PhD-FSTC-2016-64
The Faculty of Sciences, Technology and Communication

DISSERTATION

Defence held on 14/12/2016 in Luxembourg

to obtain the degree of

DOCTEUR DE L'UNIVERSITÉ DU LUXEMBOURG

EN SCIENCES DE L'INGENIEUR

by

Andrew IGNATENKO
Born on 25 April 1982 in Minsk (Belarus)

ANALYSIS OF THE IMPACT OF ROS IN NETWORKS DESCRIBING NEURODEGENERATIVE DISEASES

Dissertation defence committee

Dr Bernhard PETERS, dissertation supervisor
Professor, Université du Luxembourg

Dr Vikas KUMAR
Rovira i Virgili University, Tarragona

Dr Rudi BALLING, Chairman
Professor, Université du Luxembourg

Dr Petr NAZAROV
Luxembourg Institute of Health

Dr Alexey KOLODKIN, Vice Chairman
VU University of Amsterdam

Declaration of Authorship

I, Andrew IGNATENKO, declare that this thesis titled, "ANALYSIS OF THE IMPACT OF ROS IN NETWORKS DESCRIBING NEURODEGENERATIVE DISEASES" and the work presented in it are my own. I confirm that:

- This work was done wholly while in candidature for a research degree at the University of Luxembourg.
- No part of this thesis has previously been submitted for a degree or any other qualification at the University of Luxembourg, or any other institution.
- Where I have consulted the published work of others, this is always clearly attributed.
- Where I have quoted from the work of others, the source is always given. With the exception of such quotations, this thesis is entirely my own work.
- I have acknowledged all main sources of help.
- Where the thesis is based on work done by myself jointly with others, I have made clear exactly what was done by others and what I have contributed myself.

Signed:

Date:

Abstract

The generation of reactive oxygen species (ROS) is an unavoidable background process during a normal functioning of a cell. However, when incompletely-reduced oxygen species are generated in excess, they can oxidize a variety of organic molecules, cause a mitochondrial dysfunction and initiate a positive feedback loop leading to the generation of even more active ROS. To prevent an oxidative stress a healthy cell manages the ROS concentration by means of the antioxidants regulation as well as the removal of impaired mitochondria (mitoptosis). The ROS management is a crucial process for a cell survival and it is controlled by a ROS-induced signaling network, which includes different proteins bound by rather complicated cross-talks. This is a good example of a nonlinear multidimensional system, which is too complex for an intuitive understanding and needs a more advanced system approach. Indeed, the ROS concentration and the mitochondrial potential are system properties of a whole cell and they depend on thousands of macromolecular interactions.

One of the goals of a system approach is to understand how a biological function emerges from a system as a whole, while it can not emerge from a single component of a system. This is closely related with the design principle studies – the research that helps to identify how certain components (subsystems, species, pathways) are responsible for a certain biological behavior of a system. Adding module by module (the domino approach [1]) one can analyze their functional role and verify how new properties appear.

In the current thesis the model of the ROS management network is built using the domino principle. The model offers insight into the design principles underlying

the ROS management network and enlightens its functionality in the diseases such as cancer and Parkinson's disease (PD). It is validated using experimental data.

The model is used for in silico study of the ROS management dynamics under the stress conditions (oxidative stress). This highlights the phenomena of both adaptation to stress and the stress accumulation effect in case of repeated stress.

This study also helps to discover the potential ways to a personalized treatment of the insufficient ROS management. The different ways of a control of the ROS management network are shown using the optimal control approach. Obtained results could be used for a seeking of the treatment strategies to fix the ROS management failures caused by an oxidative stress, neurodegenerative diseases, etc. Or, in vice versa, to develop the ways of a controllable cell death that might be used in cancer research.

Acknowledgments

First, I want to thank Prof. Dr. Bernhard Peters for being my thesis supervisor over the past four years. I admire his professionalism and his persistence that became a real example for me. The working atmosphere he created in the group was a really inspiring and motivated to demonstrate the best results. I am really thankful for all talks we had have and for the fact that he has always been available for discussions. I am thankful for an extremely useful and detailed review of this manuscript that helped me to improve it significantly.

My deep gratitude to Dr. Alexey Kolodkin who became my guide in the world of systems biology and really helped me to successfully adapt in the very beginning of my PhD. I have ever met such enthusiastic person in my life. The unique combination of persistence, fundamental knowledge and open mind makes him an ideal co-supervisor. I appreciate his critics of those part of the current thesis that concerns systems biology.

I also would like to thank Prof. Dr. Rudi Balling for very fruitful discussions. His fresh eye allowed me to reconsider some points of my work and to make it less theoretical but more potentially useful from practical point of view. I appreciate very much his thoughts and ideas concerning the model validation procedure, which really helped me to make proper steps forward.

I am deeply thankful to Prof. Dr. Hans Westerhoff and Dr. Matteo Barberis from VU Amsterdam for the hours of hot and intensive discussions, which helped me to understand better the conceptions that currently lie in the basis of my PhD.

A huge thanks to the Dr. Danyel Jennen and his group from University of Maastricht for providing in proper time the experimental data for the model parameters estimation. It was a real push for the project and allowed to make it more solid from the scientific point of view.

Thanks for Dr. Vikas Kumar, the member of my thesis committee, for the discussions, possibility to give a talk at the University of Rovira i Virgili and for his extremely hospitality.

I would like to kindly thank Dr. Petr Nazarov from Luxembourg Institute of Health, the member of my thesis committee, for the fruitful discussions and help during my first days in Luxembourg.

I should certainly mention Prof. Dr. Nicolas Gauger from TU Kaiserslautern for the discussions about mathematical aspects of stability analysis.

Dr. Nathan Brady from German Cancer Research Center gave me a really good introduction into concepts, tools and software of systems biology that has been extremely useful during my first months of my PhD and helped to manage my time resources in a proper way.

A huge thanks to all members (current and formers) of LuXDEM group for the superb friendly atmosphere. Thank you Alban, Alvaro, Amir, Brice, Edder, Florian, Gabriele, Mark, Maryam, Mehdi, Mohammad, Pascal, Xavier and Yu.

Enormous words of gratitude go to Anna, my dearest wife, who unconditionally supported and motivated me again and again and kept believing in me all these years. Without her I would never be where I am now. The sweetest thanks to my son Konstantin who has been my biggest and funniest motivator over the years. The greatest thanks for the parents of my wife Anatol and Olga for their help and sincere support. My parents Arkadiy and Ludmila have always supported me and I am grateful that they keep believing in me.

This thesis was supported with a research grant (3990461) by the Fonds National de la Recherche, Luxembourg.

Dissemination

Along with the thesis the work, carried out during the four years of PhD project, was resulted in three co-authored articles. As well the results have been presented at international conferences (15 oral and posters presentations).

Published

Andrew Ignatenko, Alexey Kolodkin, Bernhard Peters and Rudi Balling. "Comparison of ODE-based models for reactive oxygen species regulation system." In *Proceedings of ICCSA 2014*. 2014. pp. 199-203.

Ready to submission

Alexey Kolodkin, Andrew Ignatenko, Hans V. Westerhoff, Nathan Brady, Evangelos Simeonidis, Jennen Danyel, Jacco Briede, Matteo Barberis, Vineet Sangar, Thierry D.G.A. Mondeel, Nilgun Sahin, Stephan Gebel, Lilia Alberghina, Anna Maria Colangelo, Bernhard Peters, Alex Skupin and Rudi Balling. "Dynamic networks dealing with oxidative stress: From design principles to personalised therapies for Parkinson's disease." In *NPJ Systems Biology and Applications*.

Andrew Ignatenko, Alexey Kolodkin, Bernhard Peters and Rudi Balling. "Application of the MPC controller to the simulation of the ROS management network." In *PLOS One*.

Abbreviations

ADP adenosine diphosphate

ADR Adverse Drug Reaction

AO antioxidant

ATP adenosine triphosphate

CAD cardiac assist devices

cyt C cytochrome C

DMC Dynamics Matrix Control

ER endoplasmic reticulum

ETC electron transport chain

HM healthy mitochondria

IM impaired mitochondria

Keap1 Kelch-like ECH-associated protein 1

MAC Model Algorithmic Control

MDT multi-drug therapies

MDV mitochondrial-derived vesicles

MPC model predictive control

NMPC nonlinear model predictive control

NO nitric oxide

NOS nitrogen oxide species

Nrf2 NF-E2-related factor 2

ODE ordinary differential equations

p62 sequestosome-1

PD Parkinson's disease

PDE partial differential equations

PLC programmable logic controller

RE response element

ROS reactive oxygen species

SBML Systems Biology Markup Language

SOD superoxide dismutase

List of Figures

List of Tables

Contents

Chapter 1

Introduction

1.1 Reactive oxygen species

1.1.1 Creation and transformation of reactive oxygen species

ROS are the natural byproduct of a vital cell activity. They might be produced in the cytoplasm during the redox reactions (e.g. Fenton reaction [2]). Alternatively, the ROS can be released from other cell organelles, such as the endoplasmic reticulum (ER) [3], and as a result of some enzymatic and non-enzymatic reactions [4, 5]. The main internal cell supplier of the ROS is the mitochondrion – a cell organelle that is responsible for the energy production by means of the Electron Transport Chain (ETC). The reactive nitrogen species [6] might also take part in the ROS formation.

At the same time the intracellular ROS can be generated by a number of external sources. For example, as a result of a smoking or a chemical exposure (e.g., paraquat, herbicides, phenols) [7, 8]. The ROS could be generated after an ionization of water molecules by X- or γ-rays as well as after the ultra-violet light exposure of the peroxide H_2O_2 [9]. Some anti-tumor drugs and antibiotics activate an excessive generation of the ROS to provoke a diseased cell death via apoptosis [10, 11].

From the chemical point of view, typical ROS are the active compounds that contain oxygen [12, 13] and have one unpaired electron in the outer orbit (i.e., free

radicals). The most common ROS are the peroxide (H_2O_2), the superoxide ($^{\bullet}O_2^-$) and the hydroxyl radical ($^{\bullet}OH$) [14]. In general, a half-time of free radicals varies from milli- to nanoseconds that makes them short-living substances. At the same time, the free radicals are produced inside a cell in a regular or "on demand" manner creating a certain amount of the intracellular ROS.

The ROS production could be described by a set of chemical transformations. During the first step the reduction of the molecular oxygen takes place and the superoxide ($^{\bullet}O_2^-$) is produced:

$$O_2 + e^- \rightarrow {}^{\bullet}O_2^-.$$

Then the dismutation of superoxide produces hydrogen peroxide (H_2O_2):

$$2\,H^+ + {}^{\bullet}O_2^- + {}^{\bullet}O_2^- \rightarrow H_2O_2 + O_2.$$

At the last step hydrogen peroxide could be completely reduced to water or partially reduced to the hydroxil radical ($^{\bullet}OH$):

$$H_2O_2 + H_2O_2 \rightarrow 2\,H_2O + O_2$$

or

$$H_2O_2 \rightarrow OH^{\bullet} + {}^{\bullet}OH.$$

All common types of the ROS [15] are grouped in the Table 1.1.

1.1.2 Redox potential

Any chemical species in a cell has its own redox potential (electronegativity). It is a measure of the affinity of a substance for electrons in comparison with hydrogen for which the value of the redox potential is set to be 0 V. The substances that are more electronegative than hydrogen have a positive value of the redox potential and vice versa. The greater the difference between the redox potentials of two substances

ROS	Short description
$^{\bullet}O_2^-$, superoxide anion	A product of the one-electron reduction of oxygen. The superoxide is a quite toxic species and it is used by the immune system to kill danger microorganisms. At the same time it participates in the development of many diseases and the aging [16]. Superoxide formation occurs in many reactions and in the ETC [17, 18]. Superoxide might be effectively neutralized by a scavenging enzyme superoxide dismutase (SOD).
H_2O_2, hydrogen peroxide	Two-electron reduction state, formed by a dismutation of $^{\bullet}O_2^-$ or by a direct reduction of oxygen. It plays an important role in the immune system. Hydrogen peroxide might decompose into the hydroxil radical that can directly damage intracellular components, especially, mitochondria [19].
$^{\bullet}$OH, hydroxyl radical	A highly reactive neutral form of the hydroxide ion [20]. It is extremely reactive and attacks most cellular components.
ROOH, organic hydroperoxide	Formed in the reactions with cellular components (e.g. lipids) [15].
RO$^{\bullet}$, alkoxy and ROO$^{\bullet}$, peroxy radicals	Produced in the presence of oxygen and participate in lipid peroxidation reactions. It may induce a damage in lipophilic compartments [21].
HOCl, hypochlorous acid	Formed from peroxide. It performs both pro-inflammatory and anti-inflammatory functions. However, it has a high reactivity and may oxidize protein constituents [22].
$ONOO^-$, peroxynitrite	Interacts with lipids, DNA, and proteins. The peroxynitrite generation is a crucial pathogenic mechanism [23].

Table 1.1: Common reactive oxygen species and their short description.

the easier an electron can travel from the less electronegative substance to the more electronegative one. As a result a donor of an electron becomes oxidized.

If there is an oxidized form (A_{ox}) of some substance A, then to obtain a reduced form A_{red} the following reaction should take place:

$$A_{ox} + ne^{-} \leftrightarrow A_{red}, \tag{1.1}$$

where n electrons are taken from a donor.

The redox potential difference ΔE between a donor and an acceptor of the electron is related to the associated Gibbs free energy change ΔG:

$$\Delta G = nF\Delta E, \tag{1.2}$$

where n is a number of transferred electrons and $F = 96485\frac{J}{mol \cdot V}$ is Faraday's constant. The Gibbs free energy is the energy that is available to do a work. If a reaction reduces the overall Gibbs energy of a system ($\Delta G < 0$), then it is referred to a thermodynamically spontaneous reaction (favoured reaction). Using tabulated values of the redox potential for different substances inside a cell it is possible to understand a direction for an electron transfer. The typical values of the redox potential of the intracellular elements vary from -0.7 V to $+0.8$ V [24]. The values of the redox potential for typical ROS are in the range from $+1$ V to $+2.3$ V [25]. It means that the value of ΔE for the pair donor-acceptor is negative that guarantees the negativity of Gibbs free energy ΔG. Thus, the reaction of oxidation of the intracellular components is favourable from thermodynamical point of view, therefore the ROS may easily oxidize them.

1.1.3 Electron transport chain

The main function of the mitochondrion is to generate energy that is stored in the molecules of adenosine triphosphate (ATP). To do that the mitochondrion uses the electron transport chain (ETC) [26]. The ETC includes several spatially distributed redox reactions to facilitate an electron transfer between a donor and an acceptor (see Fig. 1.1).

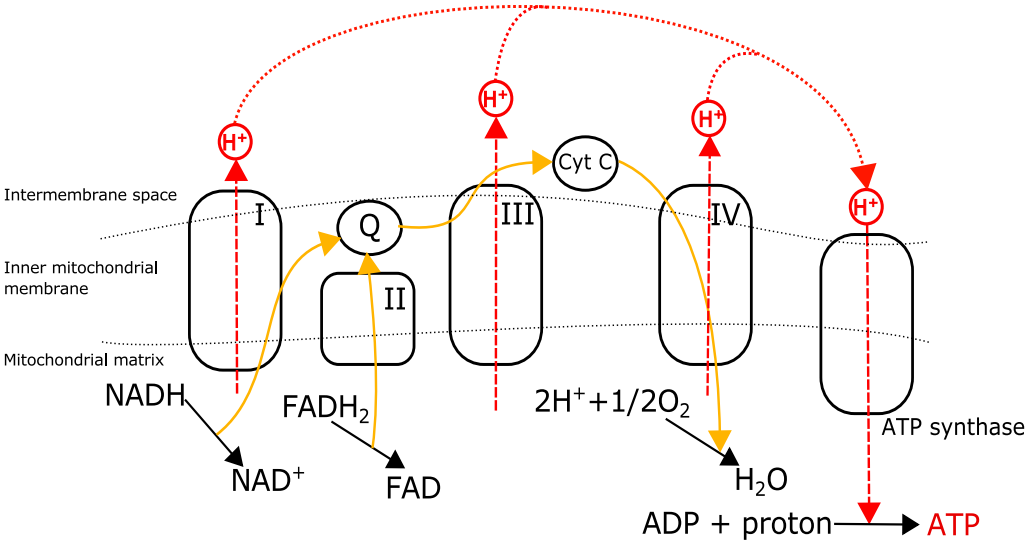

Figure 1.1: The electron transport chain (ETC) is used to create a channel for proton transfer. Protons are an important component in the process of ATP generation. The complex I accepts the electrons from NADH, and passes them to the coenzyme Q (ubiquinone) that also receives the electrons from the complex II (succinate dehydrogenase). Then the electrons are transferred into the complex III (cytochrome bc1 complex) and complex IV via cytochrome C (cyt C). Finally, in the complex IV the electrons are used for the reduction of the molecular oxygen to water.

The process starts at the inner membrane of the mitochondrion. Here the reduced forms of coenzyme nicotinamide adenine dinucleotide (NADH) and redox cofactor flavin adenine dinucleotide (FADH) are used as the donors of electrons. The electrons are passed via a transport chain and take part in the reduction of oxygen into water. The electron transfer is carried out from a donor to a more electronegative acceptor and repeated until the electron reaches oxygen. The transfer releases the energy that is used to pump the protons from the mitochondrial matrix into the intermembrane space. At the end ATP synthase uses the flow of protons to generate ATP from adenosine diphosphate (ADP).

In a normal cell about 0.1-2% of the electrons are not able to finish the transfer chain and leave the ETC to take part in the formation of active radicals [27]. However, the increase of the ROS concentration promotes electrons to escape from the ETC. As a result, ATP generation is reduced that negatively affects a cell.

1.1.4 Useful functions of the ROS

The ROS are often considered as the danger species that might damage cell components. However, the ROS also have the useful functions listed below.

- A killing of invading pathogens [28, 29, 30].
- The intracellular signalling [31, 32].
- A taking part in physiological reactions such as the immune response [33] and the mobilization of the ion transport system. For example, blood cells in the place of an injury start producing the ROS to activate the process of the wound healing.
- The regulation of a stem cell differentiation [34]. The experimental research with different stem cell lines, such as Hematopoietic Stem Cells (HSC) [35, 36], Bone Marrow Stem Cells (MSCs) [37] and neural stem cells (NSCs) [38] show the following tendency: the low ROS level correlates with quiescent cells, the medium ROS level – with active differentiating/proliferating cells and high ROS level with senescent cells. The regulatory role of the ROS might be used by cells for a kind of quorum sensing in the context of the whole body.
- The triggering of a programmed cell death (apoptosis) [39]. In contrast to necrosis of a cell (traumatic death), apoptosis is a well controlled process. It consists of a sequence of biochemical events that change a cell structure and cause its death. Unlike necrosis, the species produced by the apoptosis are quickly removed by phagocytic cells and do not pose a threat to a cell environment.

1.1.5 Cellular mechanisms for the ROS management

The ROS concentration depends on a cell functioning. For example, quiescent cells [40] have less number of mitochondria and a low metabolic activity. Their main function is to maintain themselves and to be the most protective ones. As a

result, they have a very low ROS level. Active cells have a higher metabolic load and consequently generate more ROS. A good example is dopaminergic neurons that need a lot of energy to secrete dopamine. When a cell grows older and becomes more damaged, the ROS level naturally grows further.

There are also some other factors that manipulate the ROS concentration. For example, the ROS level is highly affected by a physiological state, e.g., by anoxia. Also, the ROS level is shown to be higher when cells are at the lower cell density [41]. It might mean that a body needs to increase the proliferation and differentiation of stem cells. The ROS level would be then an easy affordable signal for a cell to monitor how many other cells are around.

Normally, a cell has two mechanisms to control the ROS concentration: enzymatic and nonenzymatic. The first found enzymatic system was the superoxide dismutase (SOD) [42, 43], which regulates the superoxide anions concentration by converting them into the peroxide:

$$2\,O_2{}^- + 2\,H^+ \rightarrow H_2O_2 + O_2$$

and then into water with a participation of the enzyme catalase:

$$H_2O_2 \rightarrow 2\,H_2O + O_2.$$

Another enzymatic system is the glutathione that catalyzes the degradation of peroxides (hydrogen and organic ones) into the alcohols. The examples of the nonenzymatic antioxydants are vitamin C and vitamin E [8].

If the antioxydants fail, a removal of impaired mitochondria might be started [44, 45]. The process of mitochondria removal is called mitophagy and might be initiated by several processes [46, 47, 48]. Alternatively, mitochondria might be recovered via the mitochondrial-derived vesicles (MDV)[49]).

The precise ROS management is a critical component for a cell survival. Roughly speaking, the ROS concentration might be regulated via antioxidants activity but

overall regulatory network is rather complicated and has other components apart from antioxidants, e.g. the proteins Nrf2, Keap1, Parkin, p62, DJ-1.

Disruptions in the ROS management might be involved in the development of many diseases. Thus, a cancer cell may deal with higher ROS concentrations and is more protected against the oxidative stress. On the contrary, in neurodegenerative diseases (Alzheimer, Parkinson, Huntington) the ROS regulation network might be disrupted and promote the death of neurons.

1.1.6 Oxidative stress

The most dangerous part of the oxidative stress is the start of an excessive generation of the ROS. Normally, the intracellular ROS concentration is low and a cell can perform a deactivation of the excessive ROS using antioxidants or just by replacing impaired mitochondria. A significant increase of the ROS concentration inside a cell may provoke an oxidative damage of a cell structures including DNA, proteins, and lipids causing different types of a cell dysfunction. For example, a damage of mitochondrial lipids could disrupt mitochondria functioning. In its turn, a mitochondrial dysfunction initiates a positive feedback loop and leads to the generation of even more active ROS.

In case of a nonreversible oxidative stress a cell might die because of either apoptosis or necrosis. In case of apoptosis an internal cell medium manages to degrade into non-toxic components, while during necrosis, a cell membrane is broken and a toxic cell content escapes to the environment and may damage other cells and tissues.

In humans an oxidative stress is a key component of many serious diseases including cancer [50], neurodegenerative diseases [51], heart failure [52], diabetes [53, 54] and others [55].

1.2 ROS and neurodegenerative diseases

Parkinson's disease (PD) is the second most widespread neurodegenerative disease, affecting $1-3\%$ of the population over 65 years old. The pathophysiology of neurodegenerative diseases is still hardly understood. For example, many investigations and publications in the area relate rather to the description of pathological consequences taking place after the disease has been developed, than to seek the explanation of the mechanisms of the disease development. Also, very limited ways of the treatment strategies are suggested: most approaches are oriented only for a maintaining of the current patient state to delay worsening.

Sometimes, the main reason of PD development is perceived as a consequence of a single mutation, for example, in the ubiquitin E3 ligase parkin [56]. However, PD is an example of multifactorial systems biological disease and can involve many processes:

- genetic predisposition, there are many genes associated with PD and their number is continuously growing [57];
- the accumulation of protein filaments in Lewy bodies [58], complexes of hyperphosphorylated tau protein [59, 60], alfa-synuclein [61];
- the inflammation [62];
- the degradation of the interactions with neighboring cells (neurons and glial cells in PD) [63];
- environmental and nutrition factors, for example, there is a positive correlation between PD and the exposure to pesticides [64].

These processes might be in a close connection with the ROS concentration and its dynamics. For example, the excessive ROS concentration might initiate the accumulation of alfa-synuclein, disrupting the generation of the protein p62. The lack of the functional p62 affects the mitophagy and may increase the ROS concentration.

1.3 Systems Biology

Systems biology is a science that aims to understand how a biological system works when it is not a standalone object and is interacting with other systems and an environment [65, 66]. Generally, to explain the functional properties of a biological system it is necessary to take into account corresponding components and their interaction with an environment. This might be possible with the use of a computer model and has become one of the goals of systems biology.

Systems biology can be defined as a science that aims to understand how biological function that is absent from macromolecules in isolation emerges when these macromolecules exist as components of a system [65].

On the one hand, biological systems consists of great number of diverse components, and, on the other hand, the way how components interact is affected by many other components of a system. Component properties are highly state-dependent – local interaction between components is affected by the state of the whole system. Systems biology proposes the solution to deal with the challenge. The information about component's state dependency (how components are related in a system) may be described in the terms of mathematical equations. When equations are integrated into a mathematical model, the emergence of a biological function may be reconstruct in silico. This may lead to principally new type of data-intensive science and, in fact, represents a shift in the way how we conceptualize and understand biological systems. For example, while running computer simulation it is possible to identify how particular design feature (e.g. a certain pattern of interactions between systems components) is responsible for systems functioning and thus one may be able to discover design principles of the system.

Since biological systems are not standalone object, one should also consider the interaction of systems components with the environment [66]. In the relation to the ROS management it is impossible to limit a model to exclusive mitochondrial ROS metabolism and it is necessary to take into account the additional processes. For example, the ROS production in the cytoplasm in iron-catalysed reactions, the

exchange of reductive potential between ROS and NOS (nitrogen oxide species), the effect of the ROS on various intracellular signalling pathways, etc.

It also seems to be impossible to answer the question about the interaction of the ROS and the mechanisms of PD if one considers the disease as a single event with an unknown cause and certain consequences. Another approach is to consider the disease as a systems event. It would allow to think of a disease as a shift of homeostasis out of the normal range due to a set of perturbations in the biomolecular network. The perception of a disease as a network perturbation [67, 68] has two important implications; first, that there may be multiple different perturbations that could result in a single disease phenotype. This agrees with the state-of-the-art understanding of many complex diseases. Second, the converse argument predicts that there could be multiple ways to return the network back to the "healthy" state by targeting several points in the network. This provides the conceptual basis for the action of polypharmacy, or multi-drug therapies (MDT) [69, 70] and the development of network targeting drugs [71, 72, 73].

When speaking about systems biology, it is worth to mention a concept of synthetic biology [74]. Some investigators [75] consider these two approaches as two sides of the same coin. While systems biology applies engineering and physics practices and principles to understand and predict the behavior of a biological network, synthetic biology can be used as a tool for systems biology to build a simpler version of a biological system.

1.4 "Domino" approach in systems biology

The "domino" approach may facilitate an implementation of systems biology ideas into the process of a model development [1]. The approach is based on the fact that there are usually only a few key metabolites or proteins that interconnect different modules in a large network. For the ROS management network the key components is the ROS, which concentration is defined via the production and consumption flows. Then, using in vitro enzyme kinetic assays or modular kinetic analysis [76] it

is possible to identify how other processes depend on the ROS concentration. In this way a first model is built with the ROS in the center and several processes around it. This model predicts how the activation of production and consumption processes affects the concentration of the key components and the steady-state fluxes. During the following steps new blocks are incorporated into the model, adding a new functionality.

One challenge in building a domino-based model of the ROS management network is related to high variability in the ROS control principles between cells, tissues, and organisms. Individual differences might be observed both on the intracellular level (gene expression, concentration of proteins etc.), and on the level of the emergent cell behavior (membrane potential, cell mobility, etc.). In other words, every living system is state dependent to a very high extent. One might think that it is necessary to build a separate ROS management model for every living system and for every particular situation. The solution could be a "blue-print" approach [65]. It assumes that the difference (the information of state-dependence) is not in the model topology but rather in the particular parameter sets and initial conditions. Consequently, a generic "blue-print" model that can be parametrized for any particular instantiation. Indeed, most processes and qualitative descriptions of biomolecular interactions should be similar between those models. They would differ in rate constants and expression levels.

1.5 Research objectives

The main research objective of this thesis is to understand the design principles of the ROS management network and its role in PD. As a rule, biological systems have a very complex and adaptive nature. Even a very small single-task biological network could have a very specific structure including tens and hundreds of components and interconnections and could demonstrate very complex interactions with an environment. This study proves that a systems biology approach could be successfully implemented for the investigation of complex biological networks.

The scope of this thesis is divided into several specific objectives. The main objective is to create a model of the ROS management network using the "domino" principle. Starting with a very simple model of the ROS management network it is possible to show how new features of the network emerge after adding new subsystems. Using certain criteria, a comparison of created models is carried out to justify the presence of particular subsystems. Finally, a validation of the model is performed using experimental data.

A computer simulation of temporal evolution provides very limited information about a network. Taking into account the possible application of the model to the problem of Parkinson's disease strategies for model control are proposed. It is well-known that PD and other neurodegenerative diseases appear as an insufficient or excessive generation of certain proteins. Under this condition the network leaves the normal working mode. The idea of a control strategy is to define possible procedures that might help to improve the state of a cell or at least maintain it on a suitable level. These recommendations might be translated into clear practical suggestions.

The idea of system control could also be expanded beyond the field of neurodegenerative diseases. Indeed, control theory might propose a strategy to kill a cell introducing a disbalance into the functioning of the ROS management network. Obtained results might be used in cancer treatment to solve the problem of a selective killing of cancer cells.

Finally, an idea of a very detailed model of the ROS management network is introduced. Special attention is drawn to the problem of personalized medicine as well as the investigation of eustress and distress phenomena.

As a conclusion, the drawbacks of the developed model and its future development are discussed.

Chapter 2

Kinetic modeling principles

2.1 Simulation methods for biological systems

Living organisms are controlled by complex molecular networks, and a prediction of network dynamics is a central challenge for systems biology. Very different mathematical and computational methods might be applied while developing a model of a biological system [77]. They include the boolean networks [78] or recently developed probabilistic boolean networks [79], for which the entities have discrete values of "ON" or "OFF" representing a protein/gene being present or absent. The continuous simulation approach generally operates with the systems of ordinary (more often – nonlinear) differential equations (ODE) [80, 81] that describe the reactions kinetics by means of the rates and the concentrations. There are also other specific approaches, including the stochastic simulation [82], a model development based on partial differential equations (PDE) [83] or stoichiometric simulation [84].

The choice of the simulation method strongly depends on information about a system to simulate. If there is comprehensive information about the elements of a system, the pathways between them as well as about kinetic data then the ODE-based approach might be an optimal choice. However, when a system has an uncertain structure or when kinetic information is unavailable, the probabilistic methods might be applied. While the discrete models bear a more intuitive charac-

ter, the continuous models reveal detailed information of the evolution of a system, particularly the paths lead to the attractors depending on the initial conditions and an external stimulation.

The change of every system species concentration is expressed through the balance and the rate equations that might be represented by an ODE system. Its solution allows simulating the kinetic behavior of a network.

Consequently, a behavior of a dynamic model is usually determined by a number of rate constants. In case of insufficient kinetic information, the literature sources and the specialized databases can be scanned to obtain additional data. Or the parameters estimation procedure using experimental data might be applied [85].

The following sections contain basic description of reactions and notations used in kinetic modelling.

2.2 Types of reactions and rate constants

2.2.1 Reactions

Reactions of synthesis and degradation

A typical reaction in the kinetic modeling [86, 87] contains a substrate and a product and has a rate constant (or constants) defining the rate of conversion of a substrate into a product (see Fig. 2.1).

Figure 2.1: A substrate (S) is converted into a product (P). A substrate can represent any specie (mRNA, a protein, ROS, an antioxidant) with some initial concentration or be just a virtual substrate with a fixed unity concentration. The latter means that a source is either unknown or has no importance for a model and the rate of the obtained product is defined only by a corresponding rate constant.

The change of the concentration of a product $[P]$ is defined as a multiplication of the concentration of a substrate $[S]$ and a corresponding rate constant k:

$$\frac{d[P]}{dt} = k[S]. \tag{2.1}$$

As a rule, along with the generation reaction, a product has a sink reaction that defines its degradation. Absence of such a reaction means unlimited accumulation of a product that makes no sense from a practical point of view. The reaction of degradation also has its own rate constant (see Fig. 2.2). However, it is possible to consider the situation when a product has the reaction of degradation but does not have the reaction of synthesis. For example, when some medicine is introduced into a network by one shot, it starts an interaction with the environment and its concentration can only decrease (reaction of degradation).

Figure 2.2: A product (P) with reactions of generation and degradation. Each reaction has its own rate constant. In principle, a product can have no reactions of generation and degradation. In this case it is assumed that a product concentration remains the same during all time of simulation.

When a product has both reaction of generation and reaction of degradation its concentration follows the difference between an input (source) and an output (sink) flows:

$$\frac{d[P]}{dt} = k_{gen}[S] - k_{deg}[P], \tag{2.2}$$

where $[S]$ and $[P]$ are the concentrations of a source and a product correspondingly, k_{gen} is a rate constant for a product generation and k_{deg} is a rate constant for a product degradation.

Michaelis-Menten kinetics

The analysis of the equation (2.1) describing the synthesis of a product from a substrate may raise the following question. Assuming that a rate constant is a constant, what happens if the concentration of a substrate begins to increase? It is obvious that the rate of the reaction will follow the change of a substrate concentration. It may happen that the reaction rate reaches its limit defined by a catalyst (enzyme) turnover. To avoid such scenario one can use a special type of kinetics: Michaelis-Menten kinetics [88]. It states the dependency of the reaction rate v and a substrate concentration $[S]$ in the following way:

$$v = \frac{d[P]}{dt} = \frac{V_{max}[S]}{K_M + [S]}, \tag{2.3}$$

where $[P]$ is a concentration of a product, V_{max} corresponds to the maximum rate achieved by the reaction at a maximum saturation $[S]$ of a substrate, K_M is the Michaelis constant that corresponds to a substrate concentration for which the reaction rate v is $0.5V_{max}$ (see Fig. 2.3). As a rule, a typical biochemical reaction with only one substrate is assumed to follow Michaelis-Menten kinetics.

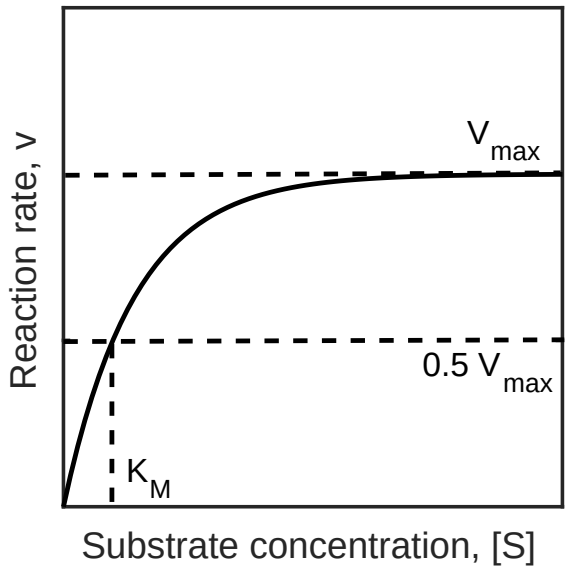

Figure 2.3: The increase of a substrate concentration $[S]$ does not lead to a linear increase of the reaction rate that is limited by a maximum value V_{max}.

However, from a practical point of view usage of the kinetics law (2.3) is not very suitable for computer models. Indeed, since a substrate $[S]$ might change in time then it might be included in the ODE-system describing network dynamics as a variable. It immediately leads to a significant sophistication of the equations by adding the fractions with variables in the denominator. Fortunately, there is a way to avoid this problem.

If the concentration of a substrate $[S]$ is much smaller than the value of K_M (i.e. $[S] \ll K_M$), then the kinetic law (2.3) can be simplified into the following equation:

$$v = \frac{d[P]}{dt} = \frac{V_{max}}{K_M}[S] = k[S], \tag{2.4}$$

where $k = \frac{V_{max}}{K_M}$. This equation is exactly the same as the law (2.1) and is called a first-order kinetics [89]. For the current thesis, first-order kinetics is used, unless otherwise is specified.

Reaction of inhibition and activation

Any biochemical reaction might be a subject for an external activation (amplification) or inhibition (suppression) (Fig. 2.4).

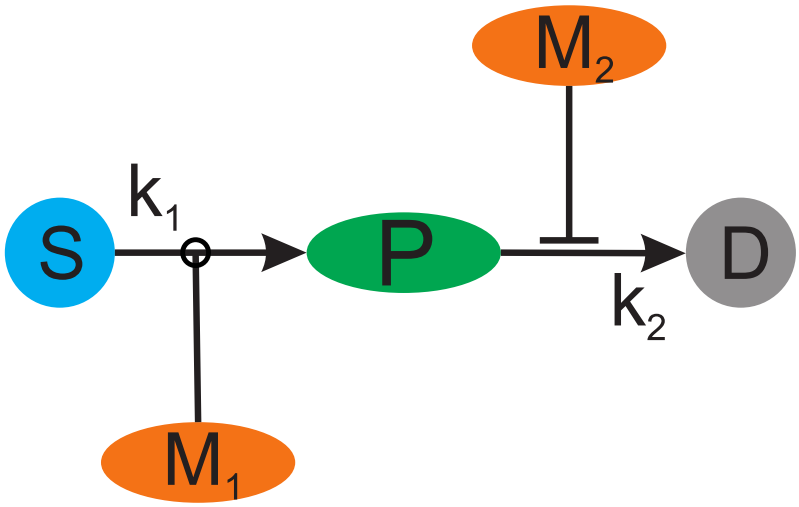

Figure 2.4: A reaction might have a modifier. A modifier can either activate ($[M_1]$) or inhibit ($[M_2]$) the reaction. In case of several modifiers a reaction might be simultaneously activated and inhibited.

When an activator $[M_1]$ modifies the rate of a reaction, the concentration of a product $[P]$ is changed according to the following law:

$$\frac{d[P]}{dt} = k[S][M_1], \tag{2.5}$$

where $[S]$ and $[M_1]$ are the concentrations of a substrate and a modifier correspondingly, k is a rate constant of the reaction of activation.

When an inhibitor $[M_2]$ modifies the rate of a reaction, the concentration of a product $[P]$ is changed as

$$\frac{d[P]}{dt} = \frac{k[S]}{K + [M_2]}, \tag{2.6}$$

where K is a parameter of dimension of concentration. Its presence does not allow unlimited growing of a product $[P]$ in case of minor concentrations of a modifier $[M_2]$. The inhibitors and activators are not consumed.

The Figure 2.4 uses some elements of Systems Biology Markup Language (SBML) notation. It is an open standard for computer models of biological processes [90]. In the current thesis three SBML elements are used (Fig. 2.5).

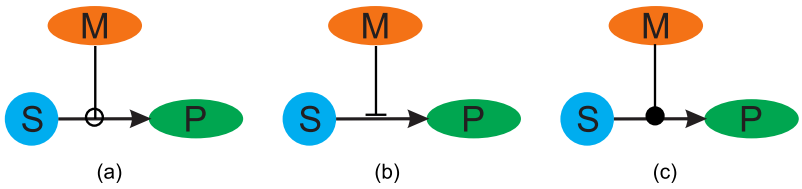

Figure 2.5: Three SBML elements are used in the thesis. (a) M is an activator of the reaction; (b) M is an inhibitor of the reaction; (c) M is consumed in the reaction.

Reversible reactions

All the reactions discussed above are assumed to be irreversible. However, if the product might have two states (for example, active and inactive) then reversible reaction may be used (Fig. 2.6)

If a product is neither synthesized nor degraded then the total concentration $[P1] + [P2]$ remains constant and is just distributed between two states. More often

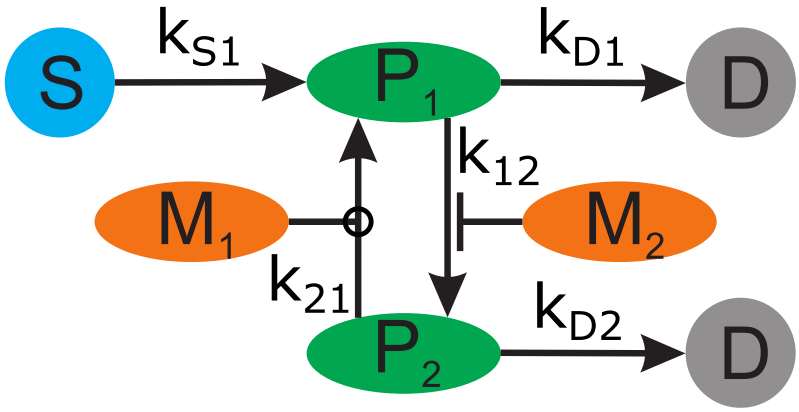

Figure 2.6: A reaction might be reversible if a product has two states ($P1$ and $P2$). Each direction of the reaction might have its own rate constant as well as modifiers.

one or both components of a product have its own sources and sinks. For example, if a product state $P1$ has a substrate $[S1]$ and a sink $[D1]$ and a product state $P2$ has only a sink $[D2]$ then for the concentration changes $\frac{d[P1]}{dt}$ and $\frac{d[P2]}{dt}$ one can write

$$\begin{aligned} \frac{d[P1]}{dt} &= k_{S1}[S1] - k_{D1}[P1] - k_{12}[P1] + k_{21}[P2], \\ \frac{d[P2]}{dt} &= -k_{D2}[P2] + k_{12}[P1] - k_{21}[P2], \end{aligned} \tag{2.7}$$

where k_{S1} is a rate constant for a synthesis of $P1$, k_{D1} and k_{D2} are rate constants for a degradation of $P1$ and $P2$ correspondingly, k_{12} and k_{21} are rate constants for the transfer from a state $P1$ to a state $P2$ and back.

2.2.2 Rate constants

Most rate constants of a model of a bioregulatory network are related to synthesis and degradation reactions. Since the parameters concern very different types of reactants (mitochondria, proteins, ROS, mRNA) then the typical timescales for the reactions also have to be different. When speaking about species that could be met in the ROS management network then all corresponding reactions could be divided into three groups: slow-rate, medium-rate and fast-rate reactions (Table 2.1).

Reaction type	**Kinetic range, s^{-1}**	**Description**
Slow-rate	$10^{-6} - 10^{-9}$	The reactions concerning mitochondria dynamics: a synthesis and a degradation. It is known that in the normal conditions (no disease, inflammation, etc.) it is necessary to spent about a $1 - 2$ weeks to change from 10% to 50% of overall number of mitochondria [91, 92].
Meduim-rate	$10^{-4} - 10^{-6}$	Reactions of protein synthesis and degradation. Indicated time range is correct for signalling proteins [93] that are assumed to take part in the ROS regulation.
Fast-rate	$10^{-1} - 10^{-4}$	Reactions of transferring between active and inactive forms of certain proteins [94].

Table 2.1: Classification of rate constants according to the reaction type.

2.3 Steady state

2.3.1 Theory of stability

Systems theory defines a steady state as a state of a system that remains unchanging in time. In terms of mathematical analysis it means that the derivative of any variable of a system in time is equal to zero. In other words, if a system is described by a set of ODE $\dot{x}(t) = f(x,t)$ then to find the steady state one should solve the system of algebraic equations:

$$f(x,t) = 0. \tag{2.8}$$

The system (2.8) might have one or more solutions (fixed points). Stability properties of a fixed point are connected with the character of a system motion in its vicinity.

If some disturbance is applied to a system being in a steady state then two scenarios are possible. Either a system manages to go back to the steady state or, if the disturbance is too large, a system leaves the steady state and starts the evolution according to a new trajectory (for example, to another steady state or to infinity).

Any steady state has an important characteristic of stability that defines the behavior of a system under the small perturbations of initial conditions. If after the perturbation a system goes back to the initial state then the corresponding steady state is called a stable one, otherwise, it is an unstable steady state.

If a system behavior is described by the ODE system

$$\begin{cases} \dfrac{dx_1}{dt} = f_1(x_1(t), x_2(t), ..., x_n(t)), \\ \dfrac{dx_2}{dt} = f_2(x_1(t), x_2(t), ..., x_n(t)), \\ ....., \\ \dfrac{dx_n}{dt} = f_n(x_1(t), x_2(t), ..., x_n(t)) \end{cases} \tag{2.9}$$

then to perform a stability analysis of the found steady state it is necessary to build the Jacobi matrix according to the following rule:

$$J = \begin{pmatrix} \frac{\partial f_1}{\partial x_1} & ... & \frac{\partial f_1}{\partial x_n} \\ ... & ... & ... \\ \frac{\partial f_n}{\partial x_1} & ... & \frac{\partial f_n}{\partial x_n} \end{pmatrix} \tag{2.10}$$

The eigenvalues of the matrix (2.10) are used to estimate a steady state stability. In general, the eigenvalues of the Jacobi matrix are complex numbers.

In an n-dimensional system the classification of the fixed point is rather difficult since there is no appropriate graphical representation. To obtain an idea about the

possible types of fixed points one could consider a 2-dimensional dynamic system, that has fixed points with two eigenvalues that can be graphically represented. Since the general solution for a motion of a dynamic system is proportional to $\sum_i e^{\lambda_i t}$, where λ_i are the calculated eigenvalues, then depending on the signs of real and imaginary parts of the eigenvalues, several types of stability might be described.

- **Both eigenvalues are imaginary.** In this case a system demonstrates pendulum behavior with a *center* (elliptic) fixed point (Fig. 2.7(a)). This type of stability corresponds to a periodic motion, i.e. an oscillation in time between two extreme points. Finally, a system flows around the fixed point, neither attracting nor repelling.

- **Both eigenvalues are real and have opposite signs**. This is an unstable fixed point of *hyperbolic* (saddle) type (Fig. 2.7(b)). The main feature of this type of stability is an existence of one direction of the attraction (in n-dimensional space the topology of the attraction might be more complicated).

- **Both eigenvalues are real and have the same sign**. Two options are possible here. If both eigenvalues are negative, then the fixed point is a *stable node*. If both eigenvalues are positive then it is an *unstable node*. In the vicinity of a node all orbits are either attracted toward to it or repelled. On the Figure 2.7(c) there is an example of a stable node. In case of unstable one the direction of the trajectories should be reversed. In contrast to the previous case an unstable node contains only the repelling trajectories. All trajectories for both stable and unstable nodes have a limiting direction in the fixed point.

- **Both eigenvalues are real and equal**. Two options are also possible here depending on the sign of the eigenvalues. In case of a negative value the fixed point is a stable improper node (Fig. 2.7(d)). If the eigenvalues are positive then the fixed point is unstable and has a type of *star* (Fig. 2.7(e)). Both types have no limiting direction and every trajectory has its own slope of an attraction or a repelling.

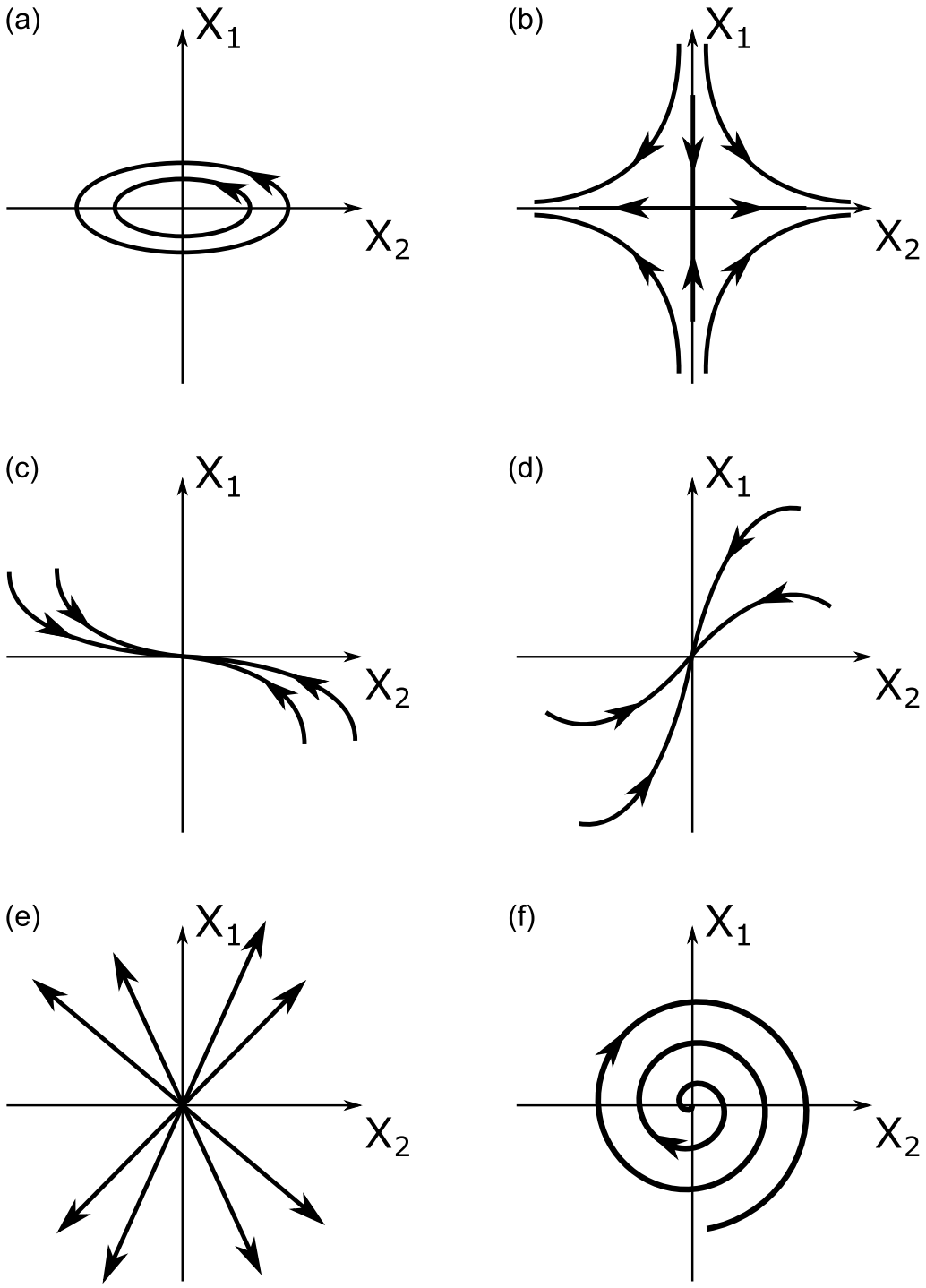

Figure 2.7: Types of a fixed point: a circle (a), a saddle (b), a node (c), an improper node (d), a star (e), a focus (f). For the simplicity it is assumed that the fixed point has the coordinates $(0, 0)$.

- **Both eigenvalues are complex**. In this case the fixed point is a *focus*. If both real parts of the eigenvalues are negative then a focus is stable. If one of the steady states has a positive real part, then a focus is unstable. On the Figure 2.7(f) there is an example of an unstable focus. In case of an unstable focus the direction of the trajectory should be reversed.

- **At least on eigenvalue is equal to zero**. In this case it is impossible to define a type of stability without additional investigations.

2.3.2 Examples of a system dynamics depending on steady states configuration

A dynamic system might have one or several steady states. Their number and type of stability might significantly change a system dynamics. It is possible to outline some characteristic cases (see Fig. 2.8). For the simplicity one dimensional case is considered.

- **One stable state.** It is the most clear case. If a system has only one stable state then its state space could be described as a gap with infinitely high walls (Fig. 2.8(a)). There would be no disturbance to make a system to leave its steady state: it always comes back.

- **One unstable state.** The only way for a system to reach an equilibrium in this case is to be placed exactly into the point of the steady state (Fig. 2.8(b)). However, even after an infinitesimal disturbance a system has to leave this steady state and it never reaches any other fixed point.

- **One stable and one unstable steady states.** When the second steady state is added to a system's state space then the dynamic of a system might be more diverse (Fig. 2.8(c)). When the second steady state is an unstable one (B), it means that there is a way for a system to leave the stable steady state (A) if the disturbance is large enough. If a system is placed in the unstable

state B then its further dynamics depends on disturbance direction. In some cases a system finds a trajectory in the direction from A to B. If a disturbance has another direction a system can choose an alternate trajectory that does not lead to the steady state A.

- **Two stable and one unstable steady states.** This scenario provides a lot of possible options for system dynamics (Fig. 2.8(d)). In addition to recently discussed trajectories several new ones are added. Thus, if a system in the unstable steady state B then after a disturbance a system might choose a trajectory to either the point A or C. In case of more dimensions there is also an option of a trajectory that leads to neither the state A nor the state C. Also, there is a possibility to make a transfer between the stable states A and C.

It is also necessary to make an important note about the special case of an unstable steady state in multidimensional state spaces. When only one of the eigenvalues of the Jacobi matrix has a positive real part then this fixed point is called "saddle" (Fig. 2.9).

The point A is a fixed point of a system. If a system is under a disturbance that shifts it strictly along the trajectory BAC then it relaxes again in the point A. Thus, one can observe a "stable" behaviour for an unstable steady state. This case represents a particular interest for a multidimensional spaces when the number of eigenvalues of the Jacobi matrix with positive real part might be significantly smaller then the number of eigenvalues with the negative real part. In this case a system might be disturbed in a wide range but still demonstrate a "stable" behavior.

2.3.3 Basin of attraction

Any stable steady state is surrounded by a basin of attraction [95] that represents all possible initial condition sets leading to the given steady state as time approaches infinity. Normally, the basins might have different dimensions and even stretch to infinity but take only a certain part of the phase space except the case when the state space contains only one steady state (Fig. 2.8(a)). Initial conditions that lie

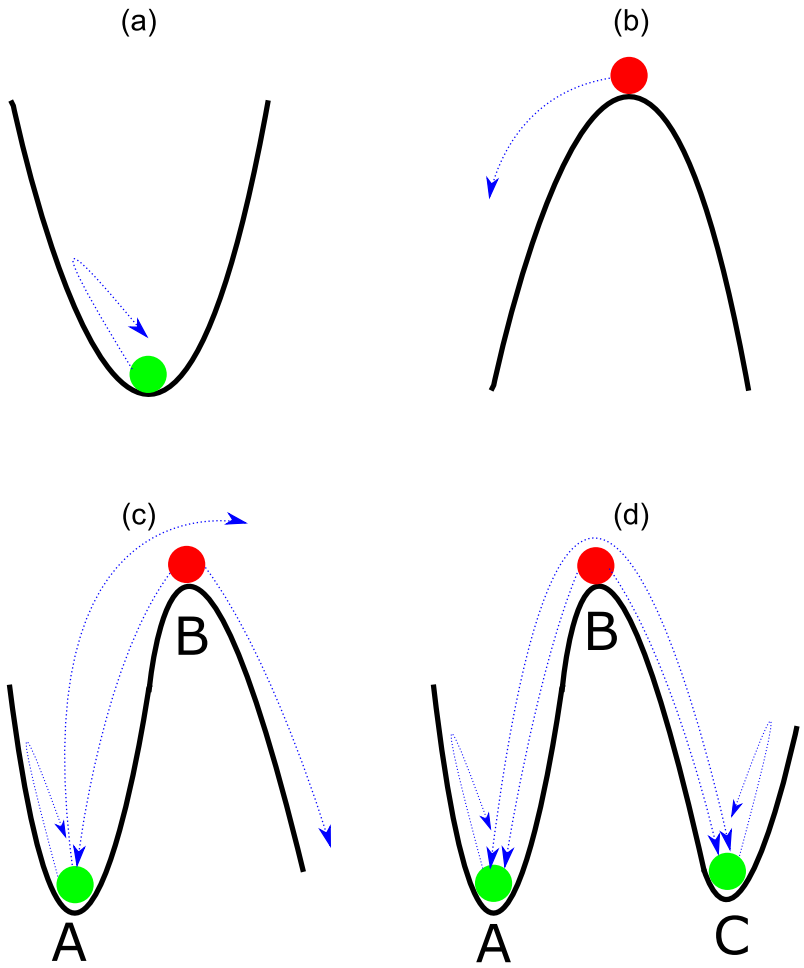

Figure 2.8: Four basic cases of steady states. Stable steady state is outlined by a green color, unstable steady state - by a red one. If a system has two and more stable steady states it might be possible to switch between them.

outside the current basin of attraction belong either for another fixed point basin or a trajectory to infinity. The concept of a basin of attraction might be used to compare different stable states or for seeking the ways of increase of stability of steady state by increasing the size of the basin.

However, analytical calculation of a basin of attraction is only possible for low dimensional problems (the number of dimensions is less or equal to 3). For a numerical calculation the Monte Carlo method or the Lyapunov's exponents [96] might be used.

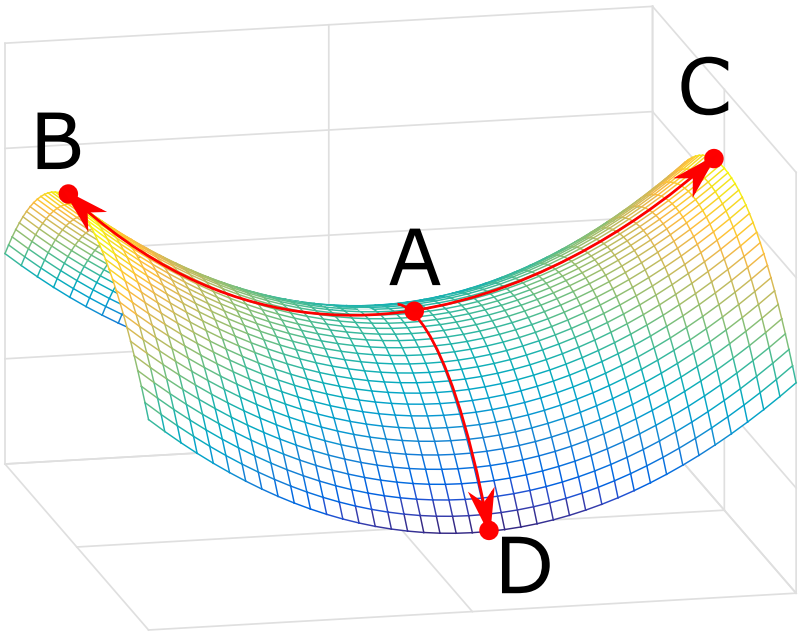

Figure 2.9: Three dimensional figure of a "saddle" point (A). The special feature of such type of an instability is that a certain type of a disturbance might cause the stable behavior of a system.

The Monte Carlo method is good enough for low-dimensional problems when it is possible to generate enough number of initial conditions and to check what fraction of them is inside the basin of attraction [95]. For high-dimensional problems the Lyapunov's exponents might provide better results. However, the application of this approach is restricted by a limited class of the problems [97].

2.3.4 Stability in biological systems

When speaking about biological systems one might be faced with several concepts describing a system stability: homeostasis, steady state (dynamic equilibrium) and chemical equilibrium. Despite the fact that all of these concepts are related to the balance of a system, they represent very different things.

- **Chemical equilibrium.** A system in equilibrium requires no energy to maintain this state [98]. If some ink is injected in a water tank with a built-in membrane in the middle, then after the diffusion the ink will have a uniform distribution for the both sides of the membrane. Afterwards, this distribution

is not changed anymore and a system is in equilibrium. No energy needs to maintain this state. A good biological example of chemical equilibrium is the value of pH. Without external impacts, pH of a biosystem remains stable as it guarantees the lowest free energy under the current conditions [99].

- **Steady state.** As it has been discussed, the main feature of a steady state is remaining constant over time. However, in contrast to a chemical equilibrium, it requires the continuous work of all regulatory systems. That is why this type of a system balance is also referred as a dynamic equilibrium. While the concept of homeostasis is applied to the entire internal environment, a steady state behavior might be restricted to specific mechanisms or subsystems. One might say, for example, that a cell is in a homeostatic state because all vital mechanisms are in steady states. The frequently used example of a steady state is an internal environment of a cell that is maintained via a constant movement of ions across the cell membrane.

- **Homeostasis.** This term is very often used specifically for animals. It is defined as maintaining of nearly constant internal environment in an animal, independently from the changes in the external environment. The key point is the presence of all necessary mechanisms to maintain a constancy within the system [100]. The good example of homeostasis is the maintaining a body temperature for mammals.

  In the current thesis the main analysis is focused on steady states. Some explicit references to the homeostasis also exist.

Chapter 3

The model of the ROS management network

3.1 The members of the ROS management network

Antioxidants

The term "antioxidant"(AO) could be referred to any molecule that could delay or even inhibit a cell damage caused by free radicals and an oxidative stress [101].

Humans have a complex antioxidant system that consists of two subsystems: enzymatic and nonenzymatic. Normally, antioxidants for everyday use are generated inside a cell (endogenous AO) but in case of necessity they could be delivered outside with medicines or a diet (exogenous AO). In some cases medicines are not necessary the AO themselves but may stimulate internal generation of the AO.

Endogenous AO play very important role since they provide necessary balance of the ROS inside a cell allowing to avoid an oxidative stress. The most efficient enzymatic AO are glutathione peroxidase, catalase and superoxide dismutase [102]. Nonenzymatic AO include the vitamins E and C, melatonin, natural flavonoids,

etc. [103]. Sometimes AO of different types could interact with each other recovering their original properties. This phenomena is known as "antioxidant network" [104].

Basically, to neutralize the ROS activity AO use two different mechanisms: a donation of one electron to a free radical and a removal of initiators of the ROS production [105]. These mechanisms provide different levels in the protection system created by AO: stopping the formation of new free radicals by reducing (glutathione peroxidase, phospholipid hydroperoxide glutathione peroxidase, etc.), scavenging active radicals (the vitamins C and E), recognizing and removing oxidated proteins (proteolytic enzymes, proteases, etc.).

Protein Parkin

Parkin is a protein that in humans is encoded by the PARK2 gene. The protein is a component of the complex that performs targeting of proteins for a degradation. It is also known that it takes part in mitophagy [106]. The mutation of the Parkin protein may cause a form of autosomal recessive juvenile Parkinson's disease [107].

Protein Sequestosome-1 (p62)

The protein p62 serves as a signaling hub for diverse cellular events such as amino acid sensing and the oxidative stress response [108]. In addition, p62 works as a selective autophagy receptor for a degradation of the ubiqutinated substrates. It recognizes toxic cellular waste, which is then scavenged.

Protein Keap1

Keap1 plays very important role in maintaining of intracellular homeostasis. The protein creates a complex with transcription factor Nrf2. This binding does not allow a transfer of Nrf2 from the cytoplasm into the nucleus and leads to the degradation of Nrf2 [109]. The lack of Keap1 is the reason of the creation of unbound Nrf2 that translocates into the nucleus causing the activation of AO generation pathways.

Protein Nrf2

The protein Nrf2 plays a vital role in maintaining cellular homeostasis, especially when a cell is under an oxidative stress. It is known as a master regulator of antioxidants and detoxifying genes via binding with their response elements (RE). Under normal conditions the protein is localized in the cytoplasm creating a complex with the protein Keap1 [110]. An oxidative stress might create a lack of Keap1 increasing the concentration of free Nrf2 that starts its transfer to the nucleus where it binds to RE. This creates a complex playing a critical role in cellular defense against oxidative stress [109, 111, 112].

Nrf2 activation increases the chances for a cell to survive under an oxidative stress via multiple mechanisms:

- an activation of many antioxidants [113] (catalase, glutathione peroxidase, superoxide dismutase, and thioredoxin) that directly or indirectly scavenge free radicals;
- a regulation of a synthesis of glutathione as the most abundant scavenger of the ROS and an important controller of redox status of proteins affecting a cell survival and death [114];
- a repair or an elimination of damaged proteins, thus, protecting a cell from a death [115];
- an activation of p62 transcription [116].

Protein Nf-κB

NF-κB (nuclear factor kappa-light-chain-enhancer of activated B cells) is a protein complex that controls transcription of DNA, cytokine production and a cell survival [117]. NF-κB is found in almost all animal cell types and is involved in the cellular responses to stimuli such as stress, cytokines, free radicals, heavy metals, ultraviolet irradiation. NF-κB plays a key role in regulating the immune response

to an infection. The incorrect regulation of NF-κB has been linked to cancer, inflammatory and autoimmune diseases.

Protein Bcl-xL

The protein Bcl-xL (B-cell lymphoma-extra large) is a transmembrane molecule in a mitochondrion. It acts as a pro-survival protein that prevents the release of the mitochondrial contents. Bcl-2 family of proteins defines whether a cell death occurs: if more Bcl-xL is present, then the cell pores become non-permeable to pro-apoptotic molecules and a cell survives.

Protein IKK

The IκB kinase (IKK) is an enzyme complex that is involved in the propagation of the cellular response to an inflammation. It is a part of the upstream NF-κB signal transduction cascade [118].

Protein DJ-1

The protein deglycase DJ-1 is also known as Parkinson's disease protein 7 (PARK7). Under the conditions of an oxidative stress the protein DJ-1 inhibits the aggregation of α-synuclein via its chaperone activity, thus, working as a redox-sensitive chaperone and as a sensor for oxidative stress. Accordingly, DJ-1 apparently protects neurons against oxidative stress and a cell death. The loss of DJ-1 results in an increased stress-induced Parkin recruitment and increased mitophagy [119].

3.2 Model I – ROS-induced mitochondrial aging

3.2.1 Model IA

Model structure

The simplest model of the ROS management network should include two components: ROS and mitochondria. A cell contains a number of organelles that can be damaged by the ROS. However, for certain reasons the mitochondrion has a special status among other organelles. At first, a mitochondrion is responsible for ATP generation. It means that a disruption in mitochondrion function could lead to the lack of energy and, possibly, to a cell disfunction or death. The ROS do not destroy the mitochondrion, instead a damage occurs and an impaired mitochondrion starts producing more ROS. These facts justify the inclusion of a mitochondrion into the model of the ROS management network. Since the mitochondrion can be in either healthy or impaired (damaged) state, a very basic model should contain three components: the ROS, healthy mitochondria and impaired mitochondria (see Fig. 3.1).

It is assumed that the healthy mitochondria concentration remains the same (no consumption in the model) but the concentrations of impaired mitochondria and the ROS could be changed in time. The model has a positive feedback loop and should demonstrate the uncontrollable increase of the concentration of both diseased mitochondria and the ROS.

Steady states and stability analysis

The seeking of the stable steady state for a model of a regulatory network is a very important task. The steady state is a key process that takes part in maintaining of homeostatic behavior of living organisms [120]. The latter property is vitally important for an organism, the best examples of homeostasis are the regulation of the body temperature, pH, glucose level, etc.

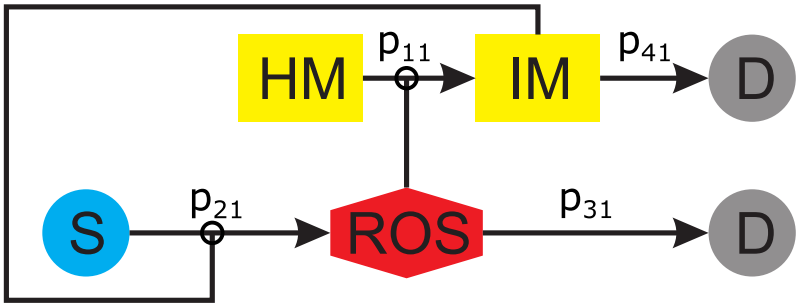

Figure 3.1: The basic model should include at least three elements: healthy mitochondria (HM), impaired mitochondria (IM) and the ROS. As any other organelle a mitochondrion moves over all life stages: from the birth to the death. The mitochondrion aging is a natural process and it is included in the model as $HM \to IM$ reaction. Aging of mitochondrion could be considered as its dysfunction. From the other hand, the mitochondrion dysfunctions can be a result of an oxidative stress against a background of the excessive ROS exposure. It means that the ROS is an activator of the reaction of mitochondrion damage. As it has been already known, impaired mitochondrion promotes further synthesis of the ROS and correspondingly could be considered as an activator of the reaction of the ROS synthesis.

The dynamics of the model IA could be described by the ODE system consisting of just two equations (only the concentrations of impaired mitochondria and the ROS can change):

$$\begin{cases} \dfrac{dx_{im}}{dt} = g_{hm} p_{11} x_{ros} - p_{41} x_{im}, \\ \dfrac{dx_{ros}}{dt} = S p_{21} x_{im} - p_{31} x_{ros}. \end{cases} \tag{3.1}$$

Where x_{im} and x_{ros} correspond to the concentrations of impaired mitochondria and the ROS, g_{hm} corresponds to a fixed concentration of healthy mitochondria, p_{11} is a rate constant for mitochondria aging reaction, p_{21} is a rate constant for the ROS production reaction, the constants p_{31} and p_{41} describe the degradation of ROS and impaired mitochondria correspondingly. The concentration S corresponding to the source of ROS.

To find the model steady state one should solve the following system of algebraic equations:

$$\begin{cases} 0 = g_{hm} p_{11} x_{ros} - p_{41} x_{im}, \\ 0 = p_{21} S x_{im} - p_{31} x_{ros}. \end{cases} \tag{3.2}$$

Evidently, the system (3.2) has only one possible trivial solution $x_{im} = 0$ and $x_{ros} = 0$ for any set of rate constants. From biological point of view the result seems to be non-realistic since it is hard to create a pure zero concentration of any network component: any fluctuation could lead to creation of non-zero concentrations. To obtain an additional proof of instability of the model IA one should perform a stability analysis. Taking into account a very simple mathematical nature of the model the analysis could be carried out analytically.

The model IA has the following Jacobi matrix.

$$J_{IA} = \begin{pmatrix} -p_{41} & g_{hm}p_{11} \\ Sp_{21} & -p_{31} \end{pmatrix} \tag{3.3}$$

The matrix has two eigenvalues

$$\begin{aligned} \lambda_1^{IA} &= \frac{1}{2}\left(-p_{41} - p_{31} - \sqrt{4Sg_{hm}p_{11}p_{21} + (p_{41} - p_{31})^2}\right), \\ \lambda_2^{IA} &= \frac{1}{2}\left(-p_{41} - p_{31} + \sqrt{4Sg_{hm}p_{11}p_{21} + (p_{41} - p_{31})^2}\right). \end{aligned} \tag{3.4}$$

Since all constant parameters and rate constants are positive then the eigenvalue λ_1^{IA} is always negative and the stability of the steady state is defined by the sign of the second eigenvalue λ_2^{IA}.

3.2.2 Model IB

Model structure

To introduce more realism and to make an attempt to obtain a stable steady state from the model it is necessary to add some mechanisms to regulate the ROS and the impaired mitochondria concentrations to avoid an uncontrolled increase of both components.

At first, the model could be complemented by the reaction of the ROS degradation with the antioxidant as an activator (the more the concentration of antioxidants

is the faster the ROS degrade). To suppress the increase of the impaired mitochondria concentration there should be a reaction of mitophagy. It removes impaired mitochondria consuming the proteins p62 and Parkin [121]. The concentrations of antioxidants, p62 and Parkin remain the same during the whole cycle of the simulation (see Fig. 3.2).

Steady states and stability analysis

Since only two species remain unfixed (newly added antioxidants, p62 and Parkin have neither sources nor sinks) then the ODE system for the model IB contains two equations:

$$\begin{cases} \dfrac{dx_{im}}{dt} = g_{hm}p_{11}x_{ros} - g_{pk}g_{p62}p_{41}x_{im}, \\ \dfrac{dx_{ros}}{dt} = Sp_{21}x_{im} - g_{ao}p_{31}x_{ros}. \end{cases} \tag{3.5}$$

Where x_{im} and x_{ros} correspond to the concentrations of impaired mitochondria and the ROS, g_{hm} corresponds to a fixed concentration of healthy mitochondria, g_{pk}, g_{p62} and g_{ao} are the constant concentrations of Parkin, p62 and antioxidants.The parameter p_{11} is a rate constant for the mitochondria aging reaction, p_{21} – for the

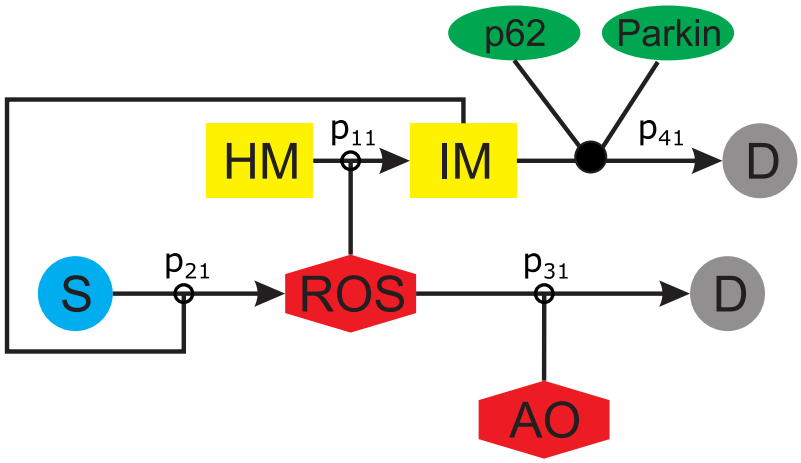

Figure 3.2: An improvement of the model IA by addition of mitophagy and the ROS degradation reactions. The mitophagy reaction is carrying out with a participation of the proteins p62 and Parkin. The proteins are not modifiers and are consumed in the mitophagy reaction: $IM + p62 + Parkin \rightarrow degradation$.

ROS production reaction, p_{31} – for the ROS degradation reaction, p_{41} – for the mitophagy reaction. S corresponds to the concentration of the source of ROS.

The steady state of the model IB is the solution of the following system of algebraic equations:

$$\begin{cases} 0 = g_{hm}p_{11}x_{ros} - g_{pk}g_{p62}p_{41}x_{im}, \\ 0 = Sp_{21}x_{im} - g_{ao}p_{31}x_{ros}, \end{cases} \tag{3.6}$$

which has evidently only a trivial solution $x_{im} = 0$ and $x_{ros} = 0$. Thus, despite the fact of an addition of some regulatory mechanisms the model IB demonstrates the same steady state solution as the model IA does. To verify if the stability type remains the same one can build the Jacobi matrix and calculate the eigenvalues.

The Jacobi matrix for the model IB could be written as:

$$J_{IB} = \begin{pmatrix} -g_{pk}g_{p62}p_{41} & g_{hm}p_{11} \\ Sp_{21} & -g_{ao}p_{31} \end{pmatrix}. \tag{3.7}$$

Two eigenvalues could be found:

$$\begin{aligned} \lambda_1^{IB} &= \frac{1}{2}\left(-g_{ao}p_{31} - g_{p62}g_{pk}p_{41} - \sqrt{D}\right), \\ \lambda_2^{IB} &= \frac{1}{2}\left(-g_{ao}p_{31} - g_{p62}g_{pk}p_{41} + \sqrt{D}\right), \end{aligned} \tag{3.8}$$

where

$$D = \left((g_{ao}p_{31} + g_{p62}g_{pk}p_{41})^2 - 4\left(-g_{hm}p_{11}Sp_{21} + g_{ao}g_{p62}g_{pk}p_{31}p_{41}\right)\right).$$

In general, the value of D could be either positive or negative and hence $\sqrt{D} = a + ib$. Taking for the simplicity $-g_{ao}p_{31} - g_{p62}g_{pk}p_{41} = -c$, where c has a positive value, one could rewrite the eigenvalues in the following form:

$$\begin{aligned} \lambda_1^{IB} &= -c - a - ib, \\ \lambda_2^{IB} &= -c + a + ib, \end{aligned} \tag{3.9}$$

	$a > 0$, $\|a\| > \|c\|$	$a > 0$, $\|a\| < \|c\|$	$a < 0$, $\|a\| > \|c\|$	$a < 0$, $\|a\| < \|c\|$	$a = 0$
$Re(\lambda_1^{IB})$	< 0	< 0	> 0	< 0	< 0
$Re(\lambda_2^{IB})$	> 0	< 0	< 0	< 0	< 0
stability	**no**	**yes**	**no**	**yes**	**yes**

Table 3.1: The solution of the steady state of the model IB can be either stable or unstable depending on values of rate constants. However, even in case of the stable steady state it could not be considered as a biologically relevant state since zero concentration can correspond only to a death state.

Then the positivity or negativity of the $Re(\lambda_i)$ depends on the signs and the values of the constants a and c. All possible combinations are provided in the Table 3.1.

Finally, the stability analysis of the model IB demonstrates the same results as for the model IA. The values of the steady state are still trivial and do not depend on model parameters.

3.2.3 Model IC

Model structure

Both previous models use the assumption of the constant concentration of healthy mitochondria. It means that a cell is supposed to have an unlimited capability to generate new mitochondria and, thus, to maintain its concentration at a fixed level regardless of the concentrations for the ROS and impaired mitochondria. In reality, a synthesizing capacity of a cell is limited. Also this assumption provides potentially unlimited capacities for a synthesis of impaired mitochondria. In reality, when the rate of mitophagy exceeds a certain level, the total mitochondrial concentration should decrease. As the result, the ROS concentration could also drop because the number of healthy mitochondria decreases. So the idea of improvement of the model IB is to add a reaction of mitochondrial synthesis (model IC). Together with mithophagy it should limit the total pool of mitochondria and provide more reasonable values for the steady state (see Fig. 3.3).

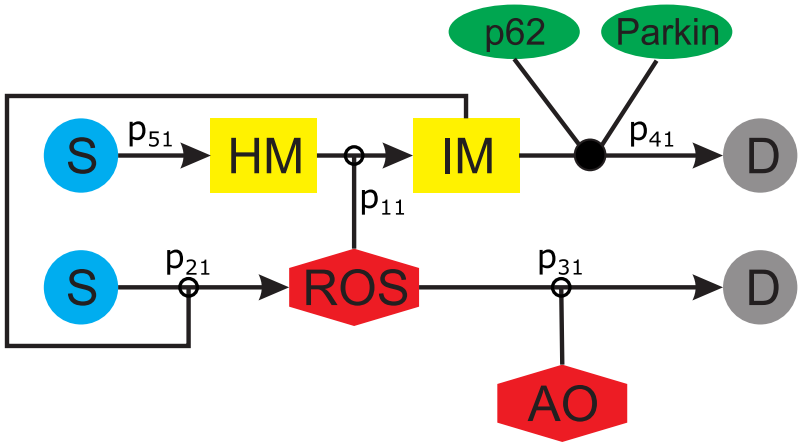

Figure 3.3: The model IC allows limiting a total mitochondrial concentration. It helps to avoid an explosive increase of the concentration of impaired mitochondria and makes the concentration of healthy mitochondria variable.

Steady states and stability analysis

Since the concentration of healthy mitochondria may change dynamically then the ODE system for the model IC consists of three equation:

$$\begin{cases} \dfrac{dx_{hm}}{dt} = Sp_{51} - p_{11}x_{hm}x_{ros}, \\ \dfrac{dx_{im}}{dt} = p_{11}x_{hm}x_{ros} - g_{pk}g_{p62}p_{41}x_{im}, \\ \dfrac{dx_{ros}}{dt} = Sp_{21}x_{im} - g_{ao}p_{31}x_{ros}. \end{cases} \tag{3.10}$$

Where x_{hm}, x_{im} and x_{ros} correspond to the concentrations of healthy, impaired mitochondria and the ROS, g_{pk}, g_{p62} and g_{ao} are constant sources of Parkin, p62 and antioxidants. The parameter p_{11} is a rate constant for mitochondria aging reaction, p_{21} – for the ROS production reaction, p_{31} – for the ROS degradation reaction, p_{41} – for the mitophagy reaction, p_{51} – for the mitochondria synthesis reaction. S corresponds to the source concentration. The model V has two sources: for healthy mitochondria and ROS. For the simplicity of analysis here and till the end of the thesis it is possible to equate every S to 1. In this case the synthesis of the corresponding product is defined exclusively by the constant rate.

Finding the solution of the system of algebraic equations

$$\begin{cases} 0 = Sp_{51} - p_{11}x_{hm}x_{ros}, \\ 0 = p_{11}x_{hm}x_{ros} - g_{pk}g_{p62}p_{41}x_{im}, \\ 0 = Sp_{21}x_{im} - g_{ao}p_{31}x_{ros} \end{cases} \tag{3.11}$$

provides one non-trivial solution:

$$\begin{aligned} x_{hm} &= \frac{g_{ao}g_{p62}g_{pk}p_{31}p_{41}}{p_{11}Sp_{21}}, \\ x_{im} &= \frac{Sp_{51}}{g_{p62}g_{pk}p_{41}}, \\ x_{ros} &= \frac{S^2p_{21}p_{51}}{g_{ao}g_{p62}g_{pk}p_{31}p_{41}}. \end{aligned} \tag{3.12}$$

It is clear that for any set of positive rate constants there is always a positive and real steady state.

The Jacobi matrix for the model IC is

$$J_{IC} = \begin{pmatrix} -p_{11}x_{ros} & 0 & -p_{11}x_{hm} \\ p_{11}x_{ros} & -g_{pk}g_{p62}p_{41} & p_{11}x_{hm} \\ 0 & Sp_{21} & -g_{ao}p_{31} \end{pmatrix}. \tag{3.13}$$

The eigenvalues λ_i of the Jacobi matrix (3.13) can be calculated after the solution of the following cubic equation:

$$\begin{aligned} &\lambda^3 + \lambda^2 \left(g_{ao}p_{31} + g_{p62}g_{pk}p_{41} + p_{11}x_{ros}\right) + \\ &\quad + \lambda \left[g_{ao}g_{p62}g_{pk}p_{31}p_{41} - p_{11}Sp_{21}x_{hm} + \left(g_{ao}p_{11}p_{31} + g_{p62}g_{pk}p_{11}p_{41}\right)x_{ros}\right] + \\ &\quad + g_{ao}g_{p62}g_{pk}p_{11}p_{31}p_{41}x_{ros} = 0, \end{aligned} \tag{3.14}$$

where the values of x_{hm} and x_{ros} should be taken from the set (3.12). The type of stability should be verified individually for every solution of (3.14). The analytical solution of the qubic equation (3.14) can be obtained with Cardano's formula [122].

3.2.4 Model parametrization

To perform further analysis of the model it is necessary to carry out its parametrization. Unfortunately, it is hardly possible to find the exact values of rate constants. However, at least, as a first approximation one can use the reactions classification provided in the section 2.2.2 at the page 20. Since it is important for the model to have a steady state then to define the values of the rate constants one should use the system or algebraic equations (3.11). To do that the desirable steady state values for the variables x_{hm}, x_{im}, x_{ros} have to be defined.

To calculate the normal concentration of mitochondria in a cell it is necessary to know both the concentration of mitochondria and a typical cell volume. Normally, the volume of a human cells varies from 30 μm^3 to 4×10^6 μm^3 [24]. However, in order to eliminate extremely small (a sperm cell) and large (a fat cell) values, one can say that a volume of a cell can be found in the range from 150 μm^3 to 5000 μm^3 that includes the volumes of the different cell types: beta cells (1000 μm^3), enterocytre (1400 μm^3), fibroblast (2000 μm^3), HeLa, cervix (3000 μm^3).

In average, a mammalian cell contains about 10^3 mitochondria [24]. Then using the value of Avogadro constant $N_A = 6.022 \times 10^{23}$ it is possible to find out the range for the concentration of mitochondria in a cell:

$$C_{mit} = \frac{n_{mit}}{N_A V_{cell}}, \tag{3.15}$$

where n_{mit} is a number of mitochondria in a cell, V_{cell} is a volume of a cell. Taking into account the typical values for n_{mit} and V_{cell} discussed above, one can find that the concentration of mitochondria in a cell can be in the range from 1 nmol/l to 110 nmol/l. For the model parametrization an average value of 55 nmol/l is taken. Since the model of the ROS management network utilizes two forms of mitochondria: healthy and impaired, then the calculated value of the total mitochondria concentration should be splitted. The rate of the mitochondria replacing starts from 3–4% per day [123]. Taking into account the fact that the number of impaired mitochondria can differ from the number of replaced mitochondria, in the current model the

Variables & Constants	**Value, nmol/l**
healthy mitochondria, x_{hm}	50
impaired mitochondria, x_{im}	5
reactive oxygen species, x_{ros}	10
antioxidants, g_{ao}	500
protein Parkin, g_{pk}	50
protein p62, g_{p62}	50

Table 3.2: Assumed steady state values for three variables of the model IC: healthy mitochondria, impaired mitochondria and the ROS and three constant concentrations: antioxidants, proteins Parkin and p62. Impaired mitochondria take about 10% of the total pool of mitochondria. This state should be considered as a healthy one since it has a normal level of the ROS in the absence of an oxidative stress [124] and a ratio of healthy and diseased mitochondria corresponds to a normal turnover process.

mentioned replacing rate is doubled. Finally, it is assumed that the concentration of impaired mitochondria is 10% of the total mitochondrial pool. The steady state concentration for the ROS (10 nmol/l) is taken from [124] where it is measured for HepG2 cells. Also the parametrization of the model IC requires the setting of the constant concentration of the antioxidants and the proteins Parkin and p62. The typical concentrations of different antioxidants are about hundreds of nM [125, 126]. Thus, as a first draft, the concentration of antioxydants is estimated as 500 nmol/l. The intracellular concentration of signaling proteins in unknown but it varies from

Reaction	**Rate constant**
Mitochondria aging, p_{11}	$2.5 \cdot 10^{-6} s^{-1} \left(\frac{nmol}{l}\right)^{-1}$
ROS synthesis, p_{21}	$4 \cdot 10^{-5} s^{-1}$
ROS degradation, p_{31}	$10^{-7} s^{-1} \left(\frac{nmol}{l}\right)^{-1}$
Mitophagy, p_{41}	$10^{-7} s^{-1} \left(\frac{nmol}{l}\right)^{-2}$
Mitochondria synthesis, p_{51}	$1.25 \cdot 10^{-3} s^{-1}$

Table 3.3: The values of the rate constants obtained after the solution of the system (3.11) using the concentrations values from Table 3.2.

10 nmol/l to 1000 nmol/l [127]. At this stage the concentration of every signaling protein is accepted to be 50 nmol/l. This value is inside the indicated range, but at the same time it does not differ too much from other concentration values. Finally, all the values for the parametrization of the model IC are grouped in the Table 3.2. Now the system (3.11) contains only five unknown values of the rate constants. Since there are only three equations the system can be considered as an underdetermined one [128]. In general, such a system has an unlimited number of solutions. The simplest way to obtain a solution is to fix certain variables by assigning some values. In the current case it is necessary to fix two values and to find the remaining ones by solving the system (3.10) of three equations with three unknowns. The possible solution is provided in the Table 3.3. To finish the model parametrization it is assumed that the concentration of source S is equal to 1 nmol/l.

One can notice that the value for the mitochondria synthesis p_{51} is outside the range specified in the Table 2.1. It might mean, that the model is incomplete and does not contain all necessary ROS regulation mechanisms. Indeed, in order to maintain the proper healthy mitochondria concentration the model produces them too fast. Hence, there might be an additional mechanism that provides more effective ROS regulation and decreases the rate of the healthy mitochondria synthesis.

3.2.5 The model response to the step-wise increase of the ROS synthesis

The ROS management network is the subject of constant challenges. Due to the different external (environmental changes, smoking, UV-rays) or internal (inflammations, various disorders) impacts the level of the ROS synthesis may be dramatically changed. One of the most important function of the ROS management network is an ability to reduce possible damage to a cell. Therefore to apply the additional verification for the model a step-wise increase of the ROS synthesis is considered (see Fig. 3.4). Indeed, a sharp ROS increase can be observed in a inflammation process [129], in a cancer therapy [130], during an insulin secretion [131].

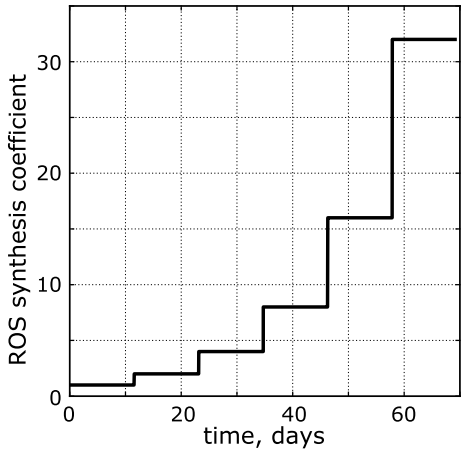

Figure 3.4: The step-wise change of the ROS synthesis (rate constant p_{21}) to check the ability of the model of the ROS management network to manage with an oxidative stress. The ROS synthesis is doubled every 10^6 seconds.

The simulation results are presented in Fig. 3.5 and have several features. At first, the model IC hardly demonstrates a homeostatic behavior. In the model IC only the healthy mitochondria concentration demonstrates the attempt of a homeostatic behavior for a first jump of the ROS synthesis when the corresponding concentration has a clear minimum and a recovery trend after that.

Another feature is the fact that the changing of the ROS concentration almost precisely repeats the dynamics of the ROS synthesis. It means that this management network has no capability to compensate the ROS synthesis jumps. A corresponding drop of the concentration of healthy mitochondria to the zero value almost guarantees the death of a cell because of lack of ATP.

3.2.6 Conclusion

A model describing a biological network should demonstrate the ability to reach the steady state. Steady state could be assigned to healthy, diseased or any intermediate state of a biological network. The evolution of a network may be represented as a set of consequential switches between steady states. The investigation of the models with the simplest structure shows that both the limited synthesis of healthy mitochondria and the mitophagy are required to reach the steady state. Despite the

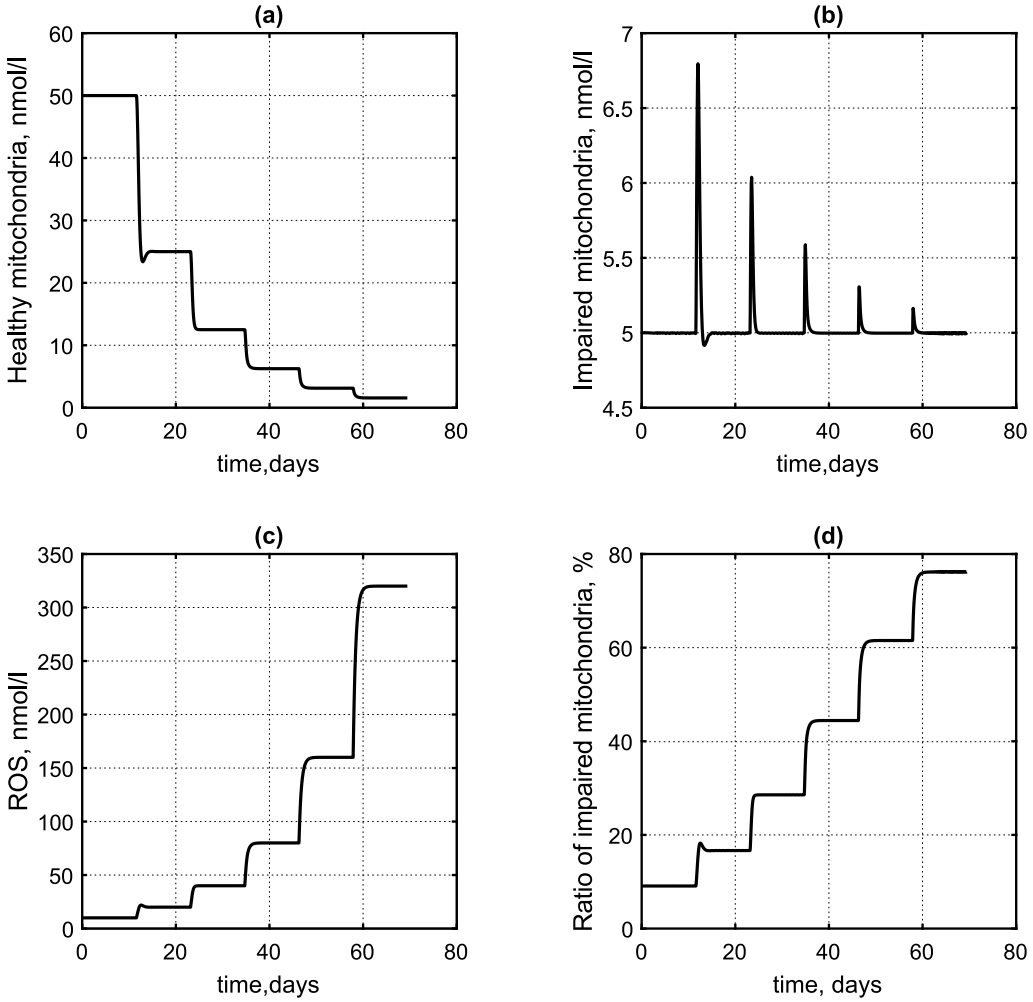

Figure 3.5: When increasing the ROS exposure three model variables have the greatest importance: healthy mitochondria (a), impaired mitochondria (b), the ROS (c) since they can be used for an estimation the state of the system. Every 10^6 seconds the ROS synthesis increases twice. Essential part of the simulation is the fact that after every jump the system has enough time to relax to the new steady state. Thus, one can avoid possible inaccuracies in post-jump dynamics because of the previous step. The figure (d) contains the ratio of impaired mitochondria in a total mitochondrial pool. The simulation is performed with MATLAB.

fact that the model IC demonstrates a steady state behavior it is not very useful from a practical point of view since it hardly demonstrates a feature of homeostasis, i.e., the regulatory function of the model does not work. However, the model IC could be used as a key one for further incorporation of additional blocks to obtain a more accurate version of the model of the ROS management network.

3.3 Model II – Keap1-Nrf2 complex

3.3.1 Model structure

In the model IC the concentrations of two species (p62 and Parkin) involved in mitophagy as well as the concentration of antioxidants are fixed. For the second stage of the model design this assumption is not a very realistic one since it guarantees a fixed level of a cell protection regardless of the ROS and impaired mitochondria concentration. Thus, the results generated by this model could not be reliable. A real cell has a dynamic pool of antioxidants with the separate reactions of synthesis and degradation. For the same reason it is necessary to make the concentrations of proteins p62 and Parkin variable as well.

In reality, a cell has one more way to modulate the mitophagy and antioxidant response. It can be done with a protein complex Keap1-Nrf2. The protein Keap1 works as ROS sensor that regulates Nrf2 degradation and its intracellular localization. The protein has two forms: active and inactive. When active, Keap1 creates a complex with Nrf2 to transfer it to the cytoplasm, and marks it for a degradation.

When the ROS oxidize cysteine residues in Keap1 molecule, Keap1 changes its conformation and becomes inactive. The higher is the concentration of ROS, the less active is Keap1 and, consequently, more Nrf2 stays in the nucleus. Higher nuclear concentration of Nrf2 provides higher expression of p62 and correspondingly increases the rate of mitophagy. The addition of Keap1-Nrf2 (see. Fig. 3.6) should change the behavior of the system qualitatively. Now, upon the increase of the ROS synthesis, one should expect a better homeostatic behavior due to the negative feed-back loop that activates the antioxidant response and mitophagy.

An addition of Keap1-Nrf2 complex and unfixing the concentration of antioxidants, p62 and Parkin immediately increase complexity of the model from mathematical point of view. Now the model has 10 variables. The full system of ODE that describes the model II could be found in the Appendix A.1.

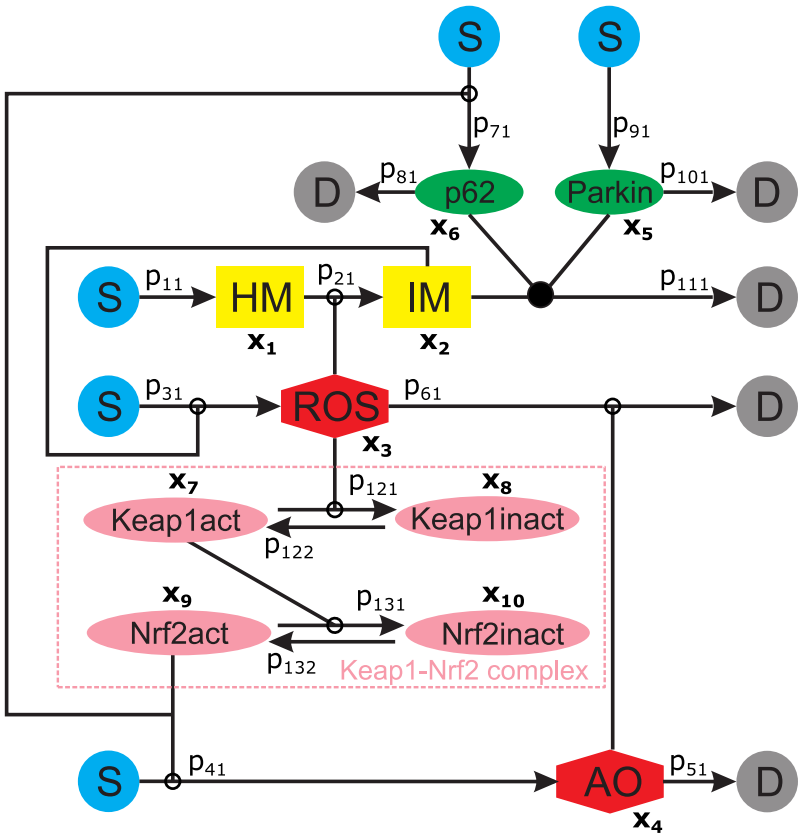

Figure 3.6: The model II with Keap1-Nrf2 complex that regulates mitophagy process. The values of the model parameters can be found in the Appendix A.1.

3.3.2 Model parametrization

The process of the model II parametrization is similar to the one for the model IC. At first, it is necessary to choose the values of the steady state the same as the model IC has. It simplifies the comparison of the models. Thus, in addition to three steady state components of the model IC seven more values are added.

It is assumed that the proteins Keap1 and Nrf2 have neither a synthesis nor a degradation. Active and inactive form of each protein create a pool and a total concentration of both forms remains the same. All reactions occur inside the pool and only between active and inactive forms.

The common parameters for the model IC and model II have the same values. Reactions of Keap1 and Nrf2 inactivation are reversible and have two rate constants.

It corresponds to a different speed of forward and backward reactions. The values of all rate constants could be found in the Appendix A.1.

3.3.3 The model response to the step-wise increase of the ROS synthesis

After an addition of a new regulatory complex and unfixing several variables one can wait that the model has to demonstrate new features and to manage with an oxidative stress better. The result of an application of the ROS jumps perturbation to the model II is shown on Fig. 3.7. The first distinction from the model IC is a better homeostatic behavior (Fig. 3.7(a)). The model II tries to recover the number of healthy mitochondria more actively. Finally, after each ROS jump it manages to reach $30 - 40\%$ of the number of healthy mitochondria before the jump. Due to this homeostatic behavior at the end of the simulation for the model II saves more healthy mitochondria then model IC, however, their concentration is still very low. Other important feature is the sharp decrease of the healthy mitochondria concentration at the moment of the first jump. The effect is even stronger that for the model IC and might be critical for ATP generation. At the same time the model demonstrates slightly better results for the ROS concentration and the ratio of impaired mitochondria.

3.3.4 Conclusion

The complex Keap1-Nrf2 provides a negative feedback loop to regulate the ROS concentration. The change of the concentration of nuclear Nrf2 via activation or deactivation of Keap1 helps to activate mitophagy and antioxidant response when the ROS concentration is increased. The model II demonstrates slightly better results concerning the temporal evolution of mitochondria and the ROS concentration than the model IC. However, it is clear that an addition of Keap1-Nrf2 complex is not enough to deal with an oxidative stress.

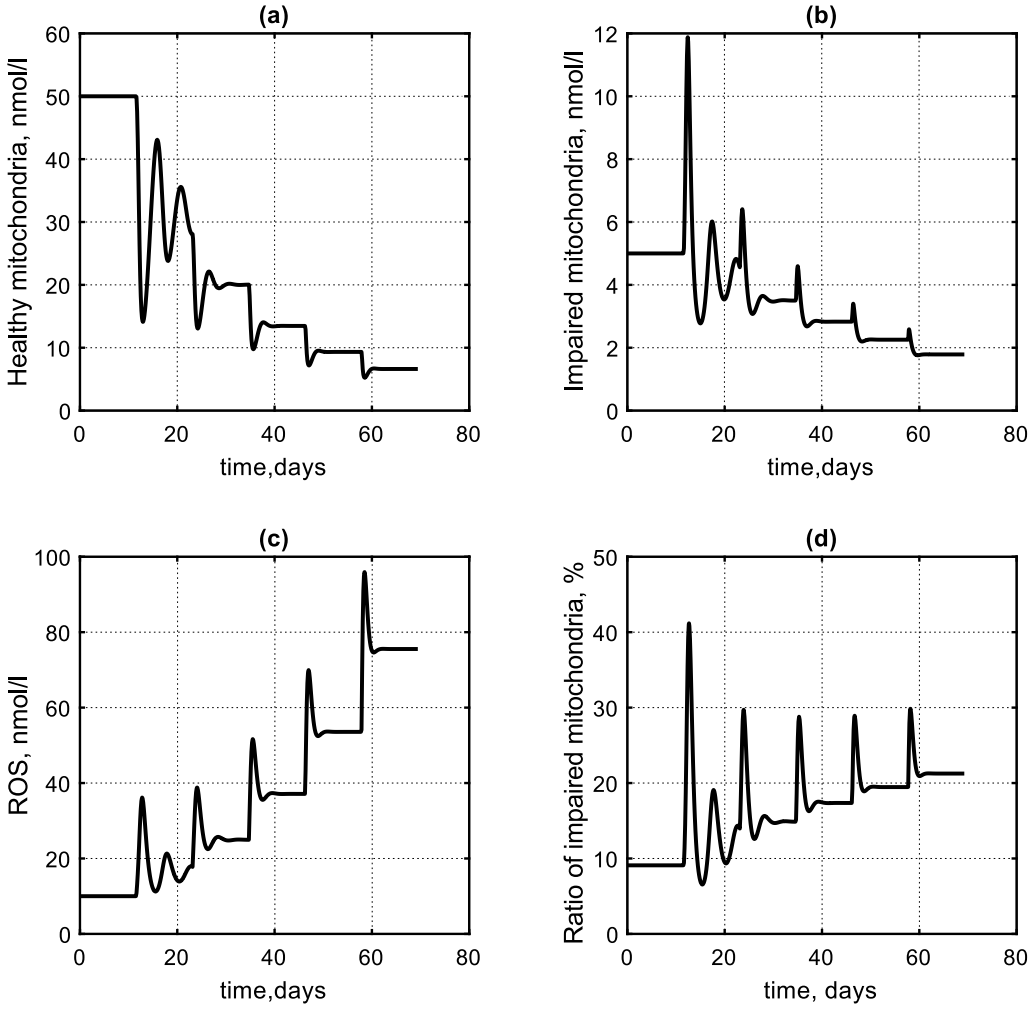

Figure 3.7: Dynamics of three variables for the model II: healthy mitochondria (a), impaired mitochondria (b), the ROS (c). since they can be used for estimation the health of the system. Every 10^6 seconds ROS synthesis increases twice. The figure (d) contains the ratio of impaired mitochondria in a total mitochondrial pool. The simulation is performed with MATLAB.

3.4 Model III – NF-κB activation

3.4.1 Model structure

The process of mitophagy decreases the concentration of impaired mitochondria and correspondingly decreases the ROS synthesis rate, thus, preventing a cell from ROS-induced damage. However, as a result, the total concentration of mitochondria can

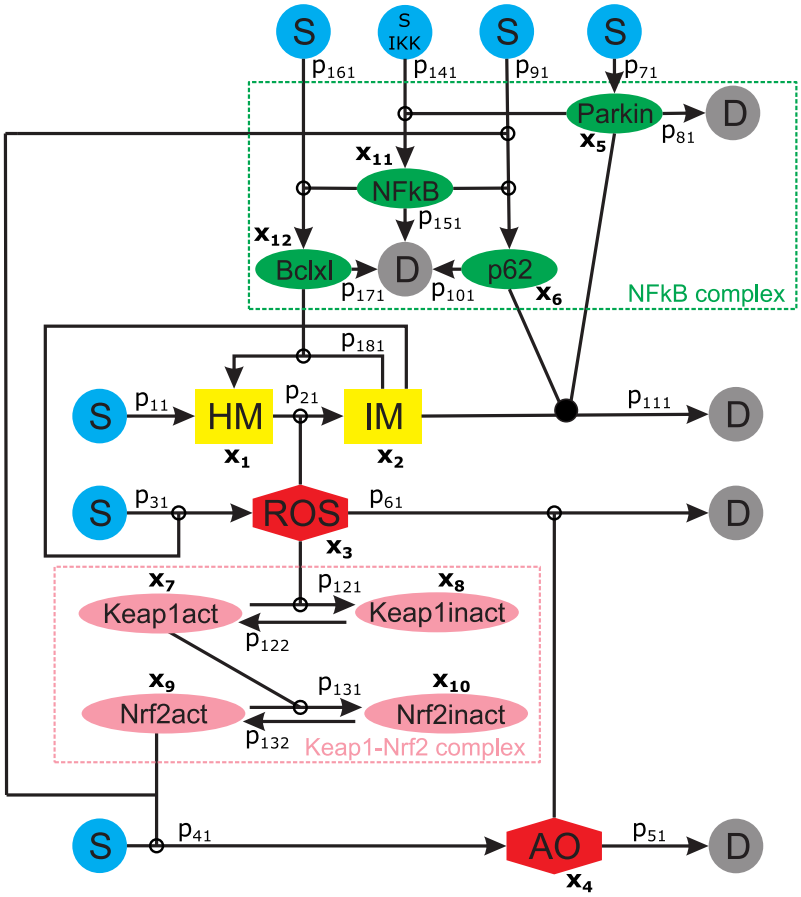

Figure 3.8: The feature of the model III is a mechanism of impaired mitochondria recovery that helps to avoid negative scenario of a cell death. The values of the model parameters can be found in the Appendix A.2.

reach a critical level when the overall energy generated by remaining mitochondria is not enough to maintain a cell functioning. This process could be considered as necrosis and result in a cell death. In the reality a cell has not only mitophagy mechanism to neutralize impaired mitochondria. Instead of being degraded impaired mitochondria might be recovered to healthy ones. To do that a cell uses a repair mechanism that is driven by Nf-κB signalling (see Fig. 3.8).

3.4.2 Model parametrization and simulation results

The model III parametrization follows the common approach accepted for the previous models and uses the same steady state values. As a result there is only one change in the values of rate constants: the rate of mitochondria aging. Full table

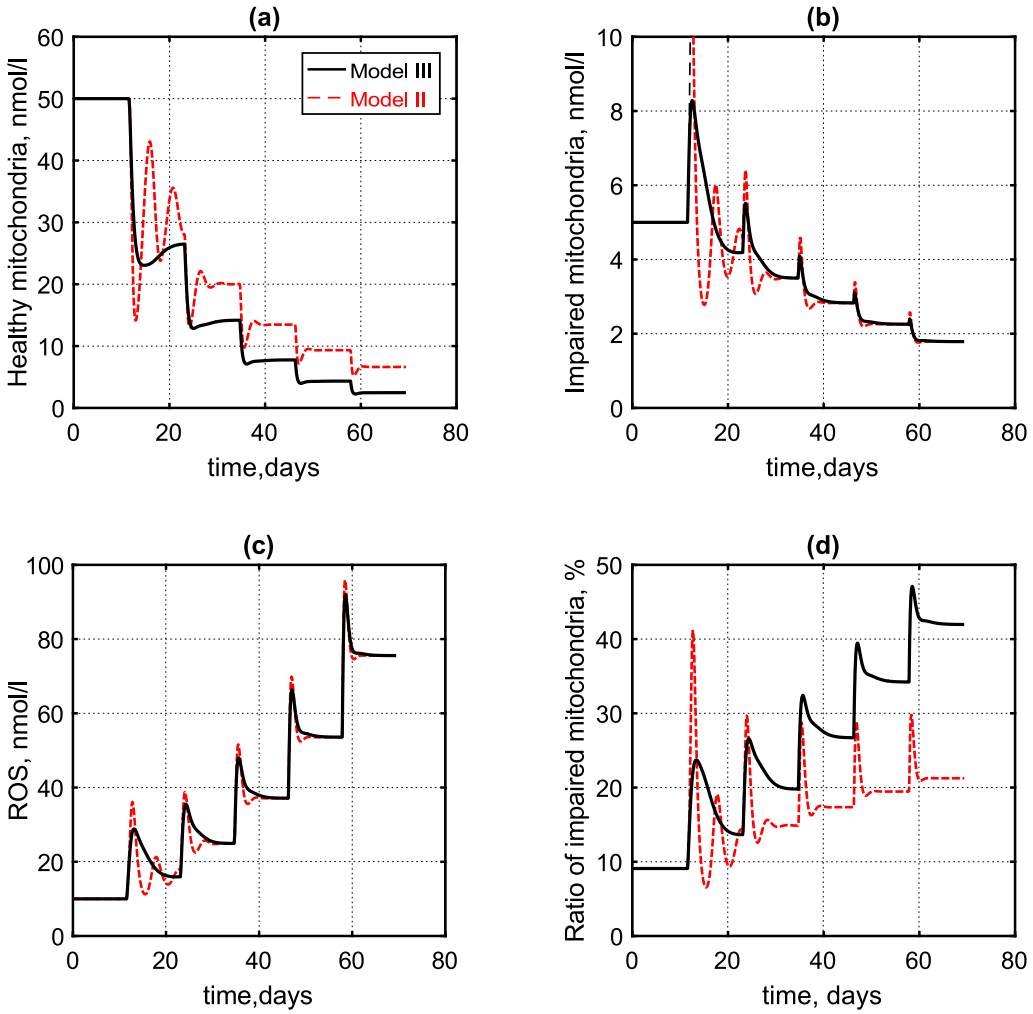

Figure 3.9: Unexpected results of the model III simulation (solid line) in comparison with the results of model II (dashed line). Dynamics of the ROS concentration and impaired mitochondria concentration are similar for the both model, however, the model III loses healthy mitochondria faster than the model II. The simulation is performed with MATLAB.

with rate constants and steady state values can be found in the Appendix (Tables A.4 and A.5).

Under the standard test with the step-wise ROS synthesis the model III demonstrates unexpected behavior: the results are worse than the model II provides. Despite of the addition of the impaired mitochondria recovery, the healthy mitochondria concentration now decreases faster than in the model II. As a result, the ratio of impaired mitochondria becomes bigger. So at the end of simulation the model III is more "diseased" than the model II (see Fig. 3.9).

One possible explanation is that a channel of impaired mitochondria recovery induced by Nf-κB could hardly be described by a single reaction. In other words, a recovery reaction in the model III is a kind of "averaged" reaction and its rate constant is a subject to investigation.

Since with the given set of parameters the model III demonstrates steady state behavior with only 9% of impaired mitochondria in the total mitochondrial pool then the value of a rate constant of the recovery reaction is enough to maintain an acceptable level of healthy mitochondria. A problem arises with the increase of the ROS synthesis. Thus, to maintain a substantial concentration of healthy mitochondria, it is necessary to increase the rate of the recovery reaction. One might expect that the higher is the rate of mitochondrial recovery, the more healthy mitochondria are.

If the mitochondrial recovery rate is doubled while the ROS synthesis is also doubled (fig 3.10(a), zone 1), then an additional activation of the recovery reaction almost allows maintaining initial steady state level for the model. After moving into the zone 2 with a normal synthesis of the ROS, the concentration of healthy mitochondria starts to increase reaching a new steady state level that exceeds the initial steady state approximately in two times. Once the model relaxes, the ROS synthesis again increases in two times (zone 3). At this step one can observe a sharp ROS jump (Fig. 3.10(a)) that corresponds to the severe oxidative stress: during the short time the concentration of ROS increases more than in 4 times.

This unexpected behavior has a rational explanation. Indeed, for the low rate of ROS synthesis and high rate of mitochondrial recovery, a cell intensively accumulates healthy mitochondria (fig 3.10(a), zone 2), but, when the ROS synthesis jumps up, all these mitochondria can be damaged. Because of high concentration of a substrate (healthy mitochondria), a quick rate of mitochondrial damage and the positive feed-back loop (ROS damage mitochondria and impaired mitochondria produce more ROS), the rate of accumulation of impaired mitochondria exceeds the rate of mitophagy. As a result, the ROS concentration grows up to a high extent and creates a strong oxidative stress.

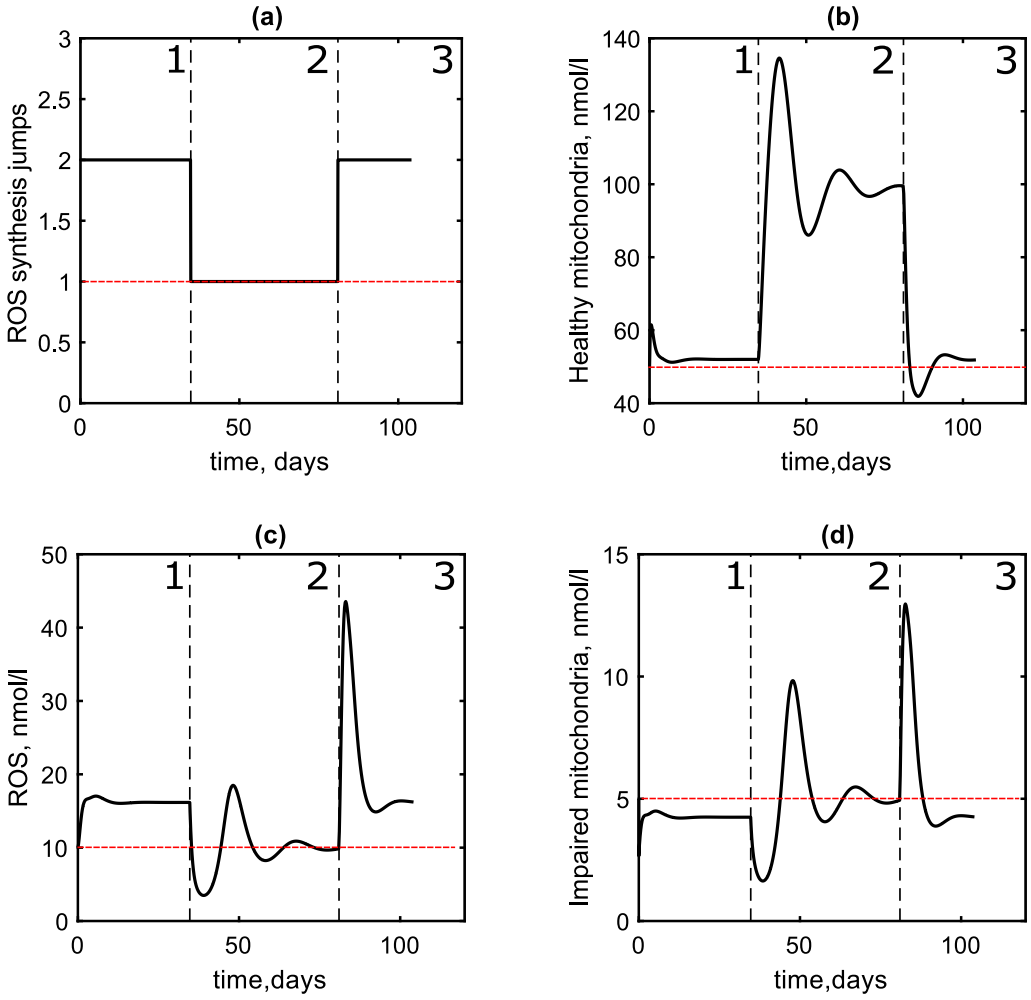

Figure 3.10: ROS synthesis (a) has three levels: 2-fold synthesis (zone 1), normal (zone 2) and again 2-fold synthesis (zone 3). Despite of the same synthesis of the ROS in zones 1 and 3 the model demonstrates different dynamics. The red line shows the steady state level for all components (observed before $t = 0$). The simulation is performed with MATLAB.

Thus, both normal and increased values of the rate constant of the recovery reaction do not provide proper functioning of the ROS management network in case of oxidative stress. The most evident solution is to let the recovery reaction be adapted to the ROS concentration. In other words, the recovery reaction should listen to the other part of the management network: there should be weak mitochondrial recovery for the low ROS level and more intensive recovery for higher ROS concentration.

3.4.3 Conclusion

The model III has a mechanism of the recovery of impaired mitochondria. This allows avoiding the situation when mitophagy is intensive enough to critically decrease the total mitochondria concentration that may result in necrosis of a cell. The recovery mechanism is driven by NFkB signalling. However, to provide an effective regulation of the recovery process a sensor of the ROS concentration should be introduced.

3.5 Model IV – DJ-1 as the ROS sensor

3.5.1 Model structure

As it has been discussed in the previous section, the model III is equipped with an important mechanism that allows recovering of impaired mitochondria instead of degrading them. However, this mechanism does not work very well until it has no connection with the ROS concentration. To introduce a pathway between ROS and Nf-κB signalling it is possible to use the protein DJ-1 that is known as a sensor of the ROS concentration [119]. Like the proteins Nrf2 and Keap1, DJ-1 can have two formations: active and inactive. When oxidized by the ROS, DJ-1 changes its state from inactive to active. Active DJ-1 modulates the activity of the various pathways in the management network, including Nf-κB and Nrf2 (see Fig. 3.11). Thus, an addition of the protein DJ-1 provides a feedback loop between the ROS and the mitochondria recovery reaction. This should make the model IV more robust to the increase of ROS synthesis.

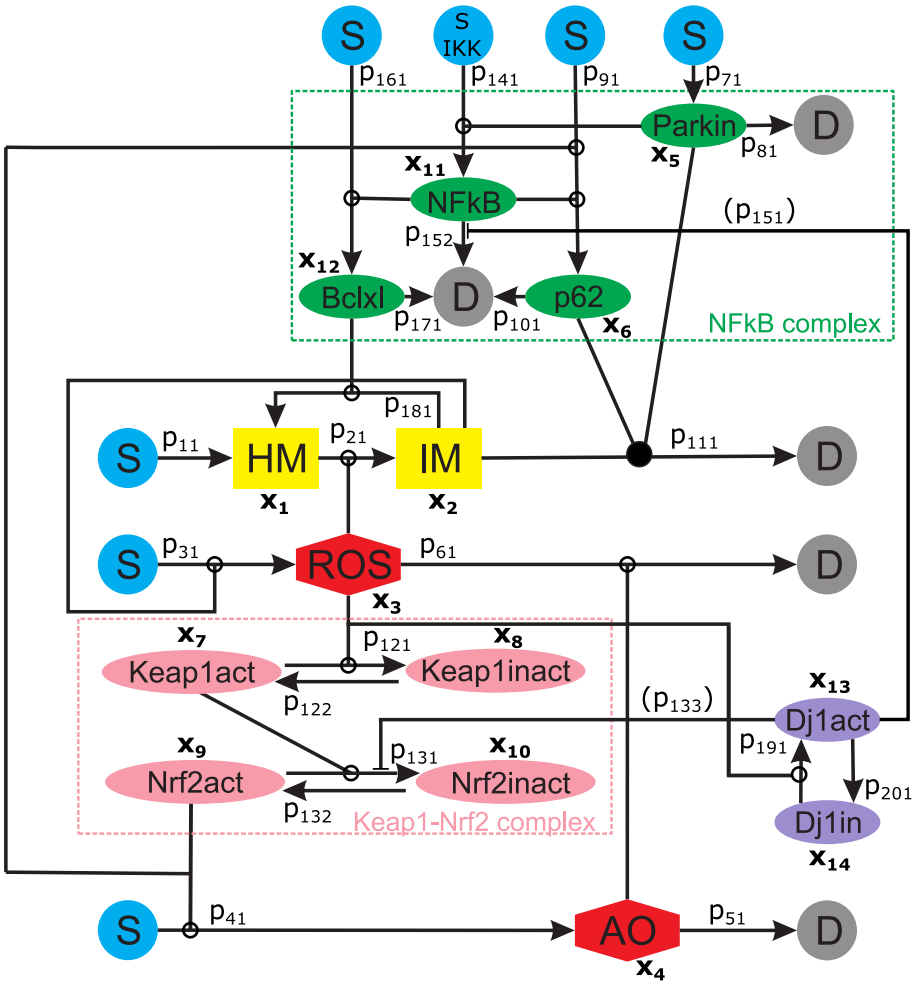

Figure 3.11: The model IV contains the protein DJ-1 that performs a regulatory function for the impaired mitochondria recovery. The non-kinetic parameters (p_{133}) and (p_{151}) allow to avoid an infinite inhibition in the case of zero concentration of the protein DJ-1. The values of the model parameters can be found in the Appendix A.3.

3.5.2 Model parametrization and simulation results for step-wise increase of the ROS synthesis

The model IV parametrization is carried out according to the procedure applied for the previous models. The full list of non-kinetic parameters and rate constants could be found in the Appendix (Tables A.7 and A.9). The results of the simulation under the step-wise ROS synthesis are shown in Fig. 3.12.

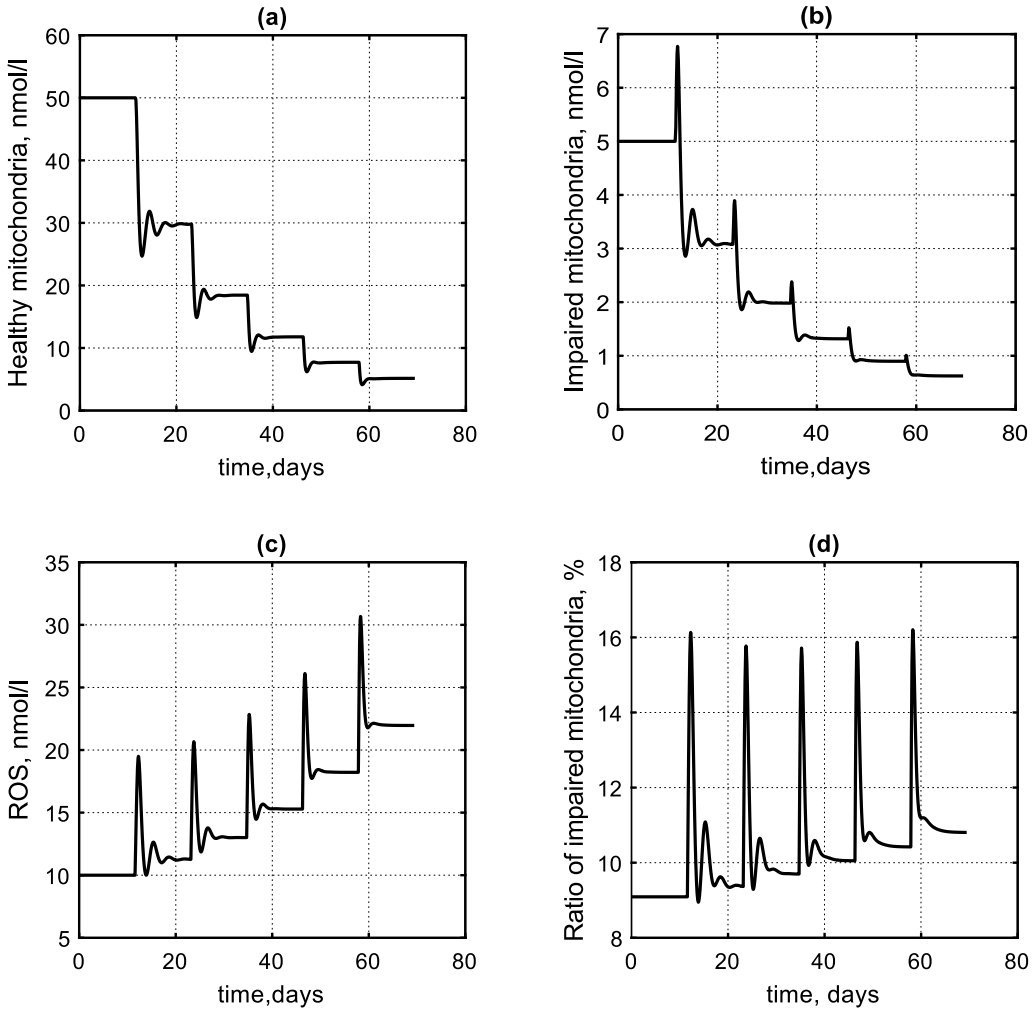

Figure 3.12: A usage of the protein DJ-1 as the ROS sensor for the reaction of mitochondria recovery. The model IV shows excellent results both for the ROS and impaired mitochondria dynamics. As well, it provides a low ratio of impaired mitochondria during whole cycle of simulation. The simulation is performed with MATLAB.

The model IV demonstrates better results than the model III. Indeed, a homeostatic behavior of the model is observed both for the ROS and healthy mitochondria concentrations. Although, after the ROS synthesis jump, the concentration of healthy mitochondria is again recovered only to $30 - 40\%$ of the before-jump level, there is no a large gap of the concentration after the first jump as it is observed in the model II.

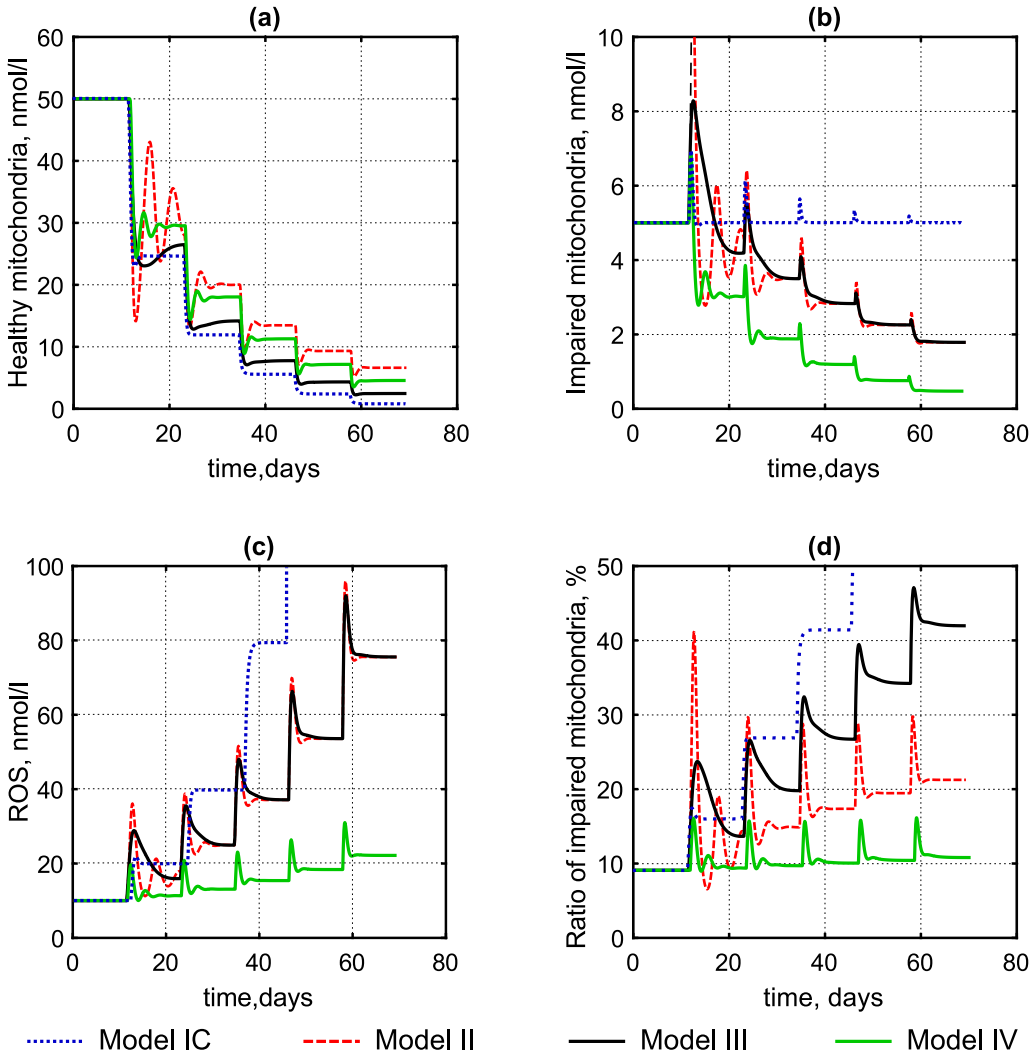

Figure 3.13: Comparison of the simulation results for the four models of the ROS management network. The model IV demonstrates the best results in the management of the oxidative stress. The simulation is performed with MATLAB.

A very good result is demonstrated for the ROS concentration. Its final value is only 2.5 larger then an initial concentration. The models II and III shows a worse result, giving about 8-fold increase of the final ROS concentration.

Normally, during all time of the simulation the ratio of impaired mitochondria leaves the range $9-11\%$ only for a short time at the moments of the ROS synthesis jumps. However, it never exceeds the value of 16%. Hence, the ratio of diseased mitochondria remains almost the same as the non-stress value.

3.5.3 Conclusion

An addition of the protein DJ-1 coordinates the mitochondrial recovery and the ROS level and helps to reach a dynamic homeostasis. This ROS sensor evidently balances the network decreasing the final ROS concentration and not increasing too much the ratio of diseased mitochondria. The comparison of the results of all four models can be found in Fig. 3.13. Evidently, the model IV that includes all three regulatory pathways (complex Keap1-Nrf2, Nf-κB signalling and the protein DJ-1) demonstrates the best results, providing the lowest level of the ROS concentration, impaired mitochondria concentration and its ratio. Only the result for the healthy mitochondria concentration demonstrates the comparable values for all three models. However, the model IV combines the good dynamics of healthy mitochondria concentration of the model II as well as the absence of the sharp gap in the concentration after the first ROS jump, provided by the model III.

3.6 Model parameters estimation

3.6.1 Parameters estimation procedure

Recently, the models of the ROS management network have been parametrized with some justified values. However, a proper model validation practice requires a stricter estimation that can be done with a usage of experimental data.

The general procedure of validation of biological models has some features that make it quite nontrivial and time-consuming. The main difficulty is the fact that even a simple model of a biological system can contain tens of parameters. Also a network model contains a large amount of "averaged" reactions. For example, the generation of any protein includes at least two phases: transcription and translation. In a model, these two phases may be replaced by an abstract source that generates a protein. An exact rate constant for this reaction can not be found.

Basically, there are several approaches for a model parameters estimation

- **Relevant literature analysis**. If a rate constant in question belongs to well-known reaction then it is possible to find some publications with numerical data.

- **Examination of specialized biomedical databases**. A very full list of the data bases can be found in the review [132]. The databases collect and systematize the data from various sources. However, if a particular rate constant (or a corresponding reaction) has not been investigated recently it is hardly possible to extract useful data from the databases.

- **Using of numerical procedure of a model parameters estimation**. It can be carried out, if there is experimental data for a model output. Then, using a tailored algorithm [133], the rate constants of a model are varying in the predefined range. The main goal is to minimize the difference between model output and an experimental data. One should remember that a found solution might not be unique. In general, this method allows to estimate any number of parameters. However, a computational complexity raises fast with the increase of the number of unknown parameters.

Unfortunately, the exact values of the rate constants used in the model of the ROS management network remains unknown. Databases and other sources might provide some information concerning the concentration of signal proteins or average values for the rates of transcription, translation and degradation [127]. The exact values for a particular protein are hardly discoverable. Therefore, to validate the model it is necessary to use the procedure of the model parameters estimation.

3.6.2 Experimental data

The data for the estimation of model's parameters are taken from the experiment of an oxidative stress application onto the human hepatoma cell line HepG2 [124]. The experiment was carried out by L. Deferme and colleagues from University of Maastricht (Department of Toxicogenomics).

In the experiment HepG2 cells were exposed to menadione, a chemical that is known for its ability to activate ROS synthesis [134, 135]. At the presence of menadione the generation of oxygen radicals is increased. One of the goals of the experiment is to measure the ROS intracellular concentration. The experiment lasted 24 hours. For the measurement the following time points were chosen: 0.5, 1, 2, 4, 6, 8 and 24 hours. The experiment was repeated three times. As a result, three experimental curves for the ROS intracellular concentration were obtained.

The base model IV can not be directly used for the parameters estimation procedure since there is no mechanism of injection of external ROS. To achieve this, the model V should be developed. It has several changes in comparison to the model IV: new mechanism of mitochondria synthesis, the subsystem of menadion injection, sources and sinks for the proteins Keap1, Nrf2 and DJ-1 to provide more flexibility for comparison with experimental data and to equip the model with additional inputs that could be used for control purposes. The detailed description of the model V is provided in the Appendix B.1.

3.6.3 Parameters estimation results

The procedure of parameters estimation was carried out with COPASI environment. It is a specialized software that supports models developed using the SBML standard and can simulate their temporal behavior using ODE-representation [136]. The software allows to define the margins for the parameters as well as to choose the method of parameters estimation. Since the exact value for the most of the model parameters are unknown then it is better to use any type of genetic algorithm [137]. The genetic algorithm is a good option if an optimization problem includes high number of variables (the model V of the ROS management network includes more that 30 rate constants). The result is shown in Fig. 3.14

The model output for the ROS dynamics is in a good agreement with experimental data. However, it is necessary to emphasize that the number of experimental points is less than the number of parameters of the model. In theory, this sit-

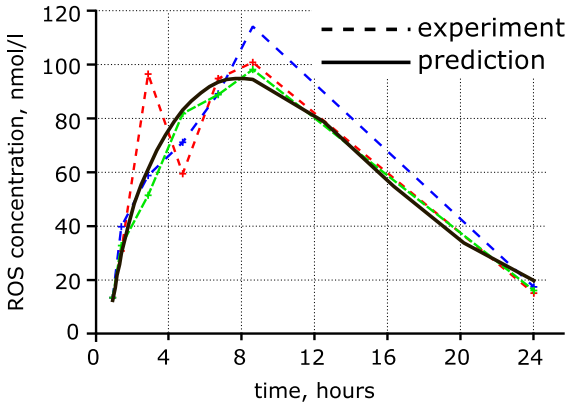

Figure 3.14: The results of the model parameters estimation. Three dotted lines correspond to the temporal ROS dynamics obtained in three experiments with human HepG2 cells. The solid line corresponds to the model prediction initialized with the estimated parameters. The estimation procedure is carried out taking into account the constraints for the rate constants from the Table 2.1 and constrains for the steady state after menadione exposure from the Appendix (Table B.1). One-time concentration of menadion is 100 μmol/l that corresponds to the experiment conditions [124]. The simulation is performed with MATLAB and Copasi.

uation might cause the problem of overfitting [138] and a bad prediction ability of the model. However, the experimental curve is smooth enough with only one clear maximum. The additional experimental points can increase the accuracy of model's parameters but hardly add new features to the experimental curve (noise, new turning points). The choice of an estimation procedure (genetic algorithm) is also defined by a low number of experimental points. The standard algorithms, for example, least squares estimation, work good only if the number of experimental point exceeds the number of model's parameters. It is also possible to make an additional check of the model's parameters estimation since the experimental group from University of Maastricht provided some additional experimental data for other elements of the ROS management network. The model predictions for these species are shown in Fig. 3.15.

It is obvious that the model demonstrates good predictions for the dynamics of antioxidants and the protein p62. Another two predictions show larger deviations. However, the experimental data have a large error that is enough to introduce an uncertainty in the results. Taking into account the standard error values one might

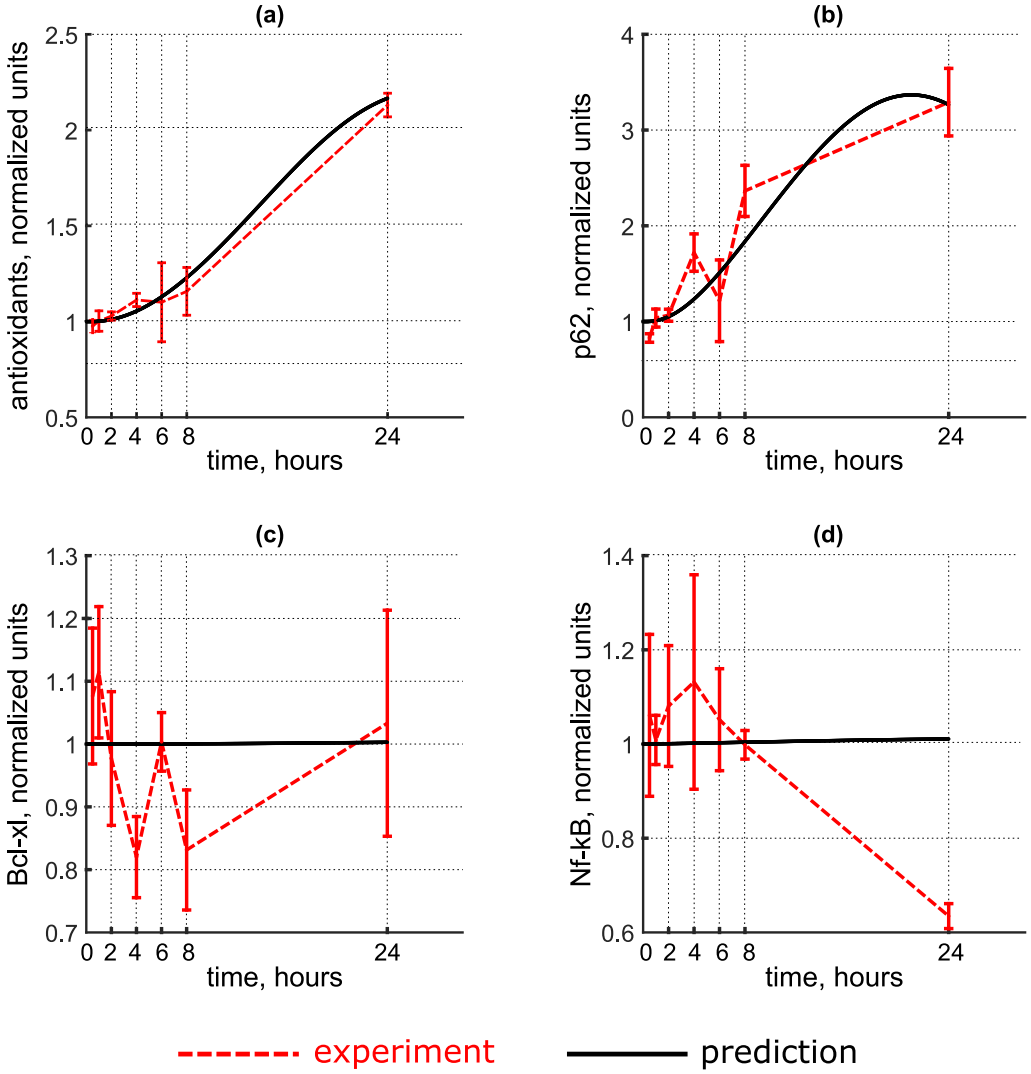

Figure 3.15: The model predictions for the dynamics of antioxidants(a) and the proteins p62(b), Bcl-xl(c), Nf-κB(d). Dashed line corresponds to the experimental data (standard error is indicated). Solid line corresponds to the model prediction initialized with the estimated parameters. The simulation is performed with MATLAB and Copasi.

conclude that the model prediction is close to the average experimental values for the the proteins Bcl-xl and Nf-κB (Fig. 3.15(c) and (d)). It is necessary to emphasize one more time that the experimental data regarding the species shown in Fig. 3.15 are not used for parameter estimation procedure.

3.7 The analysis of the parametrized model

3.7.1 Steady states

After the model has been parametrized one could calculate the steady states. Taking into account the dimension of the model state space it is hardly possible to get an analytical solution. However, the structure of ODE for the model allows a semi-analytical solution of the steady state problem. Indeed, the ODE system has several important features. At first, it is sparse. It means that every differential equation contains only a few variables rather than all variables of the system. At second, it is an autonomous system (i.e., does not explicitly contain the time). And finally, due to the polynomial nature of kinetic laws the ODE system also contains polynomial equations that simplify the analysis.

From a mathematical point of view the dimension of the ODE system allows to have a bigger number of steady states, which can be calculated numerically. However, only two steady states (presented in the Table 3.4) have real and positive values. Other steady states contain either negative or even complex values that make no sense from the biological point view since the variables of the system correspond to concentrations.

Taking into account the values for the steady states one might consider the steady state I as a healthy state of the system, corresponding to normal functioning of the ROS management network. Indeed, the concentrations of healthy and diseased mitochondria as well as the ROS and the proteins are within the normal range for a cell. On the contrary, the steady state II contains zero concentration for mitochondria and the ROS as well as abnormal values for some the proteins concentration. As a result this state might correspond to a very “diseased” state of the network. Indeed, zero concentration of mitochondria means no energy generation for a cell and its possible death.

Model variable	**Steady state I, nmol/l**	**Steady state II, nmol/l**	**Allowable range, nmol/l**
Healthy mitochondria	50	0	1–120
Impaired mitochondria	5	0	
Reactive oxygen species	10	0	20–100
Antioxidants	200	8.61	200–500
Parkin	50	50.5	10–1000
p62	50	0.1	
Keap1, active form	200	220	
Keap1, inactive form	20	0	
Nrf2, active form	20	0.9	
Nrf2, inactive from	200	200	
Nf-κB	100	4.8	
Bcl-xL	100	4.8	
DJ-1, active form	20	0	
DJ-1, inactive form	200	220	

Table 3.4: Calculated steady state values for the validated model V. The detailed solution for the steady states might be found in the Appendix B.3. The allowable ranges are taken from the section 3.2.4

3.7.2 Stability analysis

Unstable steady state

Stability analysis performed with the calculation of the eigenvalues of the Jacobi matrix for the two found steady states shows that the steady state I is a stable one and the steady state II is an unstable one. The instability of the steady state II might seem unusual, however, the analysis of instability shows that only one eigenvalue of the Jacobi matrix has a positive real part. It means that the steady state II has a type of "saddle" and it might leave this steady state only in case of disturbance along one dimension (Fig. 3.16). Indeed, the disturbance of the either the ROS or simultaneously the ROS and diseased mitochondria does not

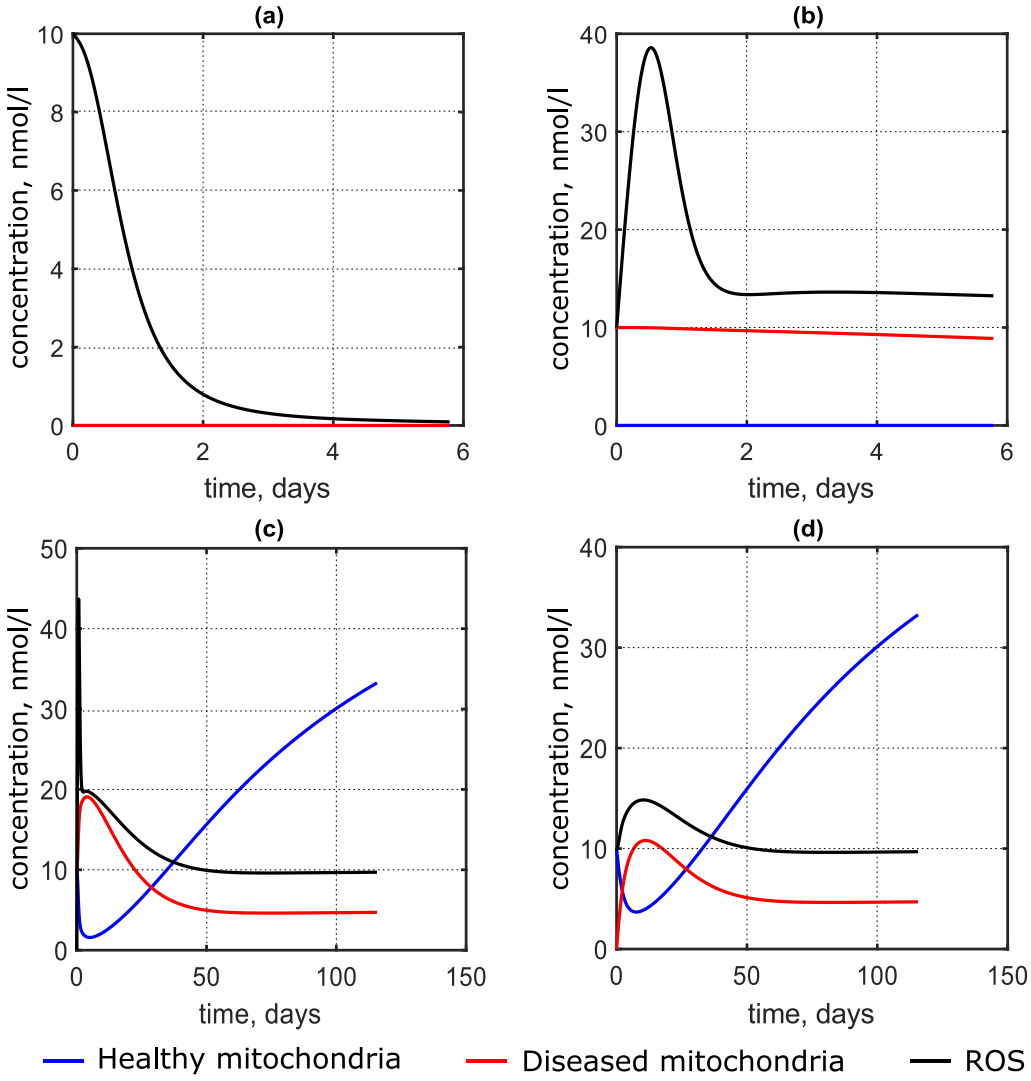

Figure 3.16: The network is disturbed when being in the unstable steady state II. (a) Only the ROS concentration is disturbed (from 0 to 10 nmol/l); (b) both the ROS and diseased mitochondria concentrations are disturbed (from 0 to 10 nmol/l); (c) both healthy and diseased mitochondria concentrations are disturbed (from 0 to 10 nmol/l); (d) both healthy mitochondria and the ROS concentrations are disturbed (from 0 to 10 nmol/l). The figures (c) and (d) shows the network dynamics on its way to the steady state I which is completed in more than 1000 days of the model timescale (not shown). The simulation is performed with MATLAB.

put the network onto the trajectory leading to the steady state I (Fig. 3.16(a) and (b)). Moreover, the concentration of healthy mitochondria stays zero. An essential requirement for escaping from this steady state is a disturbance of the healthy mitochondria concentration (Fig. 3.16(c) and (d)). However, a disturbance

of only the concentration of healthy mitochondria does not allow the network to go to the steady state I. Instead the network starts evolution to the infinity value of healthy mitochondria (Fig. 3.17).

Stable steady state

The stable steady state demonstrates a very good region of stability. The disturbed system goes back to the initial state even from a very unfavorable initial state (Fig. 3.18(a)) that may correspond to a very diseased state that also experiences an oxidative stress.

However, if the initial concentration of healthy mitochondria is equal to zero, then the transfer to the steady state II (diseased state) occurs, even if the values of all other parameters remain corresponding to the ones of the stable steady state I. In practice, a zero number of healthy mitochondria means a very low level of ATP generation and might be a reason of bad functioning of a cell.

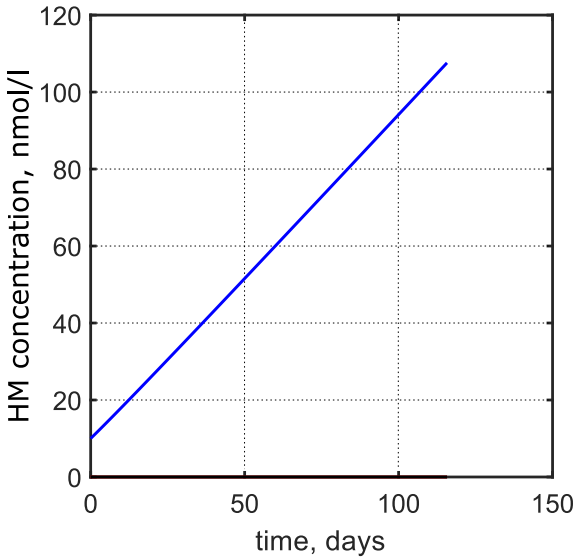

Figure 3.17: Only the concentration of healthy mitochondria (HM) is disturbed (from 0 to 10 nmol/l). This disturbance is not enough to put the network onto the trajectory to the steady state I. The simulation is performed with MATLAB.

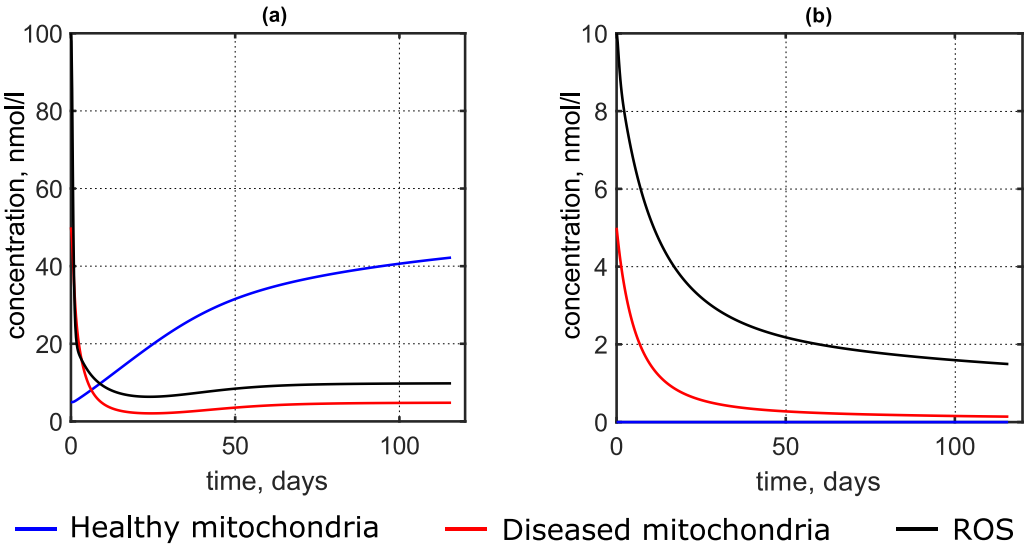

Figure 3.18: (a) The network goes back to the steady state I after the large perturbation that places the network in a bad environment of oxidative stress (the concentration of the ROS is 10 times higher than the steady state value) and with large number of diseased mitochondria (50 nmol/l). The concentration of healthy mitochondria is reduced and equal 5 nmol/l. (b) If the initial concentration of healthy mitochondria is equal to zero then the network chooses a trajectory to the steady state II. The simulation is performed with MATLAB.

3.8 Model design summary

The model of the ROS management network includes several subsystems that introduce the special features. In the basis of the model there is a principle of the ROS-induced mitochondrial aging that includes two forms of mitochondria (healthy and diseased). The damage of a mitochondrion is activated by the ROS. Diseased mitochondria activate the generation of additional ROS. To provide an adequate antioxidant response the model uses Keap1-Nrf2 complex to control the antioxidant concentration.

Diseased mitochondria jeopardize a cell and become a reason of an oxidative stress and lack of ATP. A cell has two mechanisms to regulate the concentration of healthy mitochondria: mitophagy and mitochondria recovery. The first process takes place with a consumption of the protein p62. The second one is activated using the protein Nf-κB.

It has been shown that the rate of a mitochondrial recovery should not be fixed but sensitive to the ROS concentration. If the mitochondria recovery is too intensive then the large pool of healthy mitochondria might be accumulated. A sudden and intensive oxidative stress may initiate the damage of this pool producing the high concentration of impaired mitochondria that amplifies an existing oxidative stress. Thus, to regulate the recovery process the protein DJ-1 is used as the ROS sensor.

The model IV might be considered as a base one that implements main features of the ROS management, describing both ROS effects and a cell reaction to the oxidative stress. Moreover, the inclusion of the protein DJ-1 allows to use this model for investigation both in neurodegenerative diseases and cancer research.

Summarizing the previous conclusion, several design principles might be identified.

1. *The ROS and mitochondria are mutually affected by each other.*
2. *Mitophagy and antioxidant response are dynamically changing with using a protein complex Keap1-Nrf2.*
3. *The process of mitochondria recovery needs a regulation mechanism.*
4. *The protein DJ-1 is a ROS sensor for mitochondrial recovery.*

Chapter 4

Model dynamics and predictive control

4.1 Control of biological networks

First attempts to bind a control theory and a biological system were done many decades ago starting with the works of french physiologist Claude Bernard [139] and his idea of "milieu intérieur" (inner environment). Bernard proposed the idea that any vital organism should have capabilities to protect an internal equilibrium independently of the changes in an external environment. The idea is very closed to the definition of homeostasis that is described as a property of a system to perform an active regulation of a certain variable to keep its value nearly constant. The next significant step was done by american physiologist Walter Cannon [100] who expanded Bernard's concept of homeostasis using the practical examples of steady states for glucose concentration and a body temperature. In 1948 Norbert Wiener published his famous book "Cybernetics: Or Control and Communication in the Animal and the Machine" [140] where he discussed different aspects of self-regulating mechanisms, neuroscience and artificial intelligence as well as introduced the term "cybernetics".

Nonetheless, the problem of application of a control theory onto biological systems and networks has emerged only in the recent years [74, 75, 141] and achieved some significant results in the field of a biomedical control.

One of the good examples is the application of control theory to improve cardiac assist devices (CAD). CAD are electromechanical devices ensuring a proper blood circulation in a patient body in case of a partial of a full heart dysfunction. The control theory might be applied to define the operation mode of the CAD as a function of a patient state (physical activity, positive or negative stress, etc.). First CAD with the output control were developed and approved in 1998 [142]. However, to set the desired output the device required a manual regulation performed by a patient. The recently developed CAD include a real-time monitoring of a physical and an emotional strain as well as an realization of the predictive control principle [143, 144].

Another important application of the control theory is a development of the device to control glucose level for patients with the diabetes of type 1. Such a device includes a glucose sensor, which monitors the current glucose level. An integrated pump performs an automatic injection of insulin using the data provided by the glucose sensor. To make a decision about a dosage of insulin the sensor uses an algorithm of nonlinear control [145].

At the same time it is still rather difficult to create a control device, which might be physically incorporated into a biological network. There are number of problems: micro and nano dimensions of the components of biological networks, the necessity to eliminate the rejection of an alien substance for a body, an incorporation of the power supply to feed a controller. Nevertheless, there were some attempts to create control devices to drive biological systems from inside [146]. One possible way is the usage of magnetic nanoparticles [147] as the objects that are capable to change internal state of a biological object or a network.

Biological systems and networks often perform a specific function that could be bound to a particular organism state. For example, the immune system is being active when alien substances or organisms are introduced into a human body. In

theory, the immune system should manage with any disease by itself. However, in practice, for many diseases medicines are needed to provide an additional support for the immune system to control a disease development.

Thus, the problem of control of biological systems or networks is of high importance. Moreover, the control theory is not necessary used to develop a strategy of positive system dynamics. In some cases, it can be useful to make a system dead. The most typical example is a cancer cell when it is desirable rather to kill a cell then to save it.

Finally, when speaking about the system control two classes of problems are raised: how to control a system to maintain a homeostatic behavior and how to control a system to switch it from one state to another (for example, from a diseased state to a healthy one).

4.2 Principles of model control

Independently of the area from where a model comes (chemistry, biology, physics) it is always possible to apply a generalized approach to the problem of the model control. First of all it is necessary to define model outputs, i.e., the variables of a model that have to follow some reference signal (constant or variable). For the second step one needs to define the control variables that are used to provide the desired model output dynamics. For instance, the temperature of a reactor might be controlled to maintain a reactor output inside a given range.

A control procedure might be carried out in a continuous or a discrete manner. An example of a discrete control is a thermostat that is activated only if an environmental temperature exceeds a certain temperature limit. There is no feedback loop and error measurement. Once the temperature goes back to the limit value, a thermostat is switched off.

Another example is a climate control unit that uses the continuous control principle to change dynamically an air flow intensity and a temperature. A user sets certain temperature value as a set point. A built-in sensor reads the environmental

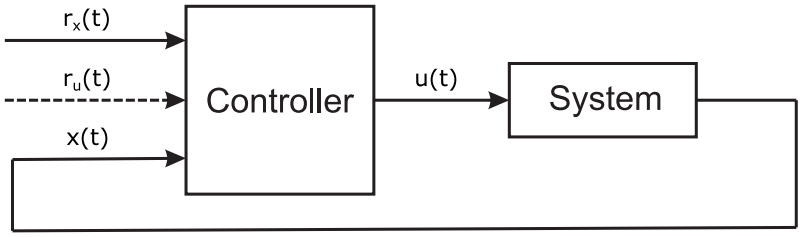

Figure 4.1: Both a system output signal $x(t)$ and a reference signal $r_x(t)$ are delivered to a controller input. A controller performs the signals comparison and provides a driving signal $u(t)$ to a system input. Optionally, a controller can put restrictions to the driving signal $u(t)$ using a separate reference signal $r_u(t)$.

temperature and compares it with a set point. In case of any deviations a sensor provides a differential signal to change a temperature and an air flow intensity to minimize the difference between actual and set points. As a rule, all control signals are generated by a special device (controller). For computer models it is possible to create a virtual controller that performs the same functions as its physical analog. A schematic representation of the control process is shown in Fig. 4.1.

As a rule, most devices, machines, and industries use the programmable logic controller (PLC) as a controlling unit [148]. PLC could be programmed to perform specific actions as a reaction to environmental changes.

The process control approach is used for three types of processes: discrete, continuous and batch. In biology both discrete (a cell division) and continuous (dynamic concentration changing) processes could be met.

4.3 Optimal control theory

When a system output is a simple (e.g., linear) function of a control variable, then, as a rule, there is a unique value for a control variable to maintain the target value of a system output. However, in practice, in complex systems such dependence might be a function of several variables, be nonlinear or unknown. In this case, there might be several solutions that provide the desired value for a system output. If a user states auxiliary restrictions for the values of controlled variables the problem

of seeking control solution turns into the optimal control problem. Thus, besides a system output, a reference signal and a controller output there is an additional restriction that is usually presented in the form of a cost function. During the seeking of a solution of the optimal control problem a cost function should be minimized or maximized. The control variables values that better optimizes a cost function is assumed to be an optimal solution. As a rule, optimal control problems have nonlinear nature and do not have an analytical solution.

One can consider a dynamic system, which is described by a set of ODE

$$\dot{x}(t) = f\left(t, x(t), u(t)\right) \tag{4.1}$$

with an initial condition $x(0) = x_0$, where $x(t)$ is a vector of system's variables, $u(t)$ is a vector of control variables and $t \in [0, \infty)$

To carry out a successful control of the object (4.1) it is necessary to fulfill two conditions:

$$\begin{aligned} \lim_{t\to\infty} \|x(t) - r_x(t)\| = 0, \\ \lim_{t\to\infty} \|u(t) - r_u(t)\| = 0, \end{aligned} \tag{4.2}$$

where $r_x(t)$ is a vector of the reference signals for a model output and $r_u(t)$ is an optional vector of the reference signals for the control variables. In practice, the vector $r_u(t)$ is set only in the case when there is an requirement for the temporal dynamic of the control variables. More often, there are some boundary conditions for the value of $u(t)$ according to the nature of control variables. For example, if a control variable corresponds to a concentration then $r_u(t)$ should be non-negative.

To make an estimation of the control efficiency a cost function is set:

$$F_0 = F_0\left(x(t), u(t)\right). \tag{4.3}$$

For example, if there is a task to find an optimal way for a car driving, then a cost function might represent the total fuel consumption or time that is needed to cover

some predefined distance or be a combination of several targets. A cost function might include both discreet and continuous parts.

Any problem of optimal control requires a seeking of such a vector of functions $u(t)$ that provides the satisfaction of the conditions (4.2), meets its own boundary conditions and minimizes (or maximizes) the cost function (4.3)

Unfortunately ODE-model (4.1) could not be a good candidate for seeking the optimal control solution. The main reason is the fact that this model is always an approximation and could not take into account all possible features of a described system. Moreover, there might be unpredictable changes in the state of an original system. Finally, it leads to a disagreement between the real and predicted trajectories. To improve the situation one could consider predictive model instead:

$$\dot{\bar{x}}(\tau) = \bar{f}\left(\tau, \bar{x}(\tau), \bar{u}(\tau)\right) \tag{4.4}$$

with an initial condition $\bar{x}(\tau = t) = x(t)$.

The predictive model (4.4) in every moment of time $\tau = t$ is initialized by a real system state. It means that independently of any external variation and changing of original system, the model (4.4) provides better results then the model (4.1), which is initialized by the system state only at the moment of time $t = 0$.

Using the predictive model (4.4) it is possible to build the prediction of the system trajectory for time range $\tau \in [t, t + T_p]$ where $T_p > 0$. It is obvious that the smaller value of T_p the more precise estimation is. The variable T_p is known as a prediction horizon.

The fact that the initialization of the predictive model is done at every simulation time step simplifies this model as it has to predict a system trajectory for a very small time range. Sometimes it is even possible to use a linearization of the model (4.1) as a predictive model.

Several possibilities for prediction strategies might be considered.

- **One-time prediction**. Let the predictive model has the prediction horizon $T_p = \infty$. It is evidently that there is some solution $\bar{u}(t)$, which could be

transformed into the solution $u(t)$ for the model (4.1). However, for a large time scale the difference in the models (4.1) and (4.4) provides a considerable error between an estimated and a real trajectory.

- **Mutli-time prediction**. The described situation might be improved if one could implement a prediction procedure for a fixed and finite prediction horizon T_p, i.e. within the time range $[t, t+T_p]$. Found control solutions $u(t)$ are applied for a system and prediction procedure is repeated for the time range $[t+T_p, t+2T_p]$, then for the range $[t+2T_p, t+3T_p]$ and so on. However, this approach has two disadvantages. At first, the control functions $u(t)$ are applied independently for its own time range. Thus, the systems dynamics is considered as a set of independent events that might be wrong for certain systems. At second, the value of T_p might be too large that guarantees the difference between estimated and real behavior of the system.

- **Mutli-time prediction with sample time**. Second disadvantage of the previous strategy defines another strategy for seeking an optima control function $u(t)$. The control function $u(t)$ obtained for the prediction horizon T_p might be applied only for a time range $[t, t+T_s]$ where $T_s \ll T_p$. After a completion of the control step the procedure is repeated with the same value of prediction horizon but initializing the predictive model with a real system state $x(t+T_s)$. This approach should provide better results for a calculation of a control function and is schematically presented in Fig. 4.2.

The procedure of a seeking of the optimal control solution with two time parameters T_s and T_p is used in the method of the model predictive control.

4.4 Model predictive control

In the processing industry one of the most developed and well-known method of model control is the model predictive control (MPC). It has been widely used in chemical and refining industries starting from 1960s. During recent decades this

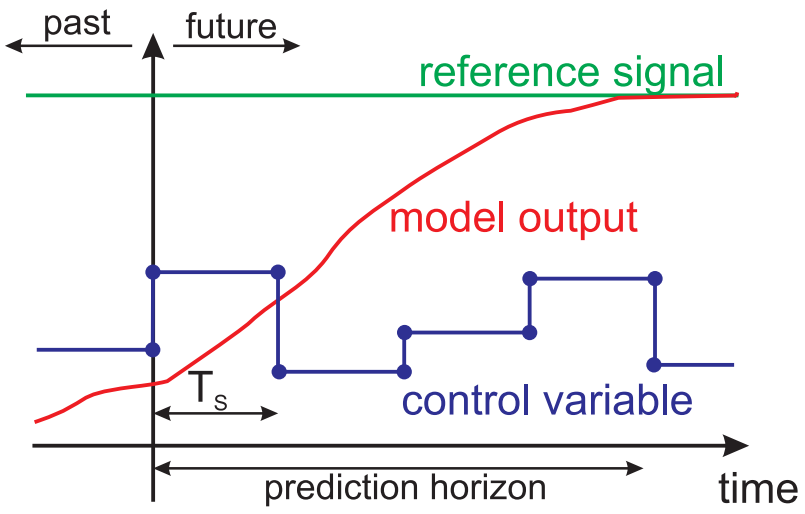

Figure 4.2: A model trajectory (red line) is estimated for prediction horizon time T_p using the current system state as an initial condition. A corresponding driving signal is generated to minimize the difference between a model output and a reference signal (green line). A driving signal (violet line) is applied for the sample time T_s that should be smaller than a prediction horizon. Then the algorithm is repeated starting from the time point $t + T_s$.

method has begun its expansion in other industries. Usually, it is applied to the systems that are describing by models of high level of complexity when other approaches might fail.

Initially, the MPC methods has been introduced using two independent but very similar methods: Dynamics Matrix Control (DMC) developed by specialists of American company Shell Oil [149] and Model Algorithmic Control (MAC) developed in France by specialists of the chemical industry [150].

The main advantages of the MPC method are a relative simplicity of a feedback loop creation as well as the excellent adaptive properties. Last feature allows using the MPC approach together with multidimensional and multicomponent models to provide a real-time optimization taking into account model restrictions and uncertainties in a model definition. Beside, it is possible to consider the change of restrictions during a simulation as well as the change of the state of a system (i.e. a breakdown).

The MPC method includes four main stages:

1. A simple mathematical model of a system is considered. It might be a linearized model in respect to a certain working point. The current state of a system is considered as an initial state. Using these assumptions one could integrate the equations of a simplified model and estimate a trajectory for a model dynamics for some limited time frame (a prediction horizon).

2. To minimize the difference between the reference signal and the estimated value of a model output obtained at the previous stage a certain optimization is carrying out. It takes into account all restrictions for both output values and control variables.

3. An optimal control strategy found at the stage 2 is applied for a time step that should be much smaller than a prediction horizon (a sample time). Model outputs are measured.

4. A prediction horizon is shifted for a time step used during the stage 3 and stages 1 – 3 are repeated.

As a rule, the MPC controller uses a linearized predictive model, however, there is the MPC method, which allows using a nonlinear model – Nonlinear Model Predictive Control (NMPC) [151]. The application of this method is a quite specific since the computational complexity is higher than in the case of ordinary MPC. NMPC is used to be applied to systems with high sampling rates or when a real-time operation is crucial, for example, in automotive industry, aerospace [152].

There is another class of MPC – robust MPC [153, 154] that is used to deal with the systems demonstrating unexpected disturbances or uncertainties. This class of problems could not be solved by the ordinary MPC approach since under a considerable disturbance a system state could be outside the boundary conditions stated for a controller, thus, failing the optimal control algorithm.

However, despite the fact that in most cases a controller could not be sufficiently incorporated inside a biological network, the concept of a model predictive controller can provide the ideas of how to control a particular biological system using an

external impact. It could be an injection of the medicines to change a translation or a degradation rate of particular proteins or a direct injection of antioxidants or the ROS.

Straightforward software realization of the MPC approach might be challenging. However, there are number of commercial software available for building and setting the MPC controller [155]. One possible solution is Simulink environment [156]. The example of the creation of the MPC controller in Simulink is provided in the Appendix C.

4.5 Implementation of model predictive control for the ROS management network

4.5.1 Preliminary notes

The usage of Simulink controller assumes choosing some inputs and outputs for a model. An output signal of a model is compared with a reference signal and a driving signal for model inputs is generated. A model might have one or several inputs and outputs.

For the output of the ROS management network three concentrations might be chosen: the ROS, healthy or diseased mitochondria. Since the concentration of healthy mitochondria reflects the ability of a cell to produce ATP, then it might be a preferable choice for the model output. Indeed, zero concentration of the healthy mitochondria corresponds to the very diseased state of a cell or even death. The reference value of 50 nmol/l taken from the Table (3.4) corresponds to the healthy state.

The model input might be presented by the generation rates of certain proteins. The Simulink controller allows to include any number of inputs to control. However, in practice, the simultaneous change of several inputs might be difficult.

4.5.2 Network relaxation

If a dynamic system is in its stable fixed point and there is no control activated, then any perturbation can put a system onto some trajectory that may lead back to a stable state. In some cases, when the perturbation is too large a system might choose another trajectory. The final point depends on the configuration of the state space (a number of steady states, a topology of the basin of attraction). Normally, a relaxation process takes some time and depends on the trajectory and the distance between the initial point and the final steady state.

In biological networks the relaxation process might mean a recover from disturbed (diseased) state to healthy one. The time factor might be a very important since the uncontrolled relaxation may take a definite time that the system may not have.

As it has been already shown in Fig. 3.16 (page 66) the total time needed for a network recovery might be measured by tens and even hundreds of days.

If this time is too large it may negatively affect on other subsystems and make a harm to a whole organism. To investigate the possible ways of a network recovery acceleration it is possible to introduce a controller into a network and analyze possible solutions (see Fig. 4.3). Three possible strategies might be considered.

Strategy A

The controller utilizes 6 inputs – generation rates of the ROS, AO and the proteins Bcl-xL, Parkin, p62, DJ-1 that are main players in the ROS regulation process. As well, the controller reads one model output (the concentration of healthy mitochondria) and have the reference signal corresponding to the concentration of healthy mitochondria in the healthy state (50 nmol/l). The simulation starts from the diseased steady state II (see Table 3.4) and the controller tries to move the system into the healthy state.

As a result, the controller uses only two inputs: ROS and Bcl-xL (Fig. 4.3 (a1)) to drive the network. The result is not very good. The concentration of healthy

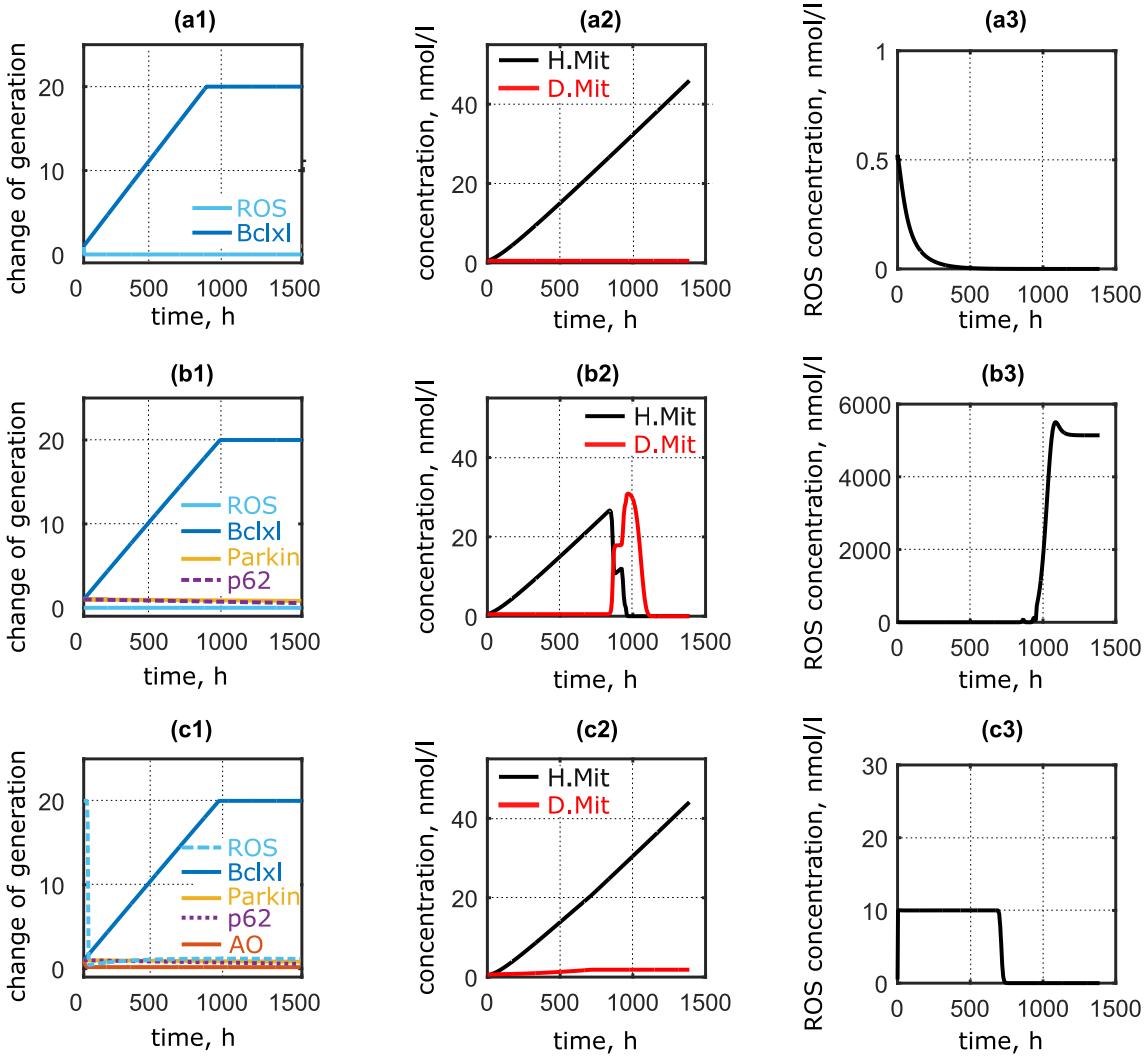

Figure 4.3: A simulation of the network recovery after a strong disturbance to the state that is close to the diseased state of the ROS management network. In (a)-series the model has six controlled inputs for the generation rates: ROS, Bcl-xL, AO, p62, DJ-1, Parkin and one output signal. In (b)-series one model output is added (impaired mitochondria). In (c)-series the third model output is added (the ROS). The first strategy (a) is not effective since the controller manages to change only the concentration of healthy mitochondria. The second strategy (b) demonstrates an unexpected collapse of the network against a background of a strong oxidative stress. The third strategy (c) demonstrates the best result allowing to effectively control three model outputs. The dynamics of the controlled network relaxation is better than the one of the uncontrolled relaxation (Fig. 3.16). The simulation is performed with Simulink.

mitochondria increases (Fig. 4.3 (a2)), however, the concentration of both impaired mitochondria and the ROS stays near zero value (Fig. 4.3 (a3)). It means that the regulatory network does not work properly: there should be a certain balance between non-zero concentrations of the healthy and impaired mitochondria as well as the ROS. On the other hand, as it has been discussed in previous chapters, a cell needs non-zero concentration of ROS to perform certain specific functions. The current simulation results can be explained after the analysis of the strategy proposed by the controller. Indeed, it includes maximum allowed increase of Bcl-xL generation, that maximizes the recovery process, and almost complete suppression of the ROS synthesis. These two actions definitely helps to increase the concentration of healthy mitochondria. However, all other important components have near zero concentrations. It means that all subsystems of the antioxidant response stay inactivated. Therefore, after the controller is switched off the network is not ready to work in the healthy state conditions.

Strategy B

The controller utilizes the same 6 inputs but 2 model outputs. In addition, the concentration of diseased mitochondria is added as an output, as well as a new reference signal that corresponds to the concentration of diseased mitochondria in healthy state (5 nmol/l). In this scenario the controller utilizes more inputs (ROS, Bcl-xL, Parkin and p62) to control the network (Fig. 4.3 (b1)). It helps to control both the concentration of the healthy and diseased mitochondria. However, the network does not demonstrate a proper behavior. After the accumulation of healthy mitochondria (Fig. 4.3 (b2)) the network suddenly collapses against a background of a strong oxidative stress (Fig. 4.3 (b3)). Thus, a usage of two model outputs is still not enough to effectively control the network relaxation process.

Strategy C

The controller utilizes the same 6 inputs but 3 model outputs. In addition, the concentration of the ROS is added as an output, as well as a new reference signal that corresponds to the concentration of the ROS in the healthy state (10 nmol/l). In this scenario the controller uses almost all available model inputs (Fig. 4.3 (c1)) trying to control three model outputs. Apparently, this control strategy is better than the previous ones. After 600 hours of simulation the concentrations of the ROS and diseased mitochondria are close to the target values (Fig. 4.3 (c2) and (c3)), as well as the concentration of the healthy mitochondria is large enough. If to compare with the results of uncontrolled relaxation (Fig. 3.16), one can find that a controlled approach demonstrates a faster dynamics of the network relaxation. If the controller is not switched off after 600 hours then one can observe the ROS concentration collapse, since further increasing of Bcl-xL synthesis suppresses the synthesis of diseased mitochondria, which are essential sources of the ROS. At the same time the ROS degradation is not affected. The combination of these two processes gives the decreasing of the ROS concentration.

Conclusion

The strategy of the controlled relaxation of the ROS management network includes an intensive control of the protein Bcl-xL generation. This provides a quick enough accumulation of healthy mitochondria. The drawback of the strategy is a slow accumulation of impaired mitochondria and the ROS. This factor does not allow to provide a proper functioning of the antioxidant response. The best result of the controlled network relaxation is achieved when the controller drives three model outputs (ROS, healthy mitochondria and impaired mitochondria).

4.5.3 Network controllable death

The model of the ROS management network demonstrates a very large basin of attraction for the stable steady state. Since there is a very little chance to exactly

calculate the basin (because of a dimension of the system) then it is hardly possible to define a minimum necessary disturbance that could make the model to leave its steady state. On the other hand, such situation might be observed in case of a cancer cell that demonstrates an impressive viability. One possible way to kill a cancer cell is to cause a strong oxidative stress.

To find the possible ways of killing a cell one may consider the healthy ROS management network and then to use a controller to switch it to the diseased state with zero (or about zero) concentration of healthy mitochondria. Indeed, a very small concentration of healthy mitochondria directly leads to the lack of ATP and, as a result, to the corresponding negative processes in a cell: a decrease in the intracellular pH, a start of harmful enzymatic processes, a fragmentation of the nucleus, a cell death [157].

There are three possible scenarios of the controlled cell death via significant reduction of the concentration of healthy mitochondria (Fig. 4.4).

Strategy A

The controller can use nine inputs to drive a model. They are the generation rates of seven proteins Bcl-xL, IKK, Keap1, Nrf2, p62, DJ-1, Parkin, the ROS and antioxidants. As an output the concentration of healthy mitochondria is used. The reference signal is a constant value corresponding to the zero concentration of healthy mitochondria. As a result of the simulation the controller utilizes only three model inputs (Fig. 4.4 (a1)). All other inputs remain are not set in motion by the controller and, hence, are not shown. The effective and rather fast decrease of the concentration of healthy mitochondria (Fig. 4.4 (a2)) is guaranteed by a sharp increase of the ROS synthesis (up to 20-fold increase that is a maximum value set for the controller) and simultaneous cut of the generation of AO and Bcl-xL. The cut of Bcl-xL completely suppresses the mitochondria recovery process. The combination of above conditions creates a very strong oxidative stress (Fig. 4.4 (a3)) that quickly kills a cell.

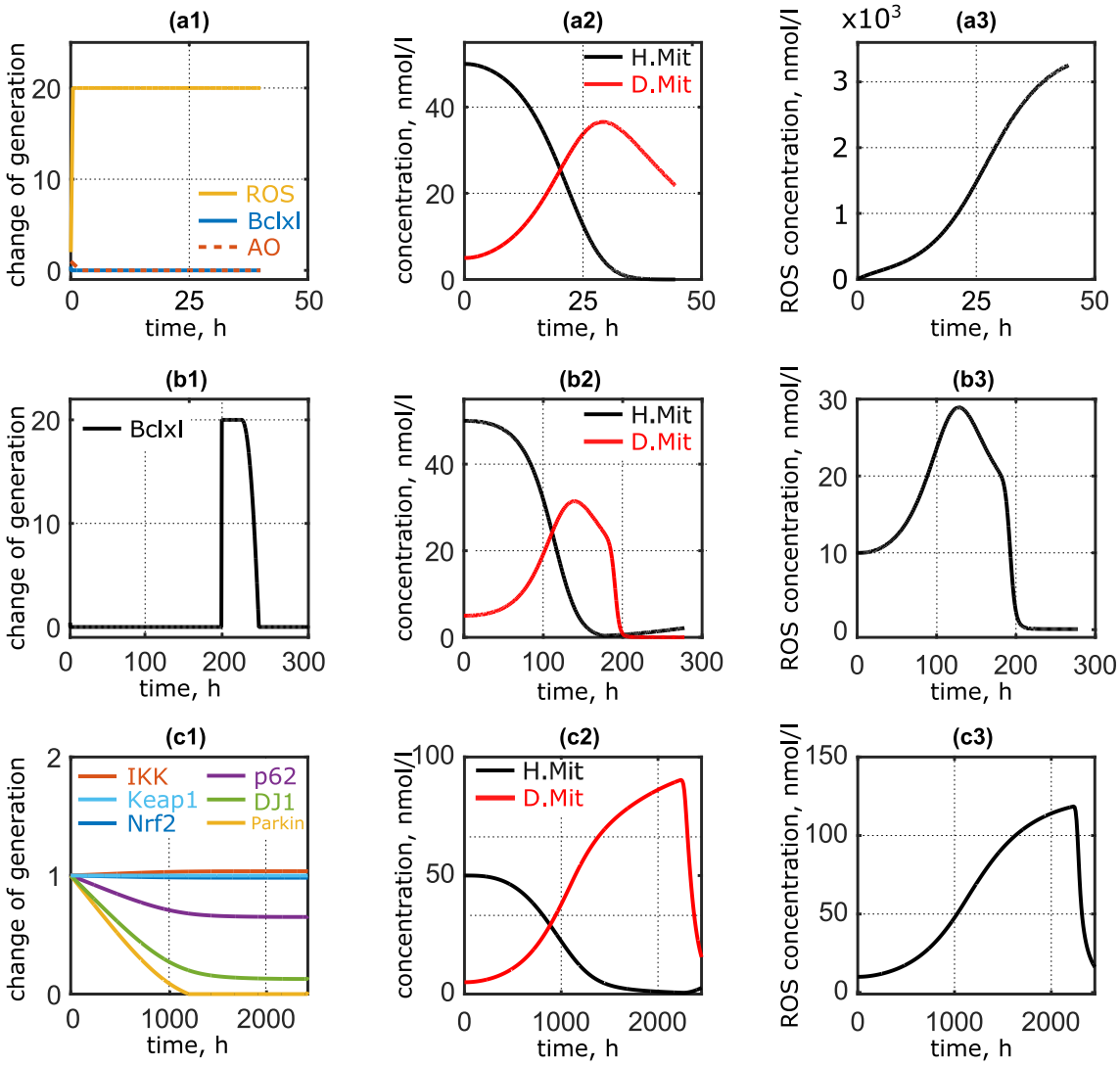

Figure 4.4: A simulation of the network death via significant reducing the concentration of healthy mitochondria. In (a)-series the model has nine controlled inputs for the generation rates: ROS, Bcl-xL, AO, IKK, Keap1, Nrf2, p62, DJ-1, Parkin. Only three inputs are driven by the controller during the simulation: ROS, Bcl-xL and AO (a1). The concentration of healthy mitochondria significantly reduces (a2) against the background of a very strong oxidative stress (a3). In (b)-series there is no control for the ROS and AO generation. Only one input for Bcl-xL (b1) is controlled, all other inputs remains inactive. The time needed for a significant reducing of the concentration of healthy mitochondria is twice larger than in the (a)-series. There is no strong oxidative stress. In (c)-series the control of Bcl-xL generation is switched off. All remaining inputs take part in the control process (c1). The time for the reducing of the concentration of healthy mitochondria is increased significantly (b2) against the background of a strong oxidative stress (c3). The simulation is performed with Simulink.

Strategy B

In this simulation series the controller can use only seven inputs. It is not able to regulate the ROS and antioxidant generation anymore. The model output and the reference signal remain the same. The controller chooses the protein Bcl-xL as a main player (Fig. 4.4 (b1)), leaving all other inputs inactive. To reduce the concentration of healthy mitochondria the controller cut the mitochondria recovery process by a suppressing the generation of Bcl-xL. As a result there is no strong oxidative stress (Fig. 4.4 (b3)). This strategy is not so effective as a previous one and requires double time to kill a cell (Fig. 4.4 (b2)). The Figure 4.4 (a1) also demonstrates a feature of using the Simulink controller. When the concentration of healthy mitochondria reaches its reference value, the controller increases the generation of the protein Bcl-xL up to the maximal permitted value and then decreases it again to zero value. Thus, the controller prevents a further decrease of the concentration into the region of negative values. Therefore, the appearance of this peak is caused by the realization of the MPC algorithm. Finally, it means that any strategy proposed by the controller should be additionally verified to eliminate the artificial dynamics created by the features of the MPC algorithm realization.

Strategy C

In this simulation series the controller utilizes only 6 inputs. The regulation of the protein Bcl-xL is switched off. The model output and the reference signal remain the same. In this case the controller utilizes all remaining inputs to reach the reference value (Fig. 4.4 (c1)). It suppresses the generation of Parkin and significantly decreases the generation of p62. This makes mitophagy process slower and leads to the accumulation of diseased mitochondria and corresponding increasing of the ROS concentration providing the conditions for the oxidative stress (Fig. 4.4 (b3)). As well, the controller decreases the generation of DJ-1 violating the antioxidation response. This strategy is not effective (Fig. 4.4 (c3)). To decrease significantly

the concentration of healthy mitochondria it takes 10 times more time than the strategy B does.

Conclusion

According to the obtained results there are two good strategies. The first one is to increase the ROS synthesis and to decrease the AO and the protein Bcl-xL generation. This causes an oxidative stress and cut the antioxidant response. Another way is to suppress the generation of Bcl-xL, thus, significantly reducing the rate of mitochondria recovery. The latter method allows to save diseased mitochondria that generate additional ROS and, thus, amplify the oxidative stress.

4.5.4 Protein knockdown and knockout

In a normal situation a cell generates proteins with some rate. In case of disease or mutation one can observe a downregulation or an upreguation of proteins. As a result of a downregulation an expression of a protein is reduced (knockdown) or even completely stopped (knockout). In case of an upregulation the expression of a protein increases significantly. Both scenarios might have different effects for a cell functioning. A very good example is a violation of the protein DJ-1 generation. A downregulation of DJ-1 decreases the antioxidant defense of a cell [158], high ratio of an inactive form of DJ-1 has been observed in patients with PD and Alzheimer's disease [159]. On the other hand, an upregulation of DJ-1 might improve a mitochondrial function [160].

In case of a downregulation of DJ-1 a cell experiences either lack of healthy mitochondria or their complete absence (Fig. 4.5). The latter might mean a cell death.

In case of the DJ-1 knockdown (the generation rate of the protein decreases by the factor of two) the concentration of healthy mitochondria decreases almost twice. The concentration of impaired mitochondria and the ROS increases moder-

ately (Fig. 4.5 (a,b)). Despite the absence of a strong oxidative stress the network is in danger. The lack of healthy mitochondria means an insufficient ATP generation.

In case of the DJ-1 knockout (the generation of the protein is stopped completely) the concentration of healthy mitochondria reaches a zero value. At the same time, the network experiences a severe oxidative stress. Both factors leave a very small probability for a cell survival.

Using the MPC controller it is possible to discover the strategies to maintain the healthy mitochondria concentration in the cases of a downregulation of the DJ-1. To define possible strategies more accurately the controller measures only one model output (the concentration of healthy mitochondria) and consequently look through the different model inputs, analyzing only one input per a simulation.

The DJ-1 knockdown

In case of DJ-1 knockdown the concentration of healthy mitochondria decreases almost twice. This means that a cell experiences a lack of ATP. The MPC controller tries to find such dynamics of the controlled input to maintain the concentration of healthy mitochondria close to the steady state level as long as possible. The results of the simulation are presented in Fig. 4.6.

The protein Nrf2. A control of Nrf2 (Fig. 4.6 (a)) does not help to maintain the concentration of healthy mitochondria close to the steady state level. A minor decrease of the ROS concentration is observed.

The protein Bcl-xL. A usage of Bcl-xL as the model input gives an excellent result for the concentration of healthy mitochondria (Fig. 4.6 (b)). It is not a surprise since this protein regulates the process of the mitochondria recovery. The oscillatory nature of the signal generated by the controller is explained by the fact that the target concentration should be in the region of the steady state value. Therefore the concentration of healthy mitochondria also oscillates.

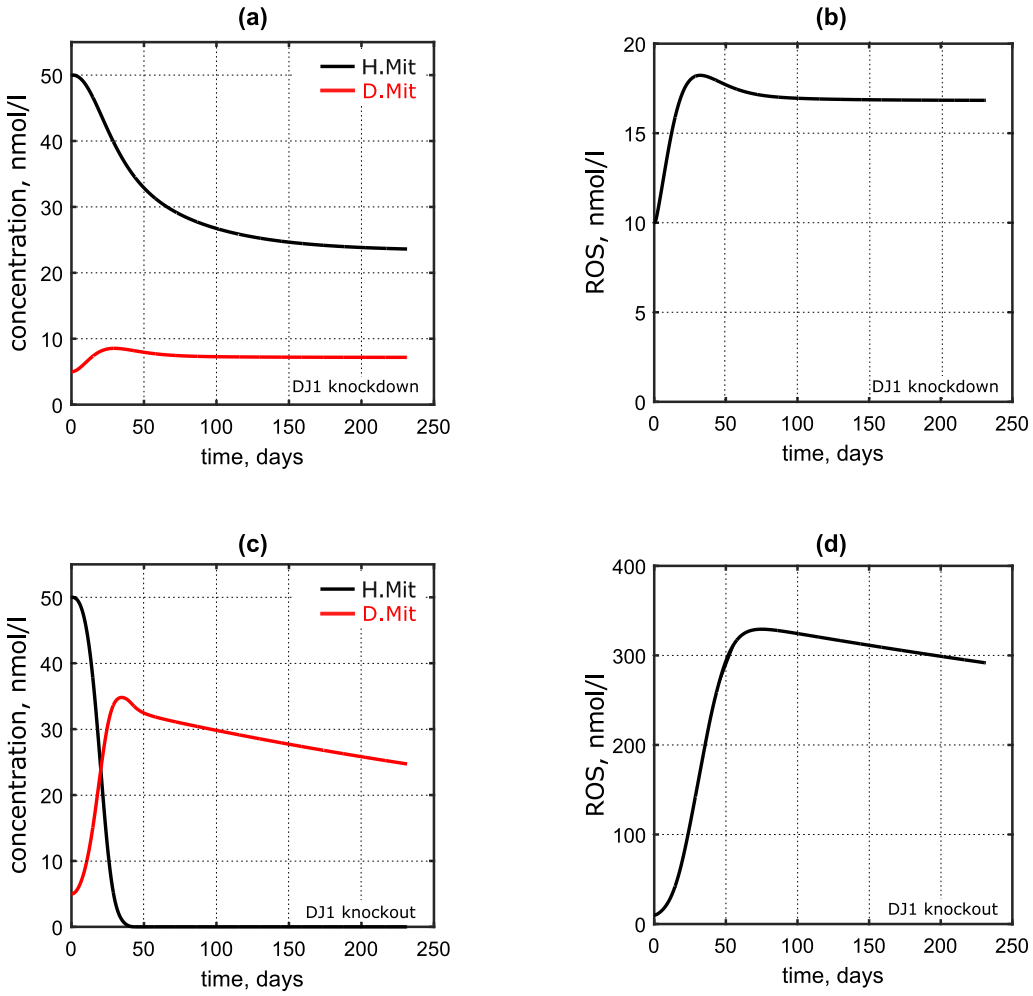

Figure 4.5: The downregulation of the protein DJ-1 accompanies neurodegenerative diseases. It can have two forms: a knockdown and a knockout. The knockdown corresponds to a partial decrease of a protein generation, the knockout is a full suppression of a protein generation. In case of the DJ-1 knockout (a double decrease of the generation rate) the concentration of healthy mitochondria significantly decreases (a), whilst the ROS concentration has a moderate increase (b). When the network experiences the DJ-1 knockout (the generation is completely cut), the concentration of healthy mitochondria drops to zero (c) against a background of a strong oxidative stress (d). The simulation is performed with Simulink.

The antioxidants. It might be expected that the AO control should help a cell to maintain the healthy mitochondria concentration. However, it only helps with the decrease of the ROS (Fig. 4.6 (c)). The concentration of diseased mitochondria is even bigger. Therefore, after the controller stops the AO regulation the accumulated impaired mitochondria might cause a strong oxidative stress.

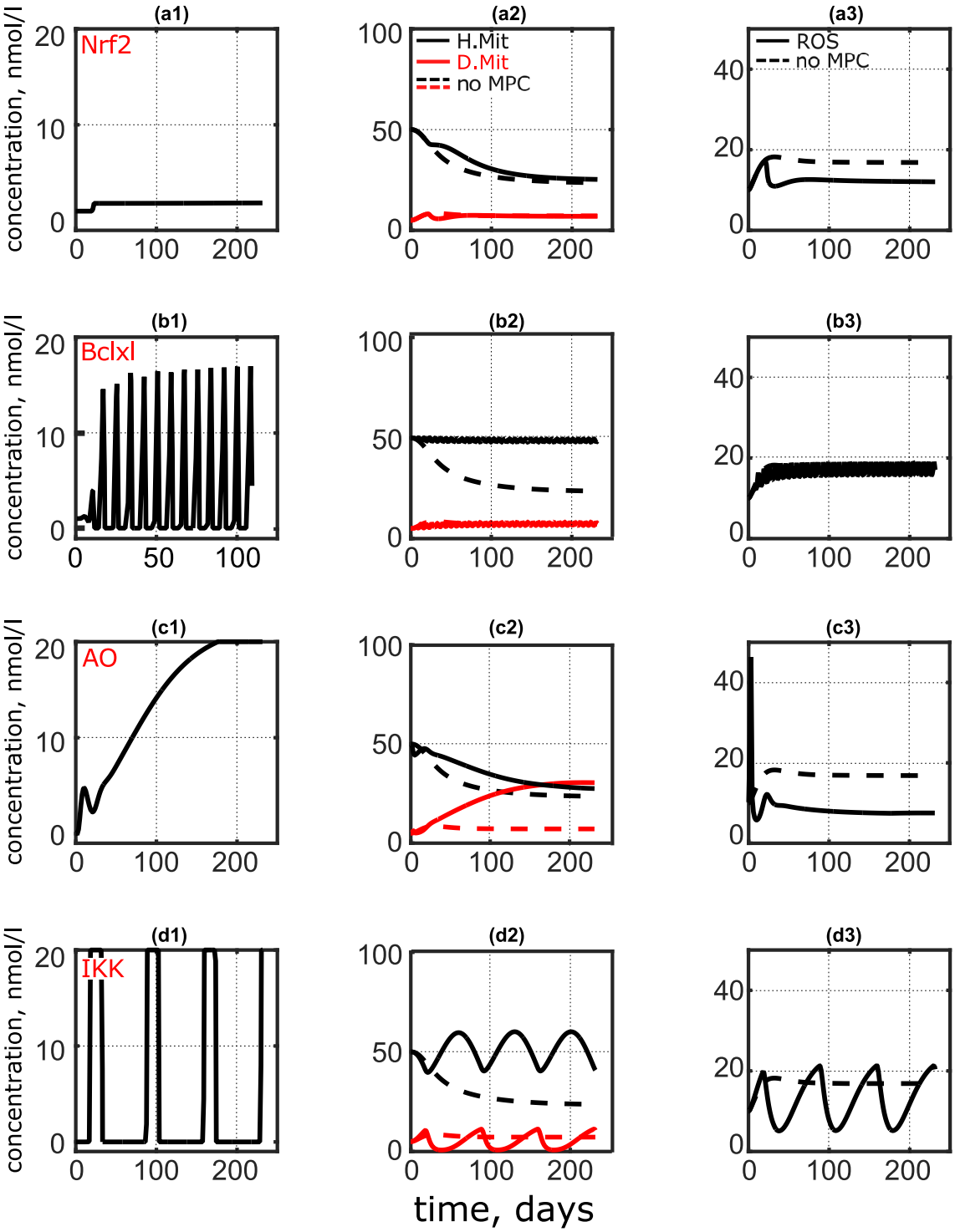

Figure 4.6: The controlled knockdown of the protein DJ-1. Every simulation set (from a to h) corresponds to a controlled generation change of one of the following species: the proteins Nrf2, Bcl-xL, IKK(Nf-κB), Parkin, p62, Keap1, the AO and the ROS. The controller uses single model output (healthy mitochondria) and one model input. In every set 1 – a dynamics of the controlled input calculated by the controller, 2 – a comparison of the mitochondria dynamics with/without controller, 3 – a comparison of the ROS dynamics with/without controller. See the next page for a continuation. The simulation is performed with Simulink.

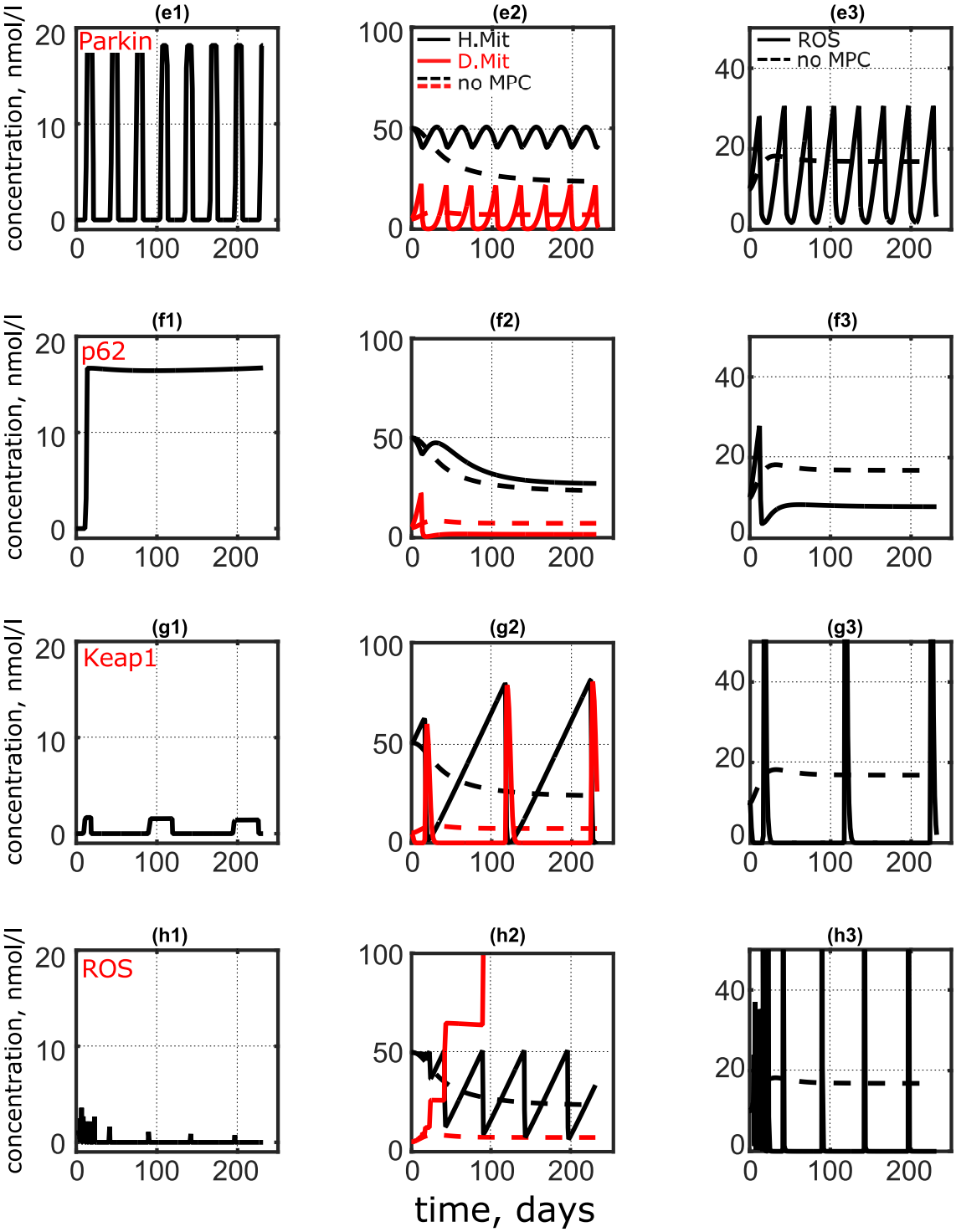

Figure 4.6: The controlled knockdown of the protein DJ-1 (cont.).

The protein IKK. Being the regulator of both Nf-κB and p62 the protein IKK can regulates simultaneously the processes of the mitophagy and mitochondria recovery. This double action should help to control three species: the ROS, healthy and impaired mitochondria (Fig. 4.6 (d)). Using a set of the pulses that drive the IKK generation, the controller manages to maintain the concentration of healthy mitochondria and reduce the overall oxidative stress via a periodical suppression of the ROS and impaired mitochondria concentrations.

The protein Parkin. Using this model input the controller again demonstrates a good efficiency that could be comparable with the usage of the protein IKK (Fig. 4.6 (e)). The only significant difference is the bigger periodic oxidative stress, caused by a higher amplitude of the oscillation of the ROS concentration.

The protein p62. This control strategy helps to decrease the ROS and impaired mitochondria concentrations (Fig. 4.6 (f)). However, the healthy mitochondria concentration (and, hence, ATP generation) is not changed by the controller.

The protein Keap1. The control of this protein makes the network unbalanced when the concentrations are changed in a high range (Fig. 4.6 (g)).

ROS. A change of the ROS synthesis can hardly affect the concentration of healthy mitochondria. Indeed, like the case of the Keap1 control, the network becomes unstable and experiences a sharp ROS oscillation and the increase of the impaired mitochondria concentration (Fig. 4.6 (h)).

The DJ-1 knockdown

In case of complete suppression of the DJ-1 generation a cell might quickly die because of lack of the energy, since the healthy mitochondria concentration goes to zero. It is hardly possible that any control strategy might prevent a cell death. However, it might postpone the time when the healthy mitochondria concentration

reaches zero. The simulation is carrying out within the same conditions as for the case of the DJ-1 knockdown. The results of the simulation are presented on Fig. 4.7.

Surprisingly, almost any control strategy helps to prolong a cell life. The only exception is a regulation via Keap1 (Fig. 4.7 (g)) when the ROS management network loses healthy mitochondria quickly and at the same time experiences a sharp pulse of oxidative stress. There are three good candidates to maintain the concentration of healthy mitochondria in the network experiencing DJ-1 knockdown

- **The protein Bcl-xL.** Using this protein as a controlled input gives good results for the healthy mitochondria concentration (Fig. 4.7 (b)). The network lives, at least, 10 times longer than in the case without a participation of the controller. However, after a short decrease, the ROS concentration quickly rises. As well, impaired mitochondria concentration gradually increases with time.

- **The protein IKK.** This control strategy acts slightly better (Fig. 4.7 (d)). It demonstrates the comparable results for healthy mitochondria and the ROS concentrations. The strategy manages to keep a relatively low level of impaired mitochondria.

- **The protein Parkin.** This approach demonstrates the best result for all three species. It manages the concentrations of both healthy and impaired mitochondria as well as restrains the increase of the ROS during some time.

However, almost all strategies do not manage to deal with an increasing oxidative stress. Only using the antioxidants allows to contain the ROS concentration below the level defined by the simulation without the control.

4.6 Model control conclusion

An application of the control theory to the models of biological systems and networks allows to find control strategies that can demonstrate unusual system's behavior.

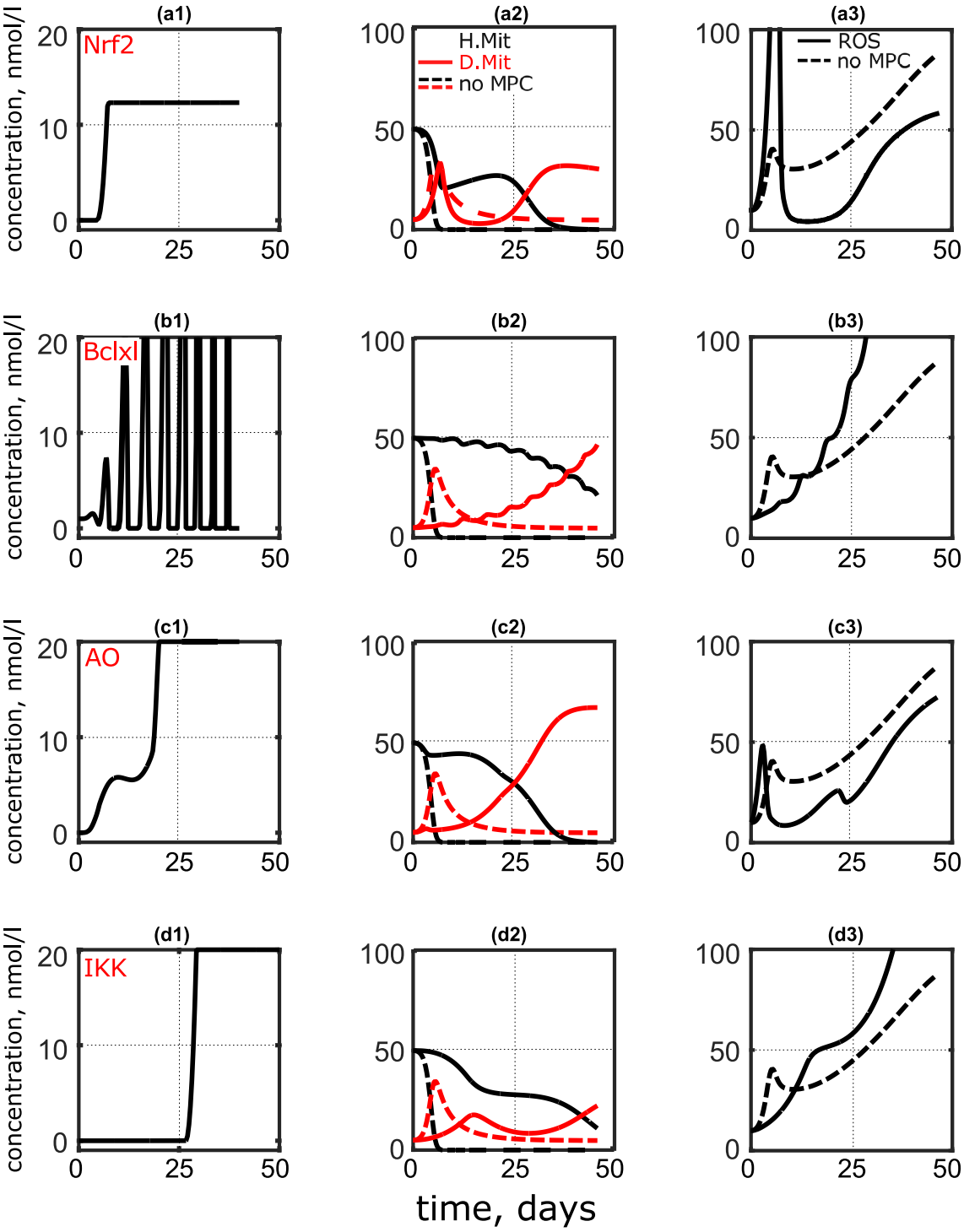

Figure 4.7: The controlled knockout of the protein DJ-1. Every simulation set (from a to h) corresponds to a controlled generation change of one of the following species: the proteins Nrf2, Bcl-xL, IKK(Nf-κB), Parkin, p62, Keap1, the AO and the ROS. The controller uses single model output (healthy mitochondria) and one model input. In every set 1 – a dynamics of the controlled input calculated by the controller, 2 – a comparison of the mitochondria dynamics with/without controller, 3 – a comparison of the ROS dynamics with/without controller. See the next page for a continuation. The simulation is performed with Simulink.

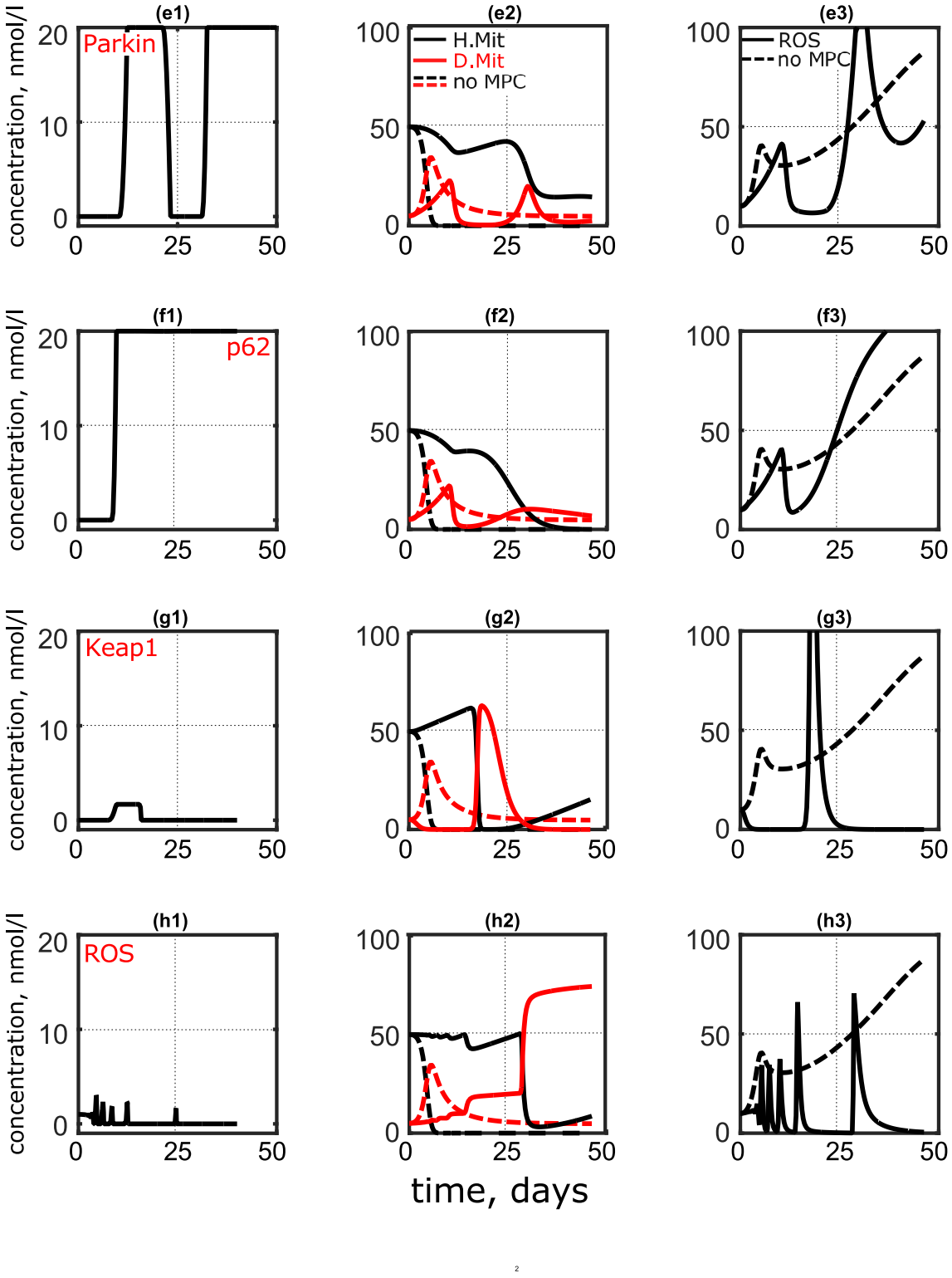

Figure 4.7: The controlled knockout of the protein DJ-1 (cont.).

When starting from a particular initial condition a system chooses a trajectory that describes its evolution. A usage of the MPC controller allows to create the additional trajectories that can not be chosen by an uncontrolled system.

An effective usage of the MPC controller requires a proper choice of model inputs and outputs. By changing the inputs in time the MPC controller tries to provide the best agreement of model outputs and the reference signals. The reference signal might either stay constant or change in time.

A practical implementation of an obtained driving signal strongly depends on its characteristic. In case of biological systems it can correspond to a medicine injection or any other external impact (radiation, chemical influence) and, therefore, can hardly contain sharp gradients or quick oscillations.

For the particular problem of the DJ-1 downregulation the MPC approach demonstrates good results. It generates some strategies for maintaining the healthy mitochondria concentration in case of the DJ-1 knockdown and knockout. The best results are demonstrated when the controller regulates the proteins Bcl-xL, IKK and Parkin. These proteins are responsible for the processes of mitophagy and impaired mitochondria recovery and, in practice, might be targeted using an external impacts (for Bcl-xL [161, 162], for IKK [163, 164], for Parkin [165, 166]).

A usage of the MPC approach for the analysis of bioregulatory networks might be a powerful tool, that can provide the suggestions for the treatment and the killing strategies (cancer research).

Chapter 5

Outlook and perspectives

5.1 Model limitations

The built model is the base one for the description of the functionality of the ROS management network. As it has been already said it includes several necessary blocks that provide the links between the mitochondrial dynamics, changing of the ROS concentration and antioxidant response. However, further usage and development of the model assume the elimination of several limitations.

ATP

The model does not contain ATP, ADP and water – the essential species that are directly used for the energy generation in a cell. Hence, the value of ATP concentration might be used for the estimation of the energy potential of a cell, where zero value of ATP might mean a cell death. At the moment, the concentration of healthy mitochondria is used as an estimator of a cell well-being. These new elements allow to consider the processes that take part in the electron transport chain. Another reason is the fact that a cell might have non-mitochondrial sources of energy [167].

Translation and transcription processes

To describe a protein generation the model uses an abstract source with an unlimited capacity and a certain rate constant. In the reality there are two stages: transcription (the process of copy of DNA into messenger RNA) and translation (usage of mRNA to generate a protein). Absence of these stages simplifies the description of a protein generation but decreases the number of parameters and, hence, complicates a validation procedure. Indeed, the documented values of a protein transcription and translation (if any) should be applied with a caution since the reaction of a protein synthesis is neither a translation reaction nor transcription one.

Protein complexes and oxidation

The model uses three protein complexes (Keap1, Nrf2 and DJ-1) that might be oxidized. The oxidation process is described via an existence of two forms of a protein: active and inactive. In reality, a protein oxidation might involve more stages and states. For example, the oxidation of the DJ-1 includes four stages [159].

Cytochrome c

The cytochrome complex (cyt c) is a protein that associated with the inner membrane of the mitochondrion. It takes part in the transfer of electrons between complexes III and IV of the ETC. This protein is also involved in the initiation of apoptosis that starts upon release of cytochrome c to the cytoplasm. Accumulation of the certain concentration of the cytochrome c might be considered as an indicator of a cell death. In the current model of the ROS management network a cell death is only connected with loosing the bigger part of the healthy mitochondria.

Other components

Several other species and interactions also might be added to the model: Pink1, that affects mitochondrial functioning [168, 169] and activates Parkin [170, 171]; the process of both Nrf2 and p62 ubiquitination by Keap1 that marks them for

a degradation [172]; mRNA layer for the proteins; more detailed layer of NFkB signalling [173, 174].

5.2 The route to personalized medicine

5.2.1 Detailed model of the ROS management network

Taking into account above-mentioned recommendations, it is possible to build the detailed model of the ROS management network that can be used to open new possibilities for the prediction and the explanation of the existing phenomena in the ROS management network (see Appendix D.1).

The detailed model would have a higher level of complexity than the model V that would complicate the validation process as well as any concerning computational task. This work could be done in the frame of a separate project and can take considerable time. The creation and analysis of the detailed model is an important step towards to a simulation of the personalizes medicine cases, when the model can be adapted to a unique case of a particular patient. This approach would allow to created personalized treatment strategies.

5.2.2 Stress adaptation

A properly working ROS management system should demonstrate the stress adaptation behavior [175], that appears in stabilization of key parameters (the mitochondria and ROS concentrations) irrespective of the oxidative stress fluctuations. Indeed, the model V is able to demonstrate such behavior (Fig. 5.1). During this simulation the model experiences a periodic changes of the ROS synthesis with a maximum coefficient of amplification of 20. Under these condition the model demonstrates an interesting phenomena: a homeostatic adaptation to the stress. The healthy mitochondria concentration reaches the local minimum and then shows the ascending trend and reaches about 80% level of the initial concentration. The number of impaired mitochondria becomes even smaller in comparison with no-stress dynam-

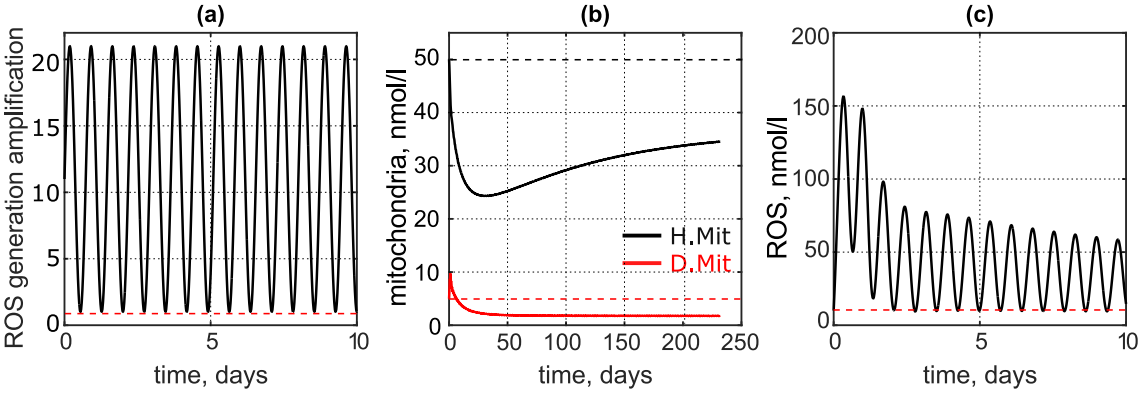

Figure 5.1: The model experiences a periodic stress caused by a harmonic oscillation of the ROS synthesis (a). Despite of the strong periodic oxidative stress (c) the model demonstrates good stress adaptation for both healthy and impaired mitochondria (b). The frequency of the stress oscillation (about 8 hours between turning points) is chosen to correspond to a usual daily cycle. The dashed lines show the components steady state level before the stress application. The simulation is performed with Simulink.

ics. All these processes occur against a background of a strong oscillatory oxidative stress. In practice, this process might be compared with an oscillatory oxidative stress caused by the intracellular calcium oscillations [176] in some specific neuronal groups affected by PD. This process might be counterbalanced by the excessive ATP generation [177]. Finally, if the stress conditions last long enough a cell might die [178, 179].

The model V does not demonstrate the full picture of this phenomenon. It manages with an oxidative stress but does not show the collapse if the stress remains. The detailed model of the ROS management network with included ATP generation is expected to demonstrate this feature. Moreover, it would let to check some strategies to treat this state or, at least, to postpone the system collapse. For example, recent research has shown the anticorrelation of drinking coffee and PD development [180]. It is known that the caffeine has a beneficial effect on the Nrf2 dynamics [181]. Hence, the increased generation of Nrf2 in the detailed model might decrease the oxidative stress and normalize ATP generation.

As well, the detailed model would allow to be consistent with experimental observations showing how the increased extracellular transport of α-synuclein (corre-

sponds to the increased concentration of α-synuclein in detailed model) may induce ROS production [182].

5.2.3 Personalized medicine

Above, the system fragility under the stress has been identified. The most probable explanation is the perturbation in p62 generation. This protein plays the essential role in the impaired mitochondria management. It is known that the dynamics of p62 is associated with PD. First, a synthesis of p62 is regulated by DJ-1 that can be downregulated by PD [183]. Second, p62 may be isolated by alfa-synuclein, that can be also related to PD [61]. Strictly speaking, these two processes can be related to a couple of different patients having PD with different mechanisms of development. And the treatment should not be the same in both cases. This idea is closely related to the quickly developing area of the personalized medicine (precision medicine, P4) [184, 185]. The main idea of this approach is to consider each disease case individually taking into account the features of the particular patient: DNA, mutations, a disease risk assessment. It has been discovered recently that the patients can respond differently to the same medicine. For example, about 40% of the patients with asthma, depression and diabetes are non-sensitive to a standard medicines [186]. The same parameter for cancer and neurodegenerative diseases can reach the value of 70%.

Another advantage of the personalized medicine is a decrease of adverse drug reactions (ADR). Many ADRs happen because of the variations in genes concerning the drug-metabolized enzymes, for example, cytochrome P450 [187]. An application of the test results for a detection of cytochrome P450 variations can significantly improve the ADR statistics [188]. Another good example is a management of the warfarin that is used to prevent the blood clots. Typically, the dosage for an individual patient varies by trial and error method. It can be dangerous for the patient causing either an excessive bleeding or further development of the blood clots. The

usage of genotyping before the application of warfarine treatment allows to define the dosage more precisely [189].

To simulate different pathophysiological scenarios for the personalized medicine the detailed model of the ROS management might be used. The current model V does not have some essential components to make this kind of simulation (VDAC, alfa-synuclein).

5.3 Adaptive model predictive control

In the previous chapters it has been shown that the application of the MPC method allows to develop different strategies for the system control. However, the fact that the MPC approach uses a linearized model, poses some limitations on its application. For example, the standard MPC controller can fail when simulating a system with a strong non-linearity or when system characteristics are changing dramatically in time. In these cases the adaptive MPC might be used [190]. This approach allows to adapt a predictive model according to the changing operating conditions. The simplest realization of the adaptive MPC is a predictive model with evolving in time parameters.

The application of the adaptive MPC method is a natural development of the control approach introduced in the current thesis. It allows to take into account a various stochastic processes that take part in genes expression [191] or when considering the chemical reactions in a single cell [192].

5.4 Further concept development

The transfer from the model V to the detailed model corresponds to the changes in the model components and the pathways between them. To get the model onto a new level more global changes might be introduced as pointed out below.

Paracellular level

The current model of the ROS management network describes only the intracellular ROS regulation. The next step would be to consider the ROS management for the cell population. Thus, some net effects may occurs. There are a number of the extracellular processes that may play an important role: a proliferation, a differentiation, a mutation, death as well as a transformation from healthy to impaired state. The ROS concentration can also depend on a cell density.

Extension of the ROS status

The current model is focused on a cell damaging role of the ROS. To consider both sides of the coin it might be possible to consider also the beneficial function of the ROS. For example, ROS take part in the immune response, in a regulation of a cell proliferation, in a management of injuries [193].

Interaction with other cellular processes

The ROS interact with cell cycle via several pathways including, the alteration of mitochondrial functioning, the oxidation of various proteins, the modulation of the activity of transcription factors (e.g. Nrf2), the crosstalk with other signalling molecules (e.g., nitric oxide – NO).

Currently, the crosstalk between ROS and NO is not taken into account. In reality, they are connected in several ways, e.g., chemical reactions [194] or ROS-induced modulation [195]. In its turn, NO modulates ROS synthesis, e.g., via the superoxide release [196]. When produced, nitric oxide modulates the expression of cell cycle regulatory proteins [197] and, thus, plays one of the central roles in the modulation the development of cancer [198]. At high concentrations, NO induces apoptosis and inhibits cancer growth, whereas at physiological concentrations, NO favors cell proliferation and tumor growth [199]. An appropriate intervening with NO may be used in a cancer therapy [199, 200]. The incorporation of NO into the

model of ROS management network could help to understand the contradictory role of NO and face the model towards cancer research.

Chapter 6

Conclusion

In the current thesis the design principles of the ROS management network were investigated. They concerned special roles of mitophagy, mitochondrial recovery, Keap1-Nrf2 complex and the protein DJ-1 in the ROS regulation. These principles were used for the step-by-step development of the models of ROS management network with an increasing complexity ("domino" approach). Every subsequent model was compared to previous one and introduced a new property of the ROS management. One of the most important conclusions is the fact that the recovery of impaired mitochondria should be correlated to the change of the intracellular ROS concentration. "Domino" methodology allowed both to investigate the roles of different regulatory mechanisms in the ROS management and to justify their inclusion in the model. As a result, the core model of the ROS management network was developed. It includes a basic but sufficient number of the ROS regulatory mechanisms and components.

The parameters of the model of the ROS management network were estimated using experimental data. To do that the resolution of the core model was increased to correspond to experimental conditions. The validated model demonstrated two real and positive steady states: one stable and one unstable. These states can correspond to a healthy and disease (oxidative stress) state of the regulatory network. It has been shown that there is a trajectory from disease to healthy state, however it

requires non-zero values for the concentrations of healthy and disease mitochondria as well as ROS. It means, for example, that the efficiency of the ROS regulation significantly decreases if the ROS concentration is too small.

A computer simulation can provide useful information on system dynamics for different environmental conditions. However, research in the field of biology and medicine implies not only a passive monitoring but also an active control. To simulate different control strategies the model of ROS management network was exported to Simulink environment where the MPC controller was set up. It has been shown that there can be different control strategies that allow to maintain the proper ROS management even in the presence of negative environmental factors. In the current thesis the cases of knockdown and knockout of the protein DJ-1 were considered. At the same time the question of controlled system death was investigated. It has been shown that even a healthy network could be switched to a very diseased state by means of dynamic control of the network inputs. These strategies can be developed further in the field of cancer research.

Using a "domino" approach, the developed core model of the ROS managements system could be augmented with additional modules and subsystems that will allow to use it for other research. Thus, the concept of a very detailed ROS management model was proposed. It includes new elements (ATP, CytC, alpha-synuclein, etc.) and higher resolution for the proteins synthesis and interaction. The detailed model can be an extremely useful for the simulation of eustress and distress behaviour as well as to be used for the personalized medicine research.

At present, the developed model does not claim the full description of the ROS management processes. However, it clearly states how research in the field of neurodegenerative diseases may benefit from design principles studies performed with the help of dynamic modelling and application of control strategies.

Appendices

Appendix A

Models description and parametrization

A.1 The model II

The model II includes the following variables (Table A.1) and is described by the ODE system (A.1).

$$\begin{cases} \frac{dx_1}{dt} = Sp_{11} - p_{21}x_1x_3, \\ \frac{dx_2}{dt} = p_{21}x_1x_3 - p_{111}x_2x_5x_6, \\ \frac{dx_3}{dt} = Sp_{31}x_2 - p_{61}x_3x_4, \\ \frac{dx_4}{dt} = -p_{51}x_4 + Sp_{41}x_9, \\ \frac{dx_5}{dt} = Sp_{71} - p_{81}x_5 - p_{111}x_2x_5x_6, \\ \frac{dx_6}{dt} = -p_{101}x_6 - p_{111}x_2x_5x_6 + Sp_{91}x_9 \\ \frac{dx_7}{dt} = p_{122}\left(S_{keap1} - x_7\right) - p_{121}x_3x_7, \\ \frac{dx_9}{dt} = p_{132}\left(S_{nrf2} - x_9\right) - p_{131}x_7x_9 \end{cases} \tag{A.1}$$

The system (A.1) does not include the variables x_8 and x_{10}. Since the concentrations for the total pool of both Keap1 and Nrf2 remain constant, then these variables can

Variable	**Reactant**	**St.state, nmol/l**
x_1	healthy mitochondria	50
x_2	impaired mitochondria	5
x_3	ROS	10
x_4	antioxidants	200
x_5	protein Parkin	50
x_6	protein p62	50
x_7	protein Keap1 (active)	200
x_8	protein Keap1 (inactive)	20
x_9	protein Nrf2 (active)	20
x_{10}	protein Nrf2 (inactive)	200

Table A.1: The variables for the model II. The values of the steady state are obtained after the model parametrization.

be excluded from the ODE system using the substitutions $x_8 = S_{keap1} - x_7$ and $x_{10} = S_{keap1} - x_9$. The values of the non-kinetic parameters and rate constants included in the system (A.1) are provided in the Table A.2 and Table A.3 correspondingly.

Non-rate constant	**Value, nmol/l**
S_{keap1}, total Keap1 concentration	220
S_{nrf2}, total Nrf2 concentration	220
S, abstract source	1

Table A.2: The values of non-kinetic parameters for the model II.

Rate constant	**Value**
p_{11}, mitochondria synthesis	$1.25 \times 10^{-3} s^{-1}$
p_{21}, mitochondria aging	$2.5 \times 10^{-6} s^{-1} \left(\frac{nmol}{l}\right)^{-1}$
p_{31}, ROS synthesis	$4 \times 10^{-5} s^{-1} \left(\frac{nmol}{l}\right)^{-1}$
p_{41}, antioxidant synthesis	$10^{-4} s^{-1} \left(\frac{nmol}{l}\right)^{-1}$
p_{51}, antioxidant degradation	$10^{-5} s^{-1}$
p_{61}, ROS degradation	$10^{-7} s^{-1} \left(\frac{nmol}{l}\right)^{-1}$
p_{71}, Parkin synthesis	$1.75 \times 10^{-3} s^{-1}$
p_{81}, Parkin degradation	$10^{-5} s^{-1}$
p_{91}, p62 synthesis	$8.75 \times 10^{-5} s^{-1} \left(\frac{nmol}{l}\right)^{-1}$
p_{101}, p62 degradation	$10^{-5} s^{-1}$
p_{111}, mitophagy	$10^{-7} s^{-1} \left(\frac{nmol}{l}\right)^{-2}$
p_{121}, Keap1 inactivation	$10^{-4} s^{-1} \left(\frac{nmol}{l}\right)^{-1}$
p_{122}, Keap1 inactivation	$10^{-2} s^{-1}$
p_{131}, Nrf2 activation	$5 \times 10^{-4} s^{-1} \left(\frac{nmol}{l}\right)^{-1}$
p_{132}, Nrf2 activation	$10^{-2} s^{-1}$

Table A.3: The values of rate constants for the model II.

A.2 The model III

The model III includes the following variables (Table A.4) and is described by the ODE system (A.2). The system (A.2) does not include the variables x_8 and x_10. Since the concentrations for the total pool of both Keap1 and Nrf2 remain constant, then these variables might be excluded from the ODE system using the substitutions $x_8 = S_{keap1} - x_7$ and $x_{10} = S_{keap1} - x_9$. The values of the non-kinetic parameters and rate constants included in the system (A.2) are provided in the Table A.6 and Table A.5 correspondingly.

Variable	**Reactant**	**St.state, nmol/l**
x_1	healthy mitochondria	50
x_2	impaired mitochondria	5
x_3	ROS	10
x_4	antioxidants	200
x_5	protein Parkin	50
x_6	protein p62	50
x_7	protein Keap1 (active)	200
x_8	protein Keap1 (inactive)	20
x_9	protein Nrf2 (active)	20
x_{10}	protein Nrf2 (inactive)	200
x_{11}	protein Nf-κB	100
x_{12}	protein Bcl-xL	100

Table A.4: The variables for the model III. The values of the steady state are obtained after the model parametrization.

$$
\begin{cases}
\frac{dx_1}{dt} = Sp_{11} - p_{21}x_1x_3 + p_{181}x_2x_{12}, \\
\frac{dx_2}{dt} = p_{21}x_1x_3 - p_{111}x_2x_5x_6 - p_{181}x_2x_{12}, \\
\frac{dx_3}{dt} = Sp_{31}x_2 - p_{61}x_3x_4, \\
\frac{dx_4}{dt} = -p_{51}x_4 + Sp_{41}x_9, \\
\frac{dx_5}{dt} = Sp_{71} - p_{81}x_5 - p_{111}x_2x_5x_6, \\
\frac{dx_6}{dt} = -p_{101}x_6 - p_{111}x_2x_5x_6 + Sp_{91}x_9x_{11} \\
\frac{dx_7}{dt} = p_{122}\left(S_{keap1} - x_7\right) - p_{121}x_3x_7, \\
\frac{dx_9}{dt} = p_{132}\left(S_{nrf2} - x_9\right) - p_{131}x_7x_9, \\
\frac{dx_{11}}{dt} = Sp_{141}x_5 - p_{151}x_{11}, \\
\frac{dx_{12}}{dt} = Sp_{161}x_{11} - p_{171}x_{12}
\end{cases}
\tag{A.2}
$$

Rate constant	**Value**
p_{11}, mitochondria synthesis	$1.25 \times 10^{-3} s^{-1}$
p_{21}, mitochondria aging	$2.5 \times 10^{-6} s^{-1} \left(\frac{nmol}{l}\right)^{-1}$
p_{31}, ROS synthesis	$4 \times 10^{-5} s^{-1} \left(\frac{nmol}{l}\right)^{-1}$
p_{41}, antioxidant synthesis	$10^{-4} s^{-1} \left(\frac{nmol}{l}\right)^{-1}$
p_{51}, antioxidant degradation	$10^{-5} s^{-1}$
p_{61}, ROS degradation	$10^{-7} s^{-1} \left(\frac{nmol}{l}\right)^{-1}$
p_{71}, Parkin synthesis	$1.75 \times 10^{-3} s^{-1}$
p_{81}, Parkin degradation	$10^{-5} s^{-1}$
p_{91}, p62 synthesis	$8.75 \times 10^{-5} s^{-1} \left(\frac{nmol}{l}\right)^{-2}$
p_{101}, p62 degradation	$10^{-5} s^{-1}$
p_{111}, mitophagy	$10^{-7} s^{-1} \left(\frac{nmol}{l}\right)^{-2}$
p_{121}, Keap1 inactivation	$10^{-4} s^{-1} \left(\frac{nmol}{l}\right)^{-1}$
p_{122}, Keap1 activation	$10^{-2} s^{-1}$
p_{131}, Nrf2 inactivation	$5 \times 10^{-4} s^{-1} \left(\frac{nmol}{l}\right)^{-1}$
p_{132}, Nrf2 activation	$10^{-2} s^{-1}$
p_{141}, Nf-κB synthesis	$2 \times 10^{-5} s^{-1} \left(\frac{nmol}{l}\right)^{-1}$
p_{151}, Nf-κB degradation	$10^{-5} s^{-1}$
p_{161}, Bcl-xL synthesis	$10^{-5} s^{-1} \left(\frac{nmol}{l}\right)^{-1}$
p_{171}, Bcl-xL degradation	$10^{-5} s^{-1}$
p_{181}, Bcl-xL mitochondrial repair	$9.75 \times 10^{-5} s^{-1} \left(\frac{nmol}{l}\right)^{-1}$

Table A.5: The values of rate constants for the model III

Non-rate constant	**Value, nmol/l**
S_{keap1}, total Keap1 concentration	220
S_{nrf2}, total Nrf2 concentration	220
S, abstract source	1

Table A.6: The values of non-kinetic parameters for the model III.

Variable	**Reactant**	**St.state, nmol/l**
x_1	healthy mitochondria	50
x_2	impaired mitochondria	5
x_3	ROS	10
x_4	antioxidants	200
x_5	protein Parkin	50
x_6	protein p62	50
x_7	protein Keap1 (active)	200
x_8	protein Keap1 (inactive)	20
x_9	protein Nrf2 (active)	20
x_{10}	protein Nrf2 (inactive)	200
x_{11}	protein Nf-κB	100
x_{12}	protein Bcl-xL	100
x_{13}	protein DJ-1 (active)	20
x_{14}	protein DJ-1 (inactive)	200

Table A.7: The variables for the model IV. The values of the steady state are obtained after the model parametrization.

A.3 The model IV

The model IV includes the following variables (Table A.7) and is described by the ODE system (A.3). The system (A.3) does not include the variables x_8 and x_{10}. Since the concentrations for the total pool of the proteins Keap1, Nrf2 and DJ-1 remain constant, then these variables might be excluded from the ODE system using the substitutions $x_8 = S_{keap1} - x_7$, $x_{10} = S_{keap1} - x_9$ and $x_{14} = S_{dj1} - x_{13}$. The values of the non-kinetic parameters and rate constants included in the system (A.3) are provided in the Table A.8 and Table A.9 correspondingly.

$$
\begin{cases}
\dfrac{dx_1}{dt} = Sp_{11} - p_{21}x_1x_3 + p_{181}x_2x_{12}, \\
\dfrac{dx_2}{dt} = p_{21}x_1x_3 - p_{111}x_2x_5x_6 - p_{181}x_2x_{12}, \\
\dfrac{dx_3}{dt} = Sp_{31}x_2 - p_{61}x_3x_4, \\
\dfrac{dx_4}{dt} = -p_{51}x_4 + Sp_{41}x_9, \\
\dfrac{dx_5}{dt} = Sp_{71} - p_{81}x_5 - p_{111}x_2x_5x_6, \\
\dfrac{dx_6}{dt} = -p_{101}x_6 - p_{111}x_2x_5x_6 + Sp_{91}x_9x_{11} \\
\dfrac{dx_7}{dt} = p_{122}\left(S_{keap1} - x_7\right) - p_{121}x_3x_7, \\
\dfrac{dx_9}{dt} = p_{132}\left(S_{nrf2} - x_9\right) - \dfrac{p_{131}x_7x_9}{p_{133} + x_{13}}, \\
\dfrac{dx_{11}}{dt} = Sp_{141}x_5 - \dfrac{p_{152}x_{11}}{p_{151} + x_{13}}, \\
\dfrac{dx_{12}}{dt} = Sp_{161}x_{11} - p_{171}x_{12}, \\
\dfrac{dx_{13}}{dt} = -p_{201}x_{13} + p_{191}x_3\left(S_{dj1} - x_{13}\right)
\end{cases}
\tag{A.3}
$$

Non-rate constant	**Value, nmol/l**
S_{keap1}, total Keap1 concentration	220
S_{nrf2}, total Nrf2 concentration	220
S_{dj1}, total DJ-1 concentration	220
S, abstract source	1
p_{133}, Nrf2 activation	5
p_{151}, NF-κB degradation	10

Table A.8: The values of non-kinetic parameters for the model IV.

Rate constant	**Value**
p_{11}, mitochondria synthesis	$1.25 \times 10^{-3} s^{-1}$
p_{21}, mitochondria aging	$2.5 \times 10^{-6} s^{-1} \left(\frac{nmol}{l}\right)^{-1}$
p_{31}, ROS synthesis	$4 \times 10^{-5} s^{-1} \left(\frac{nmol}{l}\right)^{-1}$
p_{41}, antioxidant synthesis	$10^{-4} s^{-1} \left(\frac{nmol}{l}\right)^{-1}$
p_{51}, antioxidant degradation	$10^{-5} s^{-1}$
p_{61}, ROS degradation	$10^{-7} s^{-1} \left(\frac{nmol}{l}\right)^{-1}$
p_{71}, Parkin synthesis	$1.75 \times 10^{-3} s^{-1}$
p_{81}, Parkin degradation	$10^{-5} s^{-1}$
p_{91}, p62 synthesis	$8.75 \times 10^{-5} s^{-1} \left(\frac{nmol}{l}\right)^{-2}$
p_{101}, p62 degradation	$10^{-5} s^{-1}$
p_{111}, mitophagy	$10^{-7} s^{-1} \left(\frac{nmol}{l}\right)^{-2}$
p_{121}, Keap1 inactivation	$10^{-4} s^{-1} \left(\frac{nmol}{l}\right)^{-1}$
p_{122}, Keap1 activation	$10^{-2} s^{-1}$
p_{131}, Nrf2 inactivation	$5 \times 10^{-4} s^{-1}$
p_{132}, Nrf2 activation	$10^{-2} s^{-1}$
p_{141}, Nf-κB synthesis	$2 \times 10^{-5} s^{-1} \left(\frac{nmol}{l}\right)^{-1}$
p_{152}, Nf-κB degradation	$10^{-5} s^{-1}$
p_{161}, Bcl-xL synthesis	$10^{-5} s^{-1} \left(\frac{nmol}{l}\right)^{-1}$
p_{171}, Bcl-xL degradation	$10^{-5} s^{-1}$
p_{181}, Bcl-xL mitochondrial repair	$9.75 \times 10^{-5} s^{-1} \left(\frac{nmol}{l}\right)^{-1}$
p_{191}, DJ-1 activation	$10^{-4} s^{-1} \left(\frac{nmol}{l}\right)^{-1}$
p_{201}, DJ-1 inactivation	$10^{-2} s^{-1}$

Table A.9: The values of rate constants for the model IV

Appendix B

Model validation and analysis

B.1 Model structure

To perform the procedure of parameters estimation, using the experimental data provided by University of Maastricht, the following changes are introduced into the base model IV.

- The mitochondrial recovery reaction is combined together with the reaction of mitochondrial aging. Instead, the protein Bcl-xL becomes an inhibitor of the reaction of mitochondrial aging.
- The simple reaction of healthy mitochondria synthesis is replaced by more realistic mechanism where the existing healthy mitochondria are used as a substrate for new mitochondria [201]. The mechanism uses Michaelis-Menten kinetics to avoid uncontrolled increase of the concentration of healthy mitochondria.
- Synthesis and degradation reactions are added for the proteins Keap1, Nrf2, DJ-1. It allows to use experimental data to check the results of parameter estimation procedure.
- The subsystem of menadione injection is added to the model. According to the experiment injected menadione is transformed into the internal form that

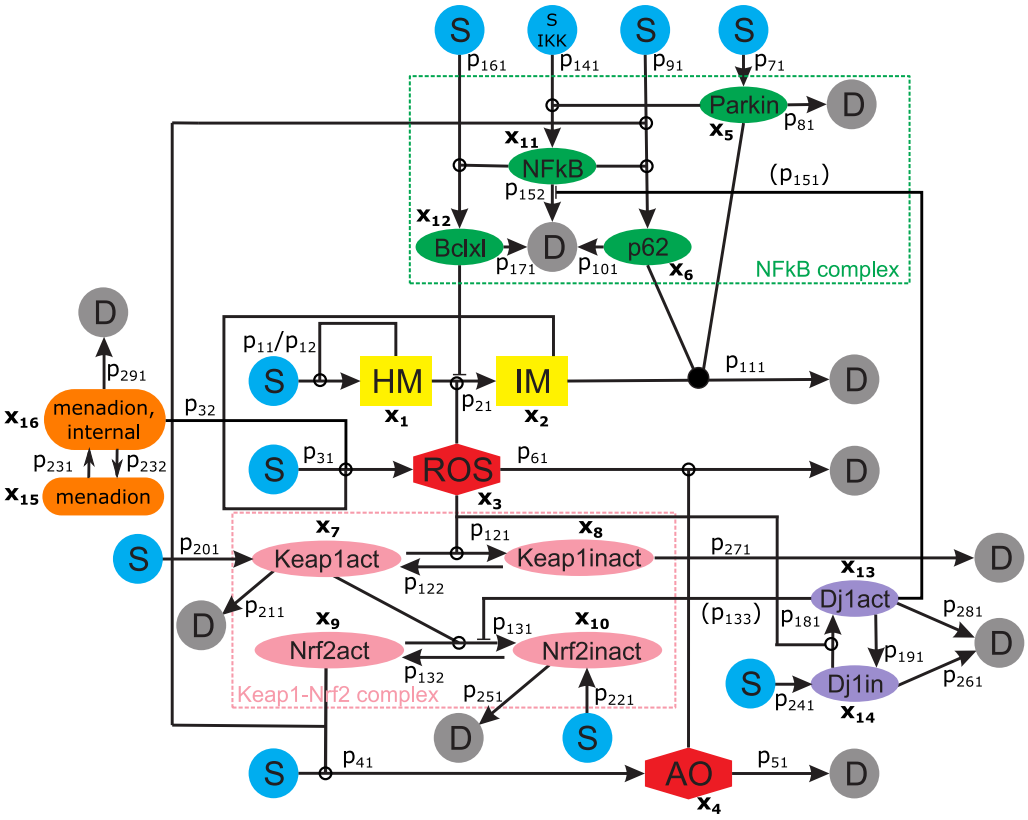

Figure B.1: The model V of the ROS management network that is validated using experimental data provided by University of Maastricht. The non-kinetic parameters (p_{133}) and (p_{151}) allow to avoid an infinite inhibition in the case of zero concentration of the protein DJ-1.

activates the ROS production inside a cell. At the same time the menadion degrades itself [202, 203].

Variable	**Reactant**	**St.state, nmol/l**
x_1	healthy mitochondria	50
x_2	impaired mitochondria	5
x_3	ROS	10
x_4	antioxidants	200
x_5	protein Parkin	50
x_6	protein p62	50
x_7	protein Keap1 (active)	200
x_8	protein Keap1 (inactive)	20
x_9	protein Nrf2 (active)	20
x_{10}	protein Nrf2 (inactive)	200
x_{11}	protein Nf-κB	100
x_{12}	protein Bcl-xL	100
x_{13}	protein DJ-1 (active)	20
x_{14}	protein DJ-1 (inactive)	200
x_{15}	menadion	10^5
x_{16}	menadion (internal)	0

Table B.1: The variables for the model V. The values of the steady state are obtained after the estimation of the model parameters using experimental data. To make simulation without menadion the variable x_{15} should be equal to zero.

B.2 Model parameters

The model V includes the following variables (Table B.1) and is described by the ODE system (B.1). The values of the non-kinetic parameters and rate constants included in the system (B.1) are provided in the Table B.2 and Table B.3 correspondingly.

$$
\begin{cases}
\dfrac{dx_1}{dt} = \dfrac{Sp_{11}x_1}{p_{12}+x_1} - \dfrac{p_{21}x_1x_3}{x_{12}}, \\
\dfrac{dx_2}{dt} = -p_{111}x_2x_5x_6 + \dfrac{p_{21}x_1x_3}{x_{12}}, \\
\dfrac{dx_3}{dt} = Sp_{31}x_2 - p_{61}x_3x_4 + p_{32}x_{16}, \\
\dfrac{dx_4}{dt} = -p_{51}x_4 + Sp_{41}x_9, \\
\dfrac{dx_5}{dt} = Sp_{71} - p_{81}x_5 - p_{111}x_2x_5x_6, \\
\dfrac{dx_6}{dt} = -p_{101}x_6 - p_{111}x_2x_5x_6 + Sp_{91}x_9x_{11}, \\
\dfrac{dx_7}{dt} = Sp_{201} - p_{211}x_7 - p_{121}x_3x_7 + p_{122}x_8, \\
\dfrac{dx_8}{dt} = p_{121}x_3x_7 - p_{122}x_8 - p_{271}x_8, \\
\dfrac{dx_9}{dt} = p_{132}x_{10} - \dfrac{p_{131}x_7x_9}{p_{133}+x_{13}}, \\
\dfrac{dx_{10}}{dt} = Sp_{221} - p_{132}x_{10} - p_{251}x_{10} + \dfrac{p_{131}x_7x_9}{p_{133}+x_{13}}, \\
\dfrac{dx_{11}}{dt} = Sp_{141}x_5 - \dfrac{p_{152}x_{11}}{p_{151}+x_{13}}, \\
\dfrac{dx_{12}}{dt} = Sp_{161}x_{11} - p_{171}x_{12}, \\
\dfrac{dx_{13}}{dt} = -p_{191}x_{13} - p_{281}x_{13} + p_{181}x_3x_{14}, \\
\dfrac{dx_{14}}{dt} = Sp_{241} + p_{191}x_{13} - p_{261}x_{14} - p_{181}x_3x_{14}, \\
\dfrac{dx_{15}}{dt} = -p_{231}x_{15} + p_{232}x_{16}, \\
\dfrac{dx_{16}}{dt} = p_{231}x_{15} - p_{232}x_{16} - p_{291}x_{16}
\end{cases}
\tag{B.1}
$$

Non-rate constant	**Value, nmol/l**
p_{12}, mitochondria generation	1
p_{133}, Nrf2 activation	1
p_{151}, NF-κB degradation	1
S, abstract source	1

Table B.2: The values of non-kinetic parameters for the model V.

The values of model V parameters show a good correspondence to the ranges, defined in the Table 2.1. However, one might notice different time scales for mitochondrial dynamics. The rate constants for the mitophagy and mitochondria aging are inside the previously defined range, but the rate constant for the mitochondrial synthesis is not. The possible explanation here is the fact that the time range for mitochondrial dynamics is defined from the value of mitochondrial turnover, the process that includes many stages, which might have different timescales. In this case the mitochondria synthesis might be a relatively fast process that is followed by slower processes of mitochondrial aging and mitophagy. So the total mitochondria turnover is found out to be a slow process.

Rate constant	**Value, s^{-1}**
p_{11}, mitochondria synthesis	$10^{-5}s^{-1}$
p_{21}, mitochondria aging	$1.96 \times 10^{-6}s^{-1}$
p_{31}, ROS synthesis (1)	$10^{-4}s^{-1}\left(\frac{nmol}{l}\right)^{-1}$
p_{32}, ROS synthesis (2)	$10^{-5}s^{-1}$
p_{41}, antioxidant synthesis	$10^{-4}s^{-1}\left(\frac{nmol}{l}\right)^{-1}$
p_{51}, antioxidant degradation	$10^{-5}s^{-1}$
p_{61}, ROS degradation	$2.5 \times 10^{-7}s^{-1}\left(\frac{nmol}{l}\right)^{-1}$
p_{71}, Parkin synthesis	$10^{-3}s^{-1}$
p_{81}, Parkin degradation	$1.98 \times 10^{-5}s^{-1}$
p_{91}, p62 synthesis	1.25×10^{-6}
p_{101}, p62 degradation	$5 \times 10^{-5}s^{-1}$
p_{111}, mitophagy	$7.8 \times 10^{-10}s^{-1}\left(\frac{nmol}{l}\right)^{-2}$
p_{121}, Keap1 inactivation (1)	$10^{-4}s^{-1}\left(\frac{nmol}{l}\right)^{-1}$
p_{122}, Keap1 inactivation (2)	$10^{-2}s^{-1}$
p_{131}, Nrf2 inactivation (1)	$1.05 \times 10^{-5}s^{-1}$
p_{132}, Nrf2 inactivation (2)	$10^{-5}s^{-1}$
p_{141}, Nf-κB synthesis	$3.6 \times 10^{-7}s^{-1}\left(\frac{nmol}{l}\right)^{-1}$
p_{152}, Nf-κB degradation	$3.8 \times 10^{-6}s^{-1}\left(\frac{nmol}{l}\right)$
p_{161}, Bcl-xL synthesis	$7 \times 10^{-6}s^{-1}\left(\frac{nmol}{l}\right)^{-1}$
p_{171}, Bcl-xL degradation	$7 \times 10^{-6}s^{-1}$
p_{181}, DJ-1 activation	$10^{-5}s^{-1}\left(\frac{nmol}{l}\right)^{-1}$
p_{191}, DJ-1 inactivation	$10^{-3}s^{-1}$
p_{201}, Keap1 synthesis	$5.06 \times 10^{-3}s^{-1}$
p_{211}, Keap1 degradation (act)	$2.3 \times 10^{-5}s^{-1}$
p_{221}, Nrf2 synthesis	$2.4 \times 10^{-3}s^{-1}$
p_{231}, Menadion activation (1)	$2.6 \times 10^{-3}s^{-1}$
p_{232}, Menadion activation (2)	$0.29s^{-1}$
p_{241}, DJ-1 synthesis	$3.3 \times 10^{-3}s^{-1}$
p_{251}, Nrf2 degradation	$1.2 \times 10^{-5}s^{-1}$
p_{261}, DJ-1 degradation (in)	$1.5 \times 10^{-6}s^{-1}$
p_{271}, Keap1 degradation (in)	$2.3 \times 10^{-5}s^{-1}$
p_{281}, DJ-1 degradation (act)	$1.5 \times 10^{-6}s^{-1}$
p_{291}, Menadion degradation	$2.9 \times 10^{-3}s^{-1}$

Table B.3: The values of rate constants for the model V

B.3 Steady state calculation

To find the steady states of the model of the ROS management network it is necessary to solve the following system of algebraic equations:

$$\begin{cases} \dfrac{p_{11}x_1}{p_{12}+x_1} - \dfrac{p_{21}x_1x_3}{x_{12}} = 0, \\ -p_{111}x_2x_5x_6 + \dfrac{p_{21}x_1x_3}{x_{12}} = 0, \\ p_{31}x_2 - p_{61}x_3x_4 + p_{32}x_{16} = 0, \\ -p_{51}x_4 + p_{41}x_9 = 0, \\ p_{71} - p_{81}x_5 - p_{111}x_2x_5x_6 = 0, \\ -p_{101}x_6 - -p_{111}x_2x_5x_6 + p_{91}x_9x11 = 0, \\ p_{201} - p_{211}x_7 - p_{121}x_3x_7 + p_{122}x_8 = 0, \\ p_{121}x_3x_7 - p_{122}p_{61} - p_{271}x_8 = 0, \\ p_{132}x_{10} - \dfrac{p_{131}x_7x_9}{p_{133}+x_{13}} = 0, \\ p_{221} - p_{132}x_{10} - p_{251}x_{10} + \dfrac{p_{131}x_7x_9}{p_{133}+x_{13}} = 0, \\ p_{141}x_5 - \dfrac{p_{152}x_{11}}{p_{151}+x_{13}} = 0, \\ p_{161}x_{11} - p_{171}x_{12} = 0, \\ -p_{191}x_{13} - p_{281}x_{13} + p_{181}x_3x_{14} = 0, \\ p_{241} + p_{191}x_{13} - p_{261}x_{14} - p_{181}x_3x_{14} = 0, \\ -p_{231}x_{15} + p_{232}x_{16} = 0, \\ p_{231}x_{15} - p_{232}x_{16} - p_{291}x_{16} = 0 \end{cases} \tag{B.2}$$

Using an elimination method numerous analytical solutions can be obtained.

Solution 1

$$\begin{cases} x_1 = 0, \\ x_2 = 0, \\ x_3 = 0, \\ x_4 = 0, \\ x_5 = \dfrac{p_{71}}{p_{81}}, \\ x_6 = 0, \\ p_{201} - p_{211}x_7 - p_{121}x_3x_7 + p_{122}x_8 = 0, \\ p_{121}x_3x_7 - p_{122}p_{61} - p_{271}x_8 = 0, \\ \boldsymbol{p_{132}\dfrac{p_{221}}{p_{251}} = 0}, \\ x_{10} = \dfrac{p_{221}}{p_{251}}, \\ p_{141}x_5 - \dfrac{p_{152}x_{11}}{p_{151} + x_{13}} = 0, \\ p_{161}x_{11} - p_{171}x_{12} = 0, \\ -p_{191}x_{13} - p_{281}x_{13} + p_{181}x_3x_{14} = 0, \\ p_{241} + p_{191}x_{13} - p_{261}x_{14} - p_{181}x_3x_{14} = 0, \\ x_{15} = 0, \\ x_{16} = 0 \end{cases} \tag{B.3}$$

The solution (B.3) is unfinished since it leads to an undetermined system of equations [204]. At the same time, in order to get $p_{132}\frac{p_{221}}{p_{251}} = 0$ either p_{132} or p_{221} should have a zero value. This scenario can correspond to the case of a reaction suppression and might require a separate investigation.

Solution 2

$$\begin{cases} x_1 = 0, \\ x_2 = 0, \\ x_3 = 0, \\ x_4 = \dfrac{p_{41}p_{71}p_{91}p_{132}p_{133}p_{141}p_{151}p_{211}p_{221}}{p_{51}p_{81}p_{101}p_{131}p_{152}p_{201}p_{251}}, \\ x_5 = \dfrac{p_{71}}{p_{81}}, \\ x_6 = \dfrac{p_{71}p_{91}p_{132}p_{133}p_{141}p_{151}p_{211}p_{221}}{p_{81}p_{101}p_{131}p_{152}p_{201}p_{251}}, \\ x_7 = \dfrac{p_{201}}{p_{211}}, \\ x_8 = 0, \\ x_9 = \dfrac{p_{132}p_{133}p_{211}p_{221}}{p_{131}p_{201}p_{251}}, \\ x_{10} = \dfrac{p_{221}}{p_{251}}, \\ x_{11} = \dfrac{p_{71}p_{141}p_{151}}{p_{81}p_{152}}, \\ x_{12} = \dfrac{p_{71}p_{141}p_{151}p_{161}}{p_{81}p_{152}p_{171}}, \\ x_{13} = 0, \\ x_{14} = \dfrac{p_{241}}{p_{261}}, \\ x_{15} = 0, \\ x_{16} = 0 \end{cases} \tag{B.4}$$

This solution always exists. Any combination of rate constants gives non-negative and real values for the steady state.

Solution 3

$$\begin{cases} x_1 = 0, \\ x_5 = 0, \\ p_{31}x_2 - p_{61}x_3x_4 + p_{32}x_{16} = 0, \\ -p_{51}x_4 + p_{41}x_9 = 0, \\ \boldsymbol{p_{71} = 0}, \\ -p_{101}x_6 - -p_{111}x_2x_5x_6 + p_{91}x_9x11 = 0, \\ p_{201} - p_{211}x_7 - p_{121}x_3x_7 + p_{122}x_8 = 0, \\ p_{121}x_3x_7 - p_{122}p_{61} - p_{271}x_8 = 0, \\ p_{132}\dfrac{p_{221}}{p_{251}} - \dfrac{p_{131}x_7x_9}{p_{133} + x_{13}} = 0, \\ x_{10} = \dfrac{p_{221}}{p_{251}}, \\ p_{161}x_{11} - p_{171}x_{12} = 0, \\ -p_{191}x_{13} - p_{281}x_{13} + p_{181}x_3x_{14} = 0, \\ p_{241} + p_{191}x_{13} - p_{261}x_{14} - p_{181}x_3x_{14} = 0, \\ x_{15} = 0, \\ x_{16} = 0 \end{cases} \tag{B.5}$$

The solution (B.5) is unfinished since a requirement $p_{71} = 0$ appears that leads to an undetermined system of equations. This scenario can correspond to the case of a reaction suppression and might require a separate investigation.

Solution 4

$$\begin{cases} x_1 = 0, \\ x_6 = 0, \\ p_{31}x_2 - p_{61}x_3x_4 + p_{32}x_{16} = 0, \\ -p_{51}x_4 + p_{41}x_9 = 0, \\ x_5 = \dfrac{p_{71}}{p_{81}}, \\ x_{11} = 0, \\ p_{201} - p_{211}x_7 - p_{121}x_3x_7 + p_{122}x_8 = 0, \\ p_{121}x_3x_7 - p_{122}p_{61} - p_{271}x_8 = 0, \\ p_{132}\dfrac{p_{221}}{p_{251}} - \dfrac{p_{131}x_7x_9}{p_{133} + x_{13}} = 0, \\ x_{10} = \dfrac{p_{221}}{p_{251}}, \\ \boldsymbol{p_{141}\dfrac{p_{71}}{p_{81}} = 0}, \\ p_{171}x_{12} = 0, \\ -p_{191}x_{13} - p_{281}x_{13} + p_{181}x_3x_{14} = 0, \\ p_{241} + p_{191}x_{13} - p_{261}x_{14} - p_{181}x_3x_{14} = 0, \\ x_{15} = 0, \\ x_{16} = 0 \end{cases} \tag{B.6}$$

The solution (B.6) is unfinished since a requirement $p_{141}\frac{p_{71}}{p_{81}} = 0$ appears that leads to an undetermined system of equations. This scenario can correspond to the case of a reaction suppression and might require a separate investigation.

Solution 5

$$
\begin{cases}
x_1 = \dfrac{-p_{12}p_{21}x_3 + p_{11}\frac{p_{161}}{p_{171}}\frac{-f_6(x_3)\pm\left(\frac{p_{141}p_{151}f_5(x_3)}{p_{111}p_{152}f_4(x_3)}+\frac{p_{141}p_{181}f_1(x_3)f_5(x_3)x_3}{p_{111}p_{152}f_4(x_3)}\right)}{2(p_{91}p_{141}p_{151}f_3(x_3)-p_{81}p_{152}+p_{91}p_{141}p_{181}f_1(x_3)f_3(x_3)x_3)}}{p_{21}x_3}, \\
\dfrac{\boldsymbol{-p_9p_{111}}}{\boldsymbol{p_{81}+p_{111}x_6(x_3)}}\boldsymbol{f_4(x_3)x_6(x_3)} + \dfrac{\boldsymbol{p_{11}x_1(x_3)}}{\boldsymbol{p_{12}+x_1(x_3)}} = \boldsymbol{0}, \\
x_3 = f_4(x_3), \\
x_4 = \dfrac{p_{41}}{p_{51}}f_3(x_3), \\
x_5 = p_{71}\left(p_{81}+p_{111}f_4(x_3)\dfrac{-p_{81}p_{101}p_{152}+p_9p_{111}p_{152}f_4(x_3)-f_5(x_3)}{2p_{101}p_{111}p_{152}f_4(x_3)}\right)^{-1}, \\
x_6 = \dfrac{-p_{81}p_{101}p_{152}+p_9p_{111}p_{152}f_4(x_3)-f_5(x_3)}{2p_{101}p_{111}p_{152}f_4(x_3)}, \\
x_7 = (p_{122}+p_{271})f_2(x_3), \\
x_8 = p_{121}f_2(x_3)x_3, \\
x_9 = f_3(x_3), \\
x_{10} = \dfrac{p_{221}}{p_{251}}, \\
x_{11} = \dfrac{-f_6(x_3)\pm\left(\frac{p_{141}p_{151}f_5(x_3)}{p_{111}p_{152}f_4(x_3)}+\frac{p_{141}p_{181}f_1(x_3)f_5(x_3)x_3}{p_{111}p_{152}f_4(x_3)}\right)}{2\left(p_{91}p_{141}p_{151}f_3(x_3)-p_{81}p_{152}+p_{91}p_{141}p_{181}f_1(x_3)f_3(x_3)x_3\right)}, \\
x_{12} = \dfrac{p_{161}}{p_{171}}\dfrac{-f_6(x_3)\pm\left(\frac{p_{141}p_{151}f_5(x_3)}{p_{111}p_{152}f_4(x_3)}+\frac{p_{141}p_{181}f_1(x_3)f_5(x_3)x_3}{p_{111}p_{152}f_4(x_3)}\right)}{2\left(p_{91}p_{141}p_{151}f_3(x_3)-p_{81}p_{152}+p_{91}p_{141}p_{181}f_1(x_3)f_3(x_3)x_3\right)}, \\
x_{13} = p_{181}f_1(x_3)x_3, \\
x_{14} = f_1(x_3)(p_{191}+p_{281}) \\
x_{15} = 0, \\
x_{16} = 0
\end{cases}
\tag{B.7}
$$

where

$$
\begin{aligned}
f_1(x_3) &= \frac{p_{241}}{p_{191}p_{261} + p_{261}p_{281} + p_{181}p_{281}x_3}, \\
f_2(x_3) &= \frac{p_{201}}{p_{122}p_{211} + p_{211}p_{271} + p_{121}p_{271}x_3}, \\
f_3(x_3) &= \frac{p_{132}p_{221}\left(p_{133} + p_{181}f_1(x_3)x_3\right)}{p_{131}p_{251}\left(p_{122} + p_{271}\right)}, \\
f_4(x_3) &= \frac{p_{41}p_{61}}{p_{31}p_{51}} f_3(x_3)x_3, \\
f_5(x_3) &= \left[\left(p_{71}p_{111}p_{152}f_4(x_3) - p_{81}p_{101}p_{152}\right)^2 + \right. \\
&\quad \left. + 4p_{71}p_{91}p_{101}p_{111}p_{141}p_{152}f_3(x_3)f_4(x_3)\left(p_{151} + p_{181}f_1(x_3)x_3\right)\right]^{1/2}, \\
f_6(x_3) &= p_9p_{141}p_{151} + p_9p_{141}p_{181}f_1(x_3) + \frac{p_{81}p_{101}p_{141}}{p_{111}f_4(x_3)}\left(p_{151} + p_{181}f_1(x_3)x_3\right).
\end{aligned}
\tag{B.8}
$$

The main idea of this solution is to chose some key variable and express all other variables of the system as a function of it. In the case of the system (B.8) the key variable is x_3. Finally, only one equation for x_3 left in the system. Depending on its order, the equation might be solved either analytically or numerically. After obtaining the solutions for x_3 all other variables values can be easily calculated.

Solution analysis

Finally, the system (B.2) has only two reasonable solutions (B.4) and (B.7). If to use the values of rate constants from the Tables B.2 and B.3 and to reject the solutions containing complex numbers, then the real steady state solutions can be found (Table B.4). The Solution 5b should be rejected since it contains negative values that makes no sense for the concentration values.

Model variable	**Solution 2, nmol/l**	**Solution 5a, nmol/l**	**Solution 5b, nmol/l**
Healthy mitochondria, x_1	0	50	-1
Impaired mitochondria, x_2	0	5	6.8×10^4
Reactive oxygen species, x_3	0	10	1200
Antioxidants, x_4	8.61	200	2.3×10^4
Parkin, x_5	50.5	50	-0.12
p62, x_6	0.1	50	-155
Keap1, active form, x_7	220	200	17
Keap1, inactive form, x_8	0	20	203
Nrf2, active form, x_9	0.9	20	2292
Nrf2, inactive from, x_{10}	200	200	200
Nf-κB, x_{11}	4.8	100	-2.36
Bcl-xL, x_{12}	4.8	100	-2.36
DJ-1, active form, x_{13}	0	20	203
DJ-1, inactive form, x_{14}	220	200	17
Menadion (external), x_{15}	0	0	0
Menadion (internal), x_{16}	0	0	0

Table B.4: The real steady states solutions for the validated model V.

Appendix C

Creation of the MPC controller in Simulink

Simulink is a graphical environment that uses a principle of visual programming. A user can utilize provided blocks to create a model and to perform an analysis and a simulation. The main advantage of Simulink is an ability to perform complex calculations just with a few clicks. Appearance of blocks used in Simulink is sometimes very similar to the designations of the different elements of electrical circuits. However, the models created in Simulink have nothing common with electrical circuits.

To demonstrate the basic principles of building a model in Simulink as well as a MPC controller one may consider a simple differential equation:

$$\frac{dx}{dt} = -ax, \tag{C.1}$$

where a is a positive constant.

The solution of (C.1) is well-known and represented by an exponential decay $x = e^{-at}$. To solve this equation in Simulink one should built a simple model (see Fig. C.1).

After applying the ODE solver in Simulink one could obtain the solution (see Fig. C.2).

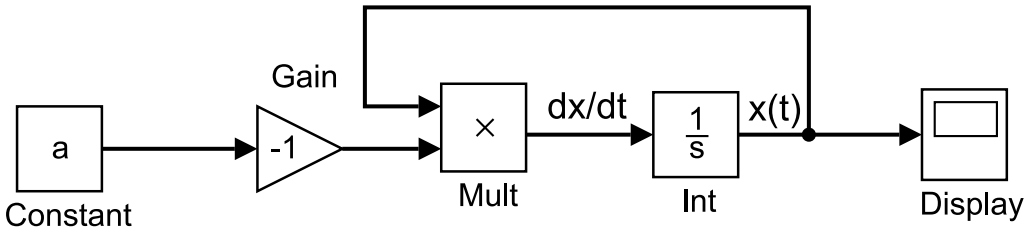

Figure C.1: The simulink model for the differential equation (C.1). The block "Int" performs an integration to obtain the solution signal $x(t)$, the block "Mult" performs a multiplication of $x(t)$ with the constant value $-a$.

The equation (C.1) might be sophisticated by an addition of a temporal dependence for the parameter a:

$$\frac{dx}{dt} = -a(t)x. \tag{C.2}$$

For the simplicity the parameter $a(t)$ might be considered as a signal generator that switches between 0 and 1 with a frequency of $2Hz$. In the current example the exact form of $a(t)$ is unimportant. However, a stepwise generator might be considered as a simulator of periodical environmental changes (daily injections, regular exposure to a stress, etc.). The Simulink model for this case is presented in Fig. C.3.

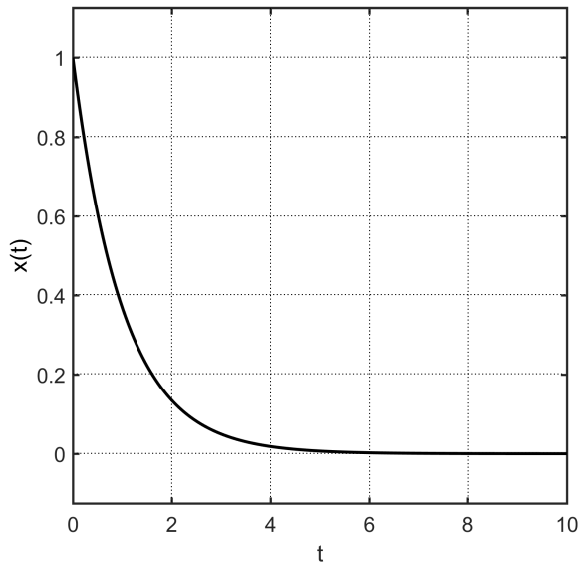

Figure C.2: The solution given by Simulink for the equation (C.1). As it was expected the solution is a damping exponent $x = e^{-at}$.

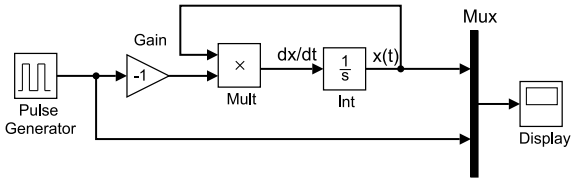

Figure C.3: Simulink model for the equation (C.2). Instead of the constant a there is a pulse generator. For simultaneous displaying of two signals (the solution $x(t)$ and the generator signal $a(t)$) the multiplexer "Mux" is used.

For the current equation it is impossible to obtain a fully analytical solution since the generator provides a discrete signal. However, one can assume that for those time points when $a = 1$ the solution will match the one of (C.1). If the generator gives 0 then the right part of (C.2) becomes also 0 and the solution is just a constant (see Fig. C.4).

As a final example the following non-trivial case is considered. One can take again the equation (C.2) and assume that there is a certain known solution $\bar{x}(t)$. The question is how the signal $a(t)$ should be changed to satisfy the equation

$$\frac{d\bar{x}}{dt} = -a(t)\bar{x}. \tag{C.3}$$

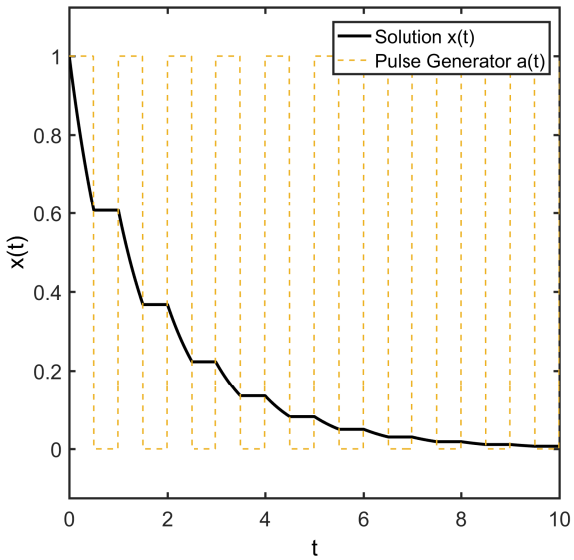

Figure C.4: The solution given by Simulink for the equation (C.2). The final solution is a mix of a damping exponent and the constant values.

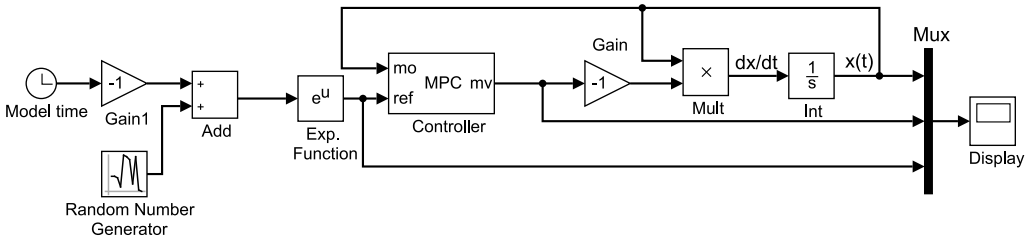

Figure C.5: Simulink model for the equation (C.3). The reference signal $\bar{x}(t)$ is e^{-at} where a is the random number with a mean value 0 and a variance 0.1. The MPC controller should generate the driving signal $a(t)$ to minimize the difference between $x(t)$ and $\bar{x}(t)$.

This problem could be solved with the MPC method. Indeed, the equation (C.3) may be considered as a model of some process, $\bar{x}(t)$ is a reference signal, $a(t)$ is a model input (or a driving signal coming from the MPC controller) and finally $x(t)$ is an output signal of the model generated under the control $a(t)$. To make the problem less trivial a random noise is introduced into the reference signal $\bar{x}(t)$ (see Fig. C.5). As a result, Simulink provides the driving signal to solve this optimal control problem (see Fig. C.6).

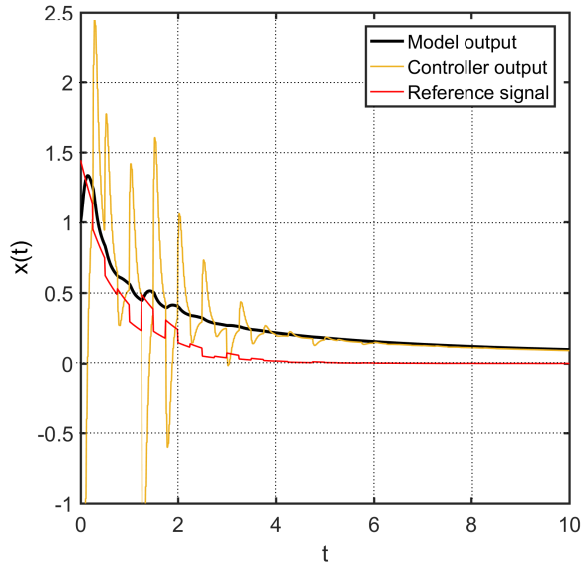

Figure C.6: The solution that is given by Simulink for the equation (C.3). A red line is the reference signal $\bar{x}(t)$, which includes random jumps, orange line is a controller output signal $a(t)$ which is used to make a model output signal (black line) as close as possible to the reference signal.

As one can see the MPC controller manages to find the driving signal that provides a satisfactory correspondence of the model output and the reference signal. Despite the factor of a random noise, the output signal manages to repeat trends of the reference signal. The result becomes more valuable if take into account that the controller has no idea about future dynamics of the reference signal because of the random component. The controller has to adapt constantly its output to follow the reference signal.

Strictly speaking, an introduction of the randomness into the reference signal increases the complexity of this problem. And the most appropriate way to find a solution is to use the theory of robust MPC. Nevertheless, even using of simple MPC controller provides good enough results.

Simulink provides the great possibilities for the simulation of the ODE systems. Once a model is built, one can perform an enormous amount of numerical experiments. For example, different types of generators could be used to present a periodical consumption of medicines or to present environmental changes of a constant, a periodical or a random nature. A usage of the MPC controller allows predicting the possible ways to change a model state that might be correspond to the seeking of the treatment strategies. Rich capabilities for signal measurements and routing allow to obtain the value of any variable (or set of variables) at the any point of a model. This simplifies the analysis of a model and helps to find the errors if any.

Appendix D

Detailed model of the ROS management network

The detailed model of the ROS management system (Figure D.1) is a natural development of the model V. Several new components and reactions are added.

- The protein Pink1 that protects a cell from the damage caused by a mitochondrial dysfunction.
- ATP, ADP and water – the essential species that are directly used for the energy generation in a cell.
- More detailed description of translation and transcription processes.
- The cytochrome complex that is involved in the initiation of apoptosis.
- The process of both Nrf2 and p62 ubiquitination by Keap1.
- More detailed layer of NF-κB signalling.

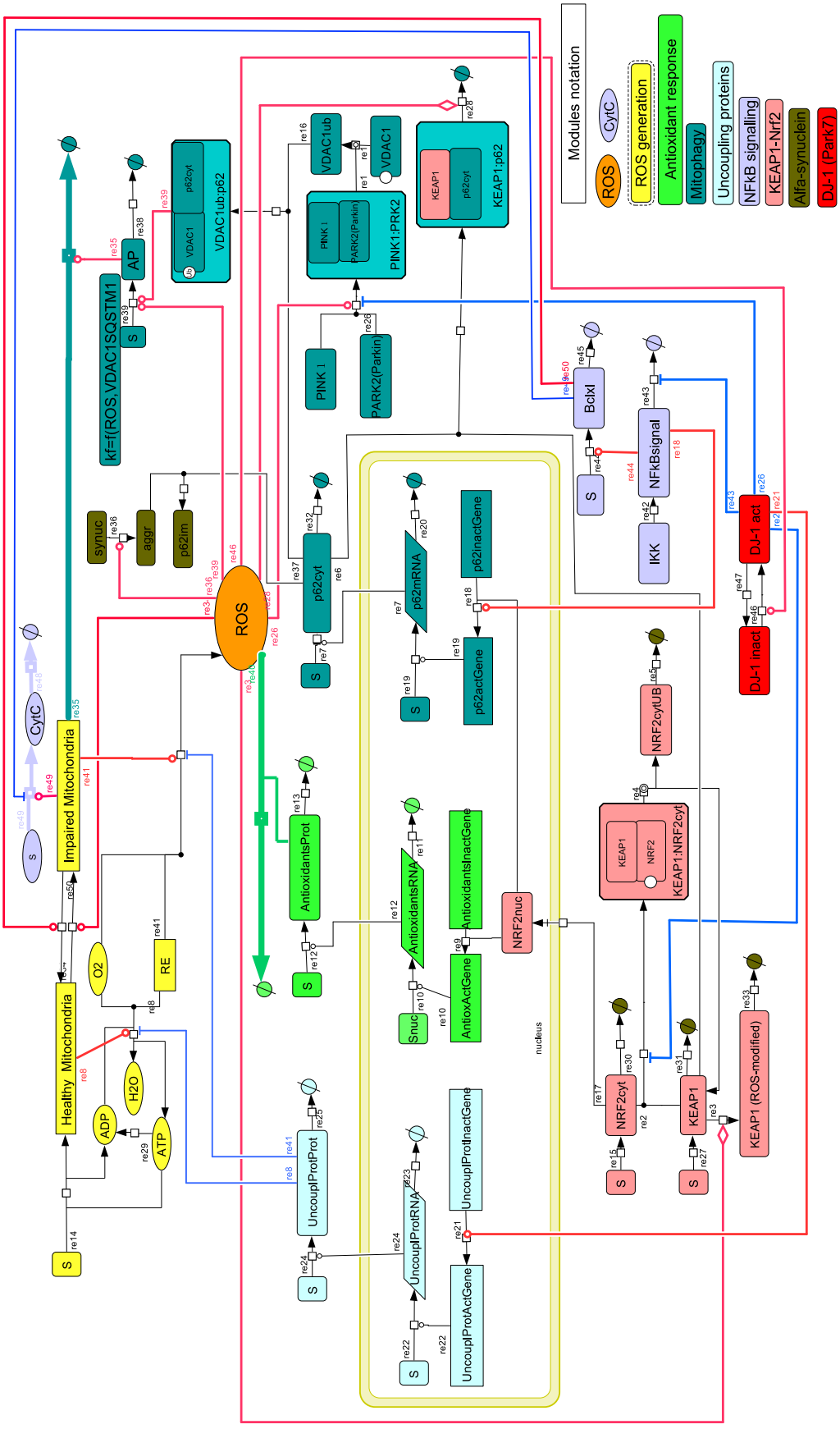

Figure D.1: The detailed model of the ROS management network that is considered as an improvement of the model V. The model is built with COPASI and CellDesigner [205].

Bibliography

[1] M. Verma, M. Zakhartsev, M. Reuss, and H. V. Westerhoff. "'Domino' systems biology and the 'A' of ATP". In: *Biochim. Biophys. Acta* 1827.1 (2013), pp. 19–29.

[2] D.B. Kell. "Towards a unifying, systems biology understanding of large-scale cellular death and destruction caused by poorly liganded iron: Parkinson's, Huntington's, Alzheimer's, prions, bactericides, chemical toxicology and others as examples". In: *Arch Toxicol.* 84.11 (2010), pp. 825–89.

[3] H.R. Kim et al. "Bax inhibitor 1 regulates ER-stress-induced ROS accumulation through the regulation of cytochrome P450 2E1". In: *J. Cell. Sci.* 122.Pt 8 (2009), pp. 1126–1133.

[4] A. Orient et al. "Novel sources of reactive oxygen species in the human body". In: *Nephrology Dialysis Transplantation* 22.5 (2007), pp. 1281–1288.

[5] K. Brieger, S. Schiavone, F. Miller Jr, and K.-H. Krause. "Reactive oxygen species: from health to disease". In: *Swiss medical weekly* 142 (2012), w13659.

[6] N.J. Finnerty et al. "Continuous real-time in vivo measurement of cerebral nitric oxide supports theoretical predictions of an irreversible switching in cerebral ROS after sufficient exposure to external toxins". In: *J Parkinsons Dis.* 3.3 (2013), pp. 351–62.

[7] K. Bagchi and S. Puri. "Free radicals and antioxidants in health and disease". In: *Eastern Mediterranean Health Journal* 4.2 (1998), pp. 350–360.

[8] T. Finkel and N. J. Holbrook. "Oxidants, oxidative stress and the biology of ageing". In: *Nature* 408.6809 (2000), pp. 239–247.

[9] J. K. Leach et al. "Ionizing radiation-induced, mitochondria-dependent generation of reactive oxygen/nitrogen". In: *Cancer Res.* 61.10 (2001), pp. 3894–3901.

[10] T. P. Szatrowski and C. F. Nathan. "Production of large amounts of hydrogen peroxide by human tumor cells". In: *Cancer Res.* 51.3 (1991), pp. 794–798.

[11] M. A. Kohanski et al. "A common mechanism of cellular death induced by bactericidal antibiotics". In: *Cell* 130.5 (2007), pp. 797–810.

[12] P.A. Riley. "Free radicals in biology: oxidative stress and the effects of ionizing radiation". In: *International journal of radiation biology* 65.1 (1994), pp. 27–33.

[13] B. Halliwell, J. Gutteridge, and C.E. Cross. "Free radicals, antioxidants, and human disease: where are we now?" In: *The Journal of laboratory and clinical medicine* 119.6 (1992), pp. 598–620.

[14] T.P.A. Devasagayam et al. "Free radicals and antioxidants in human health: current status and future prospects". In: *Japi* 52.794804 (2004), p. 4.

[15] V. Lobo, A. Patil, A. Phatak, and N. Chandra. "Free radicals, antioxidants and functional foods: Impact on human health". In: *Pharmacogn Rev* 4.8 (2010), pp. 118–126.

[16] L. Pham-Huy, H. He, and C. Pham-Huy. "Free radicals, antioxidants in disease and health". In: *Int J Biomed Sci* 4.2 (2008), pp. 89–96.

[17] D. Sawyer. "Superoxide chemistry". In: *AccessScience* (2014).

[18] I. Fridovich. "Superoxide Anion Radical (O_2^-), Superoxide Dismutases, and Related Matters". In: *Journal of Biological Chemistry* 272.30 (1997), pp. 18515–18517.

[19] D. Gough and T. Cotter. "Hydrogen peroxide: a Jekyll and Hyde signalling molecule". In: *Cell Death Dis* 2 (2011), e213.

[20] B. Lipinski. "Hydroxyl radical and its scavengers in health and disease". In: *Oxid Med Cell Longev* 2011 (2011), p. 809696.

[21] K. Rahman. "Studies on free radicals, antioxidants, and co-factors". In: *Clin Interv Aging* 2.2 (2007), pp. 219–236.

[22] C. Sam and H. Lu. "The role of hypochlorous acid as one of the reactive oxygen species in periodontal disease". In: *Journal of Dental Sciences* 4.2 (2009), pp. 45 –54.

[23] P. Pacher, J. S. Beckman, and L. Liaudet. "Nitric oxide and peroxynitrite in health and disease". In: *Physiol. Rev.* 87.1 (2007), pp. 315–424.

[24] R. Milo et al. "BioNumbers–the database of key numbers in molecular and cell biology". In: *Nucleic Acids Res.* 38.Database issue (2010), pp. D750–753.

[25] G. R. Buettner. "The pecking order of free radicals and antioxidants: lipid peroxidation, alpha-tocopherol, and ascorbate". In: *Arch. Biochem. Biophys.* 300.2 (1993), pp. 535–543.

[26] Y. Liu, G. Fiskum, and D. Schubert. "Generation of reactive oxygen species by the mitochondrial electron transport chain". In: *J. Neurochem.* 80.5 (2002), pp. 780–787.

[27] X. Li et al. "Targeting mitochondrial reactive oxygen species as novel therapy for inflammatory diseases and cancers". In: *J Hematol Oncol* 6 (2013), p. 19.

[28] B.M. Babior, R.S. Kipnes, and J.T. Curnutte. "Biological defense mechanisms. The production by leukocytes of superoxide, a potential bactericidal agent". In: *Journal of Clinical Investigation* 52.3 (1973), p. 741.

[29] B.M. Babior, J.T. Curnutte, and R.S. Kipnes. "Biological defense mechanisms. Evidence for the participation of superoxide in bacterial killing by xanthine oxidase". In: *J Lab Clin Med* 85.2 (1975), pp. 235–244.

[30] B.E. Britigan, M.S. Cohen, and G.M. Rosen. "Detection of the production of oxygen-centered free radicals by human neutrophils using spin trapping techniques: a critical perspective." In: *Journal of leukocyte biology* 41.4 (1987), pp. 349–362.

[31] M.F. Christman, R.W. Morgan, F.S. Jacobson, and B.N. Ames. "Positive control of a regulon for defenses against oxidative stress and some heat-shock proteins in Salmonella typhimurium". In: *Cell* 41.3 (1985), pp. 753–762.

[32] J.G. Scandalios. "Oxidative stress: molecular perception and transduction of signals triggering antioxidant gene defenses". In: *Brazilian Journal of Medical and Biological Research* 38.7 (2005), pp. 995–1014.

[33] C. Hall et al. "Immunoresponsive gene 1 augments bactericidal activity of macrophage-lineage cells by regulating β-oxidation-dependent mitochondrial ROS production". In: *Cell metabolism* 18.2 (2013), pp. 265–278.

[34] P. Chaudhari, Z. Ye, and Y.Y. Jang. "Roles of reactive oxygen species in the fate of stem cells." In: *Antioxid Redox Signal.* 20.12 (2014), pp. 1881–90.

[35] M. Juntilla et al. "AKT1 and AKT2 maintain hematopoietic stem cell function by regulating reactive oxygen species". In: *Blood* 115.20 (2010), pp. 4030–4038.

[36] M. Kinder et al. "Hematopoietic stem cell function requires 12/15-lipoxygenase–dependent fatty acid metabolism". In: *Blood* 115.24 (2010), pp. 5012–5022.

[37] Y. Kanda, T. Hinata, S. Kang, and Y. Watanabe. "Reactive oxygen species mediate adipocyte differentiation in mesenchymal stem cells". In: *Life sciences* 89.7 (2011), pp. 250–258.

[38] J. Le Belle et al. "Proliferative neural stem cells have high endogenous ROS levels that regulate self-renewal and neurogenesis in a PI3K/Akt-dependant manner". In: *Cell stem cell* 8.1 (2011), pp. 59–71.

[39] S. Elmore. "Apoptosis: a review of programmed cell death". In: *Toxicol Pathol* 35.4 (2007), pp. 495–516.

[40] Y. Z. Wang et al. "Concise review: Quiescent and active states of endogenous adult neural stem cells: identification and characterization". In: *Stem Cells* 29.6 (2011), pp. 907–912.

[41] C. L. Limoli et al. "Cell-density-dependent regulation of neural precursor cell function". In: *Proc. Natl. Acad. Sci. U.S.A.* 101.45 (2004), pp. 16052–16057.

[42] T. Fukai and M. Ushio-Fukai. "Superoxide dismutases: role in redox signaling, vascular function, and diseases". In: *Antioxid. Redox Signal.* 15.6 (2011), pp. 1583–1606.

[43] R. G. Alscher, N. Erturk, and L. S. Heath. "Role of superoxide dismutases (SODs) in controlling oxidative stress in plants". In: *J. Exp. Bot.* 53.372 (2002), pp. 1331–1341.

[44] N.R. Brady et al. "Coordinated behavior of mitochondria in both space and time: a reactive oxygen species-activated wave of mitochondrial depolarization." In: *Biophys. J.* 87.3 (2004), pp. 2022–2034.

[45] L.A. Kane et al. "PINK1 phosphorylates ubiquitin to activate Parkin E3 ubiquitin ligase activity". In: *J. Cell Biol.* 205.2 (2014), pp. 143–153.

[46] T. Cui et al. "Silencing of PINK1 induces mitophagy via mitochondrial permeability transition in dopaminergic MN9D cells". In: *Brain Res.* 1394 (2011), pp. 1–13.

[47] M.A. Fedorowicz et al. "Cytosolic cleaved PINK1 represses Parkin translocation to mitochondria and mitophagy". In: *EMBO Rep.* 15.1 (2014).

[48] R.M. Ivatt and A.J. Whitworth. "The many faces of mitophagy". In: *EMBO Rep.* 15.1 (2014), pp. 5–6.

[49] G. L. McLelland et al. "Parkin and PINK1 function in a vesicular trafficking pathway regulating mitochondrial quality control". In: *EMBO J.* 33.4 (2014), pp. 282–295.

[50] B. Halliwell. "Oxidative stress and cancer: have we moved forward?" In: *Biochemical Journal* 401.1 (2007), pp. 1–11.

[51] O. Hwang. "Role of oxidative stress in Parkinson's disease". In: *Experimental neurobiology* 22.1 (2013), pp. 11–17.

[52] N. Singh, A. Dhalla, C. Seneviratne, and P.K. Singal. "Oxidative stress and heart failure". In: *Cellular interactions in cardiac pathophysiology*. Springer, 1995, pp. 77–81.

[53] J. Santiago and J. Potashkin. "Shared dysregulated pathways lead to Parkinson's disease and diabetes". In: *Trends in molecular medicine* 19.3 (2013), pp. 176–186.

[54] S. A. Soleimanpour et al. "The diabetes susceptibility gene Clec16a regulates mitophagy". In: *Cell* 157.7 (2014), pp. 1577–1590.

[55] C. A. Rice-Evans and V. Gopinathan. "Oxygen toxicity, free radicals and antioxidants in human disease: biochemical implications in atherosclerosis and the problems of premature neonates". In: *Essays Biochem.* 29 (1995), pp. 39–63.

[56] R. Charan et al. "Inhibition of apoptotic Bax translocation to the mitochondria is a central function of parkin". In: *Cell death & disease* 5.7 (2014), e1313.

[57] M. Nalls et al. "Large-scale meta-analysis of genome-wide association data identifies six new risk loci for Parkinson's disease". In: *Nature genetics* 46.9 (2014), pp. 989–993.

[58] V. Gundersen. "Protein aggregation in Parkinson's disease". In: *Acta Neurol. Scand., Suppl.* 190 (2010), pp. 82–87.

[59] P. Tiraboschi, L. A. Hansen, L. J. Thal, and J. Corey-Bloom. "The importance of neuritic plaques and tangles to the development and evolution of AD". In: *Neurology* 62.11 (2004), pp. 1984–1989.

[60] S. J. Lee, H. S. Lim, E. Masliah, and H. J. Lee. "Protein aggregate spreading in neurodegenerative diseases: problems and perspectives". In: *Neurosci. Res.* 70.4 (2011), pp. 339–348.

[61] H. T. Tran et al. "α-synuclein immunotherapy blocks uptake and templated propagation of misfolded α-synuclein and neurodegeneration". In: *Cell Rep* 7.6 (2014), pp. 2054–2065.

[62] K. U. Tufekci, R. Meuwissen, S. Genc, and K. Genc. "Inflammation in Parkinson's disease". In: *Adv Protein Chem Struct Biol* 88 (2012), pp. 69–132.

[63] U. Kishore. *Neurodegenerative Diseases*. InTech, 2013.

[64] R. Pfeiffer, Z. Wszolek, and M Ebadi. *Parkinsonś disease, Second edition*. CRC Press, 2012.

[65] L. Alberghina and H.V. Westerhoff. *Systems Biology: Definitions and Perspectives*. Springer, 2005.

[66] H. V. Westerhoff et al. "Systems biology towards life in silico: mathematics of the control of living cells". In: *J Math Biol* 58.1-2 (2009), pp. 7–34.

[67] J. Hornberg, F. Bruggeman, H. Westerhoff, and J. Lankelma. "Cancer: a systems biology disease". In: *Biosystems* 83.2 (2006), pp. 81–90.

[68] A. Del Sol, R. Balling, L. Hood, and D. Galas. "Diseases as network perturbations". In: *Current opinion in biotechnology* 21.4 (2010), pp. 566–571.

[69] M. Volpe, D. Chin, and F. Paneni. "The challenge of polypharmacy in cardiovascular medicine". In: *Fundamental & clinical pharmacology* 24.1 (2010), pp. 9–17.

[70] C. Luni et al. "Confidence from uncertainty-A multi-target drug screening method from robust control theory". In: *BMC systems biology* 4.1 (2010), p. 161.

[71] B. Bakker et al. "Network-based selectivity of antiparasitic inhibitors". In: *Molecular biology reports* 29.1 (2002), pp. 1–5.

[72] J. Lehár et al. "Synergistic drug combinations tend to improve therapeutically relevant selectivity". In: *Nature biotechnology* 27.7 (2009), pp. 659–666.

[73] A. Borisy et al. "Systematic discovery of multicomponent therapeutics". In: *Proceedings of the National Academy of Sciences* 100.13 (2003), pp. 7977–7982.

[74] G. Cuccato, G. Della Gatta, and D. di Bernardo. "Systems and Synthetic biology: tackling genetic networks and complex diseases". In: *Heredity (Edinb)* 102.6 (2009), pp. 527–532.

[75] F. Menolascina, V. Siciliano, and D. di Bernardo. "Engineering and control of biological systems: A new way to tackle complex diseases". In: *FEBS Letters* 586.15 (2012), pp. 2122–2128.

[76] J. Ciapaite et al. "Modular kinetic analysis of the adenine nucleotide translocator-mediated effects of palmitoyl-CoA on the oxidative phosphorylation in isolated rat liver mitochondria". In: *Diabetes* 54.4 (2005), pp. 944–951.

[77] K. Hubner, S. Sahle, and U. Kummer. "Applications and trends in systems biology in biochemistry". In: *FEBS Journal* 278.16 (2011), pp. 2767–2857.

[78] A. Saadatpour and R. Albert. "Boolean modeling of biological regulatory networks: a methodology tutorial". In: *Methods* 62.1 (2013), pp. 3–12.

[79] J. Liang and J. Han. "Stochastic Boolean networks: an efficient approach to modeling gene regulatory networks". In: *BMC Syst Biol* 6 (2012), p. 113.

[80] K. C. Chen et al. "Integrative analysis of cell cycle control in budding yeast". In: *Mol. Biol. Cell* 15.8 (2004), pp. 3841–3862.

[81] C. Goodwin. *Temporal organization in cells; a dynamic theory of cellular control processes.* London,Academic Press, 1963, p. 184.

[82] T.Jr. Székely and K. Burrage. "Stochastic simulation in systems biology". In: *Computational and Structural Biotechnology Journal* 12.2021 (2014), pp. 14 –25.

[83] H. Resat, M. N. Costa, and H. Shankaran. "Spatial aspects in biological system simulations". In: *Meth. Enzymol.* 487 (2011), pp. 485–511.

[84] N. Jamshidi and B. ?. Palsson. "Mass action stoichiometric simulation models: incorporating kinetics and regulation into stoichiometric models". In: *Biophys. J.* 98.2 (2010), pp. 175–185.

[85] J. Beck and K. Arnold. *Parameter estimation in engineering and science*. J. Wiley, 1977.

[86] H. Resat, L. Petzold, and M. F. Pettigrew. "Kinetic modeling of biological systems". In: *Methods Mol. Biol.* 541 (2009), pp. 311–335.

[87] R. Alves, F. Antunes, and A. Salvador. "Tools for kinetic modeling of biochemical networks". In: *Nat. Biotechnol.* 24.6 (2006), pp. 667–672.

[88] W. W. Chen, M. Niepel, and P. K. Sorger. "Classic and contemporary approaches to modeling biochemical reactions". In: *Genes Dev.* 24.17 (2010), pp. 1861–1875.

[89] B. Bekins, E. Warren, and E. Godsy. "A Comparison of Zero-Order, First-Order, and Monod Biotransformation Models". In: *Ground Water* 36.2 (1998), pp. 261–268.

[90] H. Kitano. "Computational systems biology". In: *Nature* 420.6912 (2002), pp. 206–210.

[91] R. Gottlieb and Gustafsson A. "Mitochondrial turnover in the heart". In: *Biochimica et Biophysica Acta (BBA) - Molecular Cell Research* 1813.7 (2011). Mitochondria and Cardioprotection, pp. 1295 –1301.

[92] N. G. Lipsky and P. L. Pedersen. "Mitochondrial turnover in animal cells. Half-lives of mitochondria and mitochondrial subfractions of rat liver based on [14C]bicarbonate incorporation". In: *J. Biol. Chem.* 256.16 (1981), pp. 8652–8657.

[93] B. Schwanhausser et al. "Global quantification of mammalian gene expression control". In: *Nature* 473 (2011), 337342.

[94] S. Gaudet, S. Spencer, W. Chen, and P. Sorger. "Exploring the Contextual Sensitivity of Factors that Determine Cell-to-Cell Variability in Receptor-Mediated Apoptosis". In: *PLoS Comput Biol* 8.4 (2012), e1002482.

[95] J. C. Sprott and A. Xiong. "Classifying and quantifying basins of attraction". In: *Chaos* 25.8, 083101 (2015).

[96] G. Spelsberg-Korspeter et al. "Construction of Lyapunov functions for the estimation of basins of attraction". In: *J. Braz. Soc. Mech. Sci. & Eng.* 34 (2012), pp. 633–639.

[97] S. Ratschan and Z. She. "Providing a Basin of Attraction to a Target Region of Polynomial Systems by Computation of Lyapunov-Like Functions". In: *SIAM Journal on Control and Optimization* 48.7 (2010), pp. 4377–4394.

[98] A. Burton. "The properties of the steady state compared to those of equilibrium as shown in characteristic biological behavior". In: *Journal of Cellular and Comparative Physiology* 14.3 (1939), pp. 327–349.

[99] M. Schultz. "Why Equilibrium? Understanding Entropy of Mixing". In: *Journal of Chemical Education* 76.10 (1999), p. 1391.

[100] W.B. Cannon. "THe sympathetic division of the autonomic system in relation to homeostasis". In: *Archives of Neurology & Psychiatry* 22.2 (1929), pp. 282–294.

[101] B. Halliwell and J. Gutteridge. "The definition and measurement of antioxidants in biological systems". In: *Free Radical Biology and Medicine* 18.1 (1995), pp. 125–126.

[102] J. MatÉs, C. Pérez-Gómez, and I. De Castro. "Antioxidant enzymes and human diseases". In: *Clinical biochemistry* 32.8 (1999), pp. 595–603.

[103] M. McCall and B. Frei. "Can antioxidant vitamins materially reduce oxidative damage in humans?" In: *Free Radical Biology and Medicine* 26.7 (1999), pp. 1034–1053.

[104] H. Sies, W. Stahl, and A. Sevanian. "Nutritional, dietary and postprandial oxidative stress". In: *The Journal of nutrition* 135.5 (2005), pp. 969–972.

[105] C. Rice-Evans and A. Diplock. "Current status of antioxidant therapy". In: *Free Radical Biology and Medicine* 15.1 (1993), pp. 77–96.

[106] A. Tanaka. "Parkin-mediated selective mitochondrial autophagy, mitophagy: Parkin purges damaged organelles from the vital mitochondrial network". In: {*FEBS*} *Letters* 584.7 (2010). Autophagy, pp. 1386 –1392.

[107] Y. Mizuno et al. "Parkin and Parkinson's disease". In: *Curr. Opin. Neurol.* 14.4 (2001), pp. 477–482.

[108] Y. Katsuragi, Y. Ichimura, and M. Komatsu. "p62/SQSTM1 functions as a signaling hub and an autophagy adaptor". In: *FEBS J.* 282.24 (2015), pp. 4672–4678.

[109] M. Kobayashi and M. Yamamoto. "Molecular mechanisms activating the Nrf2-Keap1 pathway of antioxidant gene regulation". In: *Antioxidants & redox signaling* 7.3-4 (2005), pp. 385–394.

[110] K. Itoh et al. "Keap1 represses nuclear activation of antioxidant responsive elements by Nrf2 through binding to the amino-terminal Neh2 domain". In: *Genes & development* 13.1 (1999), pp. 76–86.

[111] K. Chan, X. Han, and Y. Kan. "An important function of Nrf2 in combating oxidative stress: detoxification of acetaminophen". In: *Proceedings of the National Academy of Sciences* 98.8 (2001), pp. 4611–4616.

[112] J. Lee et al. "Identification of the NF-E2-related factor-2-dependent genes conferring protection against oxidative stress in primary cortical astrocytes using oligonucleotide microarray analysis". In: *Journal of Biological Chemistry* 278.14 (2003), pp. 12029–12038.

[113] T. Ishii et al. "Transcription factor Nrf2 coordinately regulates a group of oxidative stress-inducible genes in macrophages". In: *Journal of Biological Chemistry* 275.21 (2000), pp. 16023–16029.

[114] F. Bea et al. "Induction of glutathione synthesis in macrophages by oxidized low-density lipoproteins is mediated by consensus antioxidant response elements". In: *Circulation research* 92.4 (2003), pp. 386–393.

[115] M. Kwak et al. "Modulation of gene expression by cancer chemopreventive dithiolethiones through the Keap1-Nrf2 pathway Identification of novel gene clusters for cell survival". In: *Journal of Biological Chemistry* 278.10 (2003), pp. 8135–8145.

[116] A. Jain et al. "p62/SQSTM1 is a target gene for transcription factor NRF2 and creates a positive feedback loop by inducing antioxidant response element-driven gene transcription". In: *J. Biol. Chem.* 285.29 (2010), pp. 22576–22591.

[117] T. D. Gilmore. "Introduction to NF-kappaB: players, pathways, perspectives". In: *Oncogene* 25.51 (2006), pp. 6680–6684.

[118] H. Hacker and M. Karin. "Regulation and function of IKK and IKK-related kinases". In: *Sci. STKE* 2006.357 (2006), re13.

[119] A. Joselin et al. "ROS-dependent regulation of Parkin and DJ-1 localization during oxidative stress in neurons". In: *Human molecular genetics* (2012), dds325.

[120] G. Fichera, M. A. Sneider, and J. Wyman. "On the existence of a steady state in a biological system". In: *Proc. Natl. Acad. Sci. U.S.A.* 74.10 (1977), pp. 4182–4184.

[121] S. Geisler et al. "PINK1/Parkin-mediated mitophagy is dependent on VDAC1 and p62/SQSTM1". In: *Nat. Cell Biol.* 12.2 (2010), pp. 119–131.

[122] M. Spiegel. *Mathematical Handbook of Formulas and Tables*. Schaum, 1968.

[123] T. Y. Kim et al. "Metabolic labeling reveals proteome dynamics of mouse mitochondria". In: *Mol. Cell Proteomics* 11.12 (2012), pp. 1586–1594.

[124] L. Deferme et al. "Time series analysis of oxidative stress response patterns in HepG2: a toxicogenomics approach". In: *Toxicology* 306 (2013), pp. 24–34.

[125] V. I. Lushchak. "Glutathione homeostasis and functions: potential targets for medical interventions". In: *J Amino Acids* 2012 (2012), p. 736837.

[126] C. D. Thomson. "Selenium-dependent and non-selenium-dependent glutathione peroxidase in human tissues of New Zealand residents". In: *Biochem. Int.* 10.4 (1985), pp. 673–679.

[127] U. Moran, R. Phillips, and R. Milo. "SnapShot: key numbers in biology". In: *Cell* 141.7 (2010), pp. 1262–1262.

[128] W. R. Madych. "Solutions of Underdetermined Systems of Linear Equations". In: *Lecture Notes-Monograph Series* 20 (1991), pp. 227–238.

[129] A. Rizzo et al. "Serum levels of reactive oxygen species (ROS) in the bitch". In: *Immunopharmacol Immunotoxicol* 31.2 (2009), pp. 310–313.

[130] C. Zhu, W. Hu, H. Wu, and X. Hu. "No evident dose-response relationship between cellular ROS level and its cytotoxicity–a paradoxical issue in ROS-based cancer therapy". In: *Sci Rep* 4 (2014).

[131] L. Fridlyand and L. Philipson. "Does the glucose-dependent insulin secretion mechanism itself cause oxidative stress in pancreatic beta-cells?" In: *Diabetes* 53.8 (2004), pp. 1942–1948.

[132] D. Zou, L. Ma, J. Yu, and Z. Zhang. "Biological databases for human research". In: *Genomics Proteomics Bioinformatics* 13.1 (2015), pp. 55–63.

[133] G. Lillacci and M. Khammash. "Parameter Estimation and Model Selection in Computational Biology". In: *PLoS Comput Biol* 6.3 (2010), pp. 1–17.

[134] D. N. Criddle et al. "Menadione-induced reactive oxygen species generation via redox cycling promotes apoptosis of murine pancreatic acinar cells". In: *J. Biol. Chem.* 281.52 (2006), pp. 40485–40492.

[135] G. Loor et al. "Menadione triggers cell death through ROS-dependent mechanisms involving PARP activation without requiring apoptosis". In: *Free Radic. Biol. Med.* 49.12 (2010), pp. 1925–1936.

[136] J. Schaber. "Easy parameter identifiability analysis with COPASI". In: *BioSystems* 110.3 (2012), pp. 183–185.

[137] M. Kumar, M. Husian, N. Upreti, and D. Gupta. "Genetic algorithm: Review and application". In: *International Journal of Information Technology and Knowledge Management* 2.2 (2010), pp. 451–454.

[138] D. Hawkins. "The problem of overfitting". In: *J Chem Inf Comput Sci* 44.1 (2004), pp. 1–12.

[139] Charles G. Gross. "Claude Bernard and the Constancy of the Internal Environment". In: *The Neuroscientist* 4.5 (1998), pp. 380–385.

[140] N. Wiener. *Cybernetics; or, Control and communication in the animal and the machine*. New York: M.I.T. Press, 1961. ISBN: 9780262730099.

[141] A. S. Khalil and J. J. Collins. "Synthetic biology: applications come of age". In: *Nat. Rev. Genet.* 11.5 (2010), pp. 367–379.

[142] J. Boston, M. Simaan, J. Antaki, and Y. Yu. "Control issues in rotary heart assist devices". In: *Proc. American Control Conference* (2000), pp. 3473–3477.

[143] S. A. Haddad, R. P. Houben, and W. A. Serdijn. "The evolution of pacemakers". In: *IEEE Eng Med Biol Mag* 25.3 (2006), pp. 38–48.

[144] R. S. Parker, F. J. Doyle, and N. A. Peppas. "A model-based algorithm for blood glucose control in type I diabetic patients". In: *IEEE Trans Biomed Eng* 46.2 (1999), pp. 148–157.

[145] A. H. Clemens. "Feedback control dynamics for glucose controlled insulin infusion system". In: *Med Prog Technol* 6.3 (1979), pp. 91–98.

[146] V.Y. Reddy et al. "Percutaneous Implantation of an Entirely Intracardiac Leadless Pacemaker". In: *New England Journal of Medicine* 373.12 (2015). PMID: 26321198, pp. 1125–1135.

[147] M. Colombo et al. "Biological applications of magnetic nanoparticles". In: *Chem. Soc. Rev.* 41 (11 2012), pp. 4306–4334.

[148] E. Alphonsus and M. Abdullah. "A review on the applications of programmable logic controllers (PLCs)". In: *Renewable and Sustainable Energy Reviews* 60 (2016), pp. 1185 –1205.

[149] P. Lundstr$\acute{}$om, J.H. Lee, M. Morari, and S. Skogestad. "Limitations of dynamic matrix control". In: *Computers & Chemical Engineering* 19.4 (1995), pp. 409 –421.

[150] R. Rouhani and R. Mehra. "Model algorithmic control (MAC); basic theoretical properties". In: *Automatica* 18.4 (1982), pp. 401 –414.

[151] R. Findeisen, F. Allgöwer, and L. Biegler. *Assessment and Future Directions of Nonlinear Model Predictive Control*. Lecture Notes in Control and Information Sciences. Springer Berlin Heidelberg, 2007.

[152] R. Kamyar and E. Taheri. "Aircraft Optimal Terrain/Threat-Based Trajectory Planning and Control". In: *Journal of Guidance Control Dynamics* 37 (2014), pp. 466–483.

[153] P. O. M. Scokaert and D. Q. Mayne. "Min-max feedback model predictive control for constrained linear systems". In: *IEEE Transactions on Automatic Control* 43.8 (1998), pp. 1136–1142.

[154] A. Richards and J. How. "Robust stable model predictive control with constraint tightening". In: *2006 American Control Conference*. 2006, 6 pp.–.

[155] S. Qin and T. Badgwell. "A survey of industrial model predictive control technology". In: *Control Engineering Practice* 11 (2003), pp. 733–764.

[156] R. Grepl. "Real-Time Control Prototyping in MATLAB/Simulink: Review of tools for research and education in mechatronics". In: *2011 IEEE International Conference on Mechatronics*. 2011, pp. 881–886.

[157] J. P. Cobb, R. S. Hotchkiss, I. E. Karl, and T. G. Buchman. "Mechanisms of cell injury and death". In: *Br J Anaesth* 77.1 (1996), pp. 3–10.

[158] C. Liu, Y. Chen, I Kochevar, and U. Jurkunas. "Decreased DJ-1 Leads to Impaired Nrf2-Regulated Antioxidant Defense and Increased UV-AInduced Apoptosis in Corneal Endothelial Cells". In: *Invest Ophthalmol Vis Sci.* 55.9 (2014), pp. 5551–5560.

[159] H. Ariga et al. "Neuroprotective function of DJ-1 in Parkinson's disease". In: *Oxid Med Cell Longev* 2013 (2013), p. 683920.

[160] Y. Zhang et al. "Overexpression of DJ-1/PARK7, the Parkinson's disease-related protein, improves mitochondrial function via Akt phosphorylation on threonine 308 in dopaminergic neuron-like cells". In: *Eur. J. Neurosci.* 43.10 (2016), pp. 1379–1388.

[161] B. Weyhenmeyer, A. C. Murphy, J. H. Prehn, and B. M. Murphy. "Targeting the anti-apoptotic Bcl-2 family members for the treatment of cancer". In: *Exp. Oncol.* 34.3 (2012), pp. 192–199.

[162] S. Besbes, M. Mirshahi, M. Pocard, and C. Billard. "New dimension in therapeutic targeting of BCL-2 family proteins". In: *Oncotarget* 6.15 (2015), pp. 12862–12871.

[163] D. F. Lee and M. C. Hung. "Advances in targeting IKK and IKK-related kinases for cancer therapy". In: *Clin. Cancer Res.* 14.18 (2008), pp. 5656–5662.

[164] C. Gamble et al. "Inhibitory kappa B Kinases as targets for pharmacological regulation". In: *Br. J. Pharmacol.* 165.4 (2012), pp. 802–819.

[165] T. R. Caulfield, F. C. Fiesel, and W. Springer. "Activation of the E3 ubiquitin ligase Parkin". In: *Biochem. Soc. Trans.* 43.2 (2015), pp. 269–274.

[166] S. Kubo, T. Hatano, M. Takanashi, and N. Hattori. "Can parkin be a target for future treatment of Parkinson's disease?" In: *Expert Opin. Ther. Targets* 17.10 (2013), pp. 1133–1144.

[167] A. S. Herrera et al. "Beyond mitochondria, what would be the energy source of the cell?" In: *Cent Nerv Syst Agents Med Chem* 15.1 (2015), pp. 32–41.

[168] V. A. Morais et al. "PINK1 loss-of-function mutations affect mitochondrial complex I activity via NdufA10 ubiquinone uncoupling". In: *Science* 344.6180 (2014), pp. 203–207.

[169] A. Rakovic et al. "Phosphatase and tensin homolog (PTEN)-induced putative kinase 1 (PINK1)-dependent ubiquitination of endogenous Parkin attenuates mitophagy: study in human primary fibroblasts and induced pluripotent stem cell-derived neurons". In: *J. Biol. Chem.* 288.4 (2013), pp. 2223–2237.

[170] D. Sha, L. S. Chin, and L. Li. "Phosphorylation of parkin by Parkinson disease-linked kinase PINK1 activates parkin E3 ligase function and NF-kappaB signaling". In: *Hum. Mol. Genet.* 19.2 (2010), pp. 352–363.

[171] A. K. Muller-Rischart et al. "The E3 ligase parkin maintains mitochondrial integrity by increasing linear ubiquitination of NEMO". In: *Mol. Cell* 49.5 (2013), pp. 908–921.

[172] D. D. Zhang et al. "Ubiquitination of Keap1, a BTB-Kelch substrate adaptor protein for Cul3, targets Keap1 for degradation by a proteasome-independent pathway". In: *J. Biol. Chem.* 280.34 (2005), pp. 30091–30099.

[173] G. Arena et al. "PINK1 protects against cell death induced by mitochondrial depolarization, by phosphorylating Bcl-xL and impairing its pro-apoptotic cleavage." In: *Cell Death Differ.* 20.7 (2013), pp. 920–30.

[174] T. Kodama et al. "BH3-only activator proteins Bid and Bim are dispensable for Bak/Bax-dependent thrombocyte apoptosis induced by Bcl-xL deficiency: molecular requisites for the mitochondrial pathway to apoptosis in platelets". In: *J. Biol. Chem.* 286.16 (2011), pp. 13905–13913.

[175] M. Schieber and N. S. Chandel. "ROS function in redox signaling and oxidative stress". In: *Curr. Biol.* 24.10 (2014), R453–462.

[176] D. J. Surmeier, J. N. Guzman, J. Sanchez-Padilla, and J. A. Goldberg. "The origins of oxidant stress in Parkinson's disease and therapeutic strategies". In: *Antioxid. Redox Signal.* 14.7 (2011), pp. 1289–1301.

[177] S. Gandhi and A. Y. Abramov. "Mechanism of oxidative stress in neurodegeneration". In: *Oxid Med Cell Longev* 2012 (2012), p. 428010.

[178] M. Cloutier, R. Middleton, and P. Wellstead. "Feedback motif for the pathogenesis of Parkinson's disease". In: *Systems Biology, IET* 6.3 (2012), pp. 86–93.

[179] M. Cloutier and P. Wellstead. "Dynamic modelling of protein and oxidative metabolisms simulates the pathogenesis of Parkinson's disease". In: *Systems Biology, IET* 6.3 (2012), pp. 65–72.

[180] A. Bjorklund and M. A. Cenci. "Recent Advances in Parkinson's disease - translational and clinical research". In: *Prog. Brain Res.* 184 (2010), pp. vii–viii.

[181] L. F. Zhang et al. "Coffee and caffeine potentiate the antiamyloidogenic activity of melatonin via inhibition of Aβ oligomerization and modulation of the Tau-mediated pathway in N2a/APP cells". In: *Drug Des Devel Ther* 9 (2015), pp. 241–272.

[182] F. Buchel et al. "Parkinson's disease: dopaminergic nerve cell model is consistent with experimental finding of increased extracellular transport of α-synuclein". In: *BMC Neurosci* 14 (2013), p. 136.

[183] Y. Wang, W. Liu, X. He, and F. Zhou. "Parkinson's disease-associated DJ-1 mutations increase abnormal phosphorylation of tau protein through Akt/GSK-3β pathways". In: *J. Mol. Neurosci.* 51.3 (2013), pp. 911–918.

[184] T. R. Egnew. "Suffering, meaning, and healing: challenges of contemporary medicine". In: *Ann Fam Med* 7.2 (2009), pp. 170–175.

[185] R. Peck and P. Smith. "Beyond Genetics-Stratified and Personalised Medicines Using Multiple Parameters". In: *Pharmaceuticals (Basel)* 3.5 (2010), pp. 1637–1651.

[186] B. B. Spear, M. Heath-Chiozzi, and J. Huff. "Clinical application of pharmacogenetics". In: *Trends Mol Med* 7.5 (2001), pp. 201–204.

[187] K. A. Phillips et al. "Potential role of pharmacogenomics in reducing adverse drug reactions: a systematic review". In: *JAMA* 286.18 (2001), pp. 2270–2279.

[188] K. K. Jain. "Applications of AmpliChip CYP450". In: *Mol. Diagn.* 9.3 (2005), pp. 119–127.

[189] S. E. Kimmel et al. "A pharmacogenetic versus a clinical algorithm for warfarin dosing". In: *N. Engl. J. Med.* 369.24 (2013), pp. 2283–2293.

[190] D. Mayne and Michalska H. "Adaptive receding horizon control for constrained nonlinear systems". In: *Decision and Control, 1993., Proceedings of the 32nd IEEE Conference on*. Vol. 2. 1993, pp. 1286–1291.

[191] M. Elowitz, A. Levine, E. Siggia, and P. Swain. "Stochastic Gene Expression in a Single Cell". In: 297.5584 (2002), pp. 1183–1186.

[192] O. Berg. "A model for the statistical fluctuations of protein numbers in a microbial population". In: *Journal of Theoretical Biology* 71.4 (1978), pp. 587–603.

[193] P. D. Ray, B. W. Huang, and Y. Tsuji. "Reactive oxygen species (ROS) homeostasis and redox regulation in cellular signaling". In: *Cell. Signal.* 24.5 (2012), pp. 981–990.

[194] G. L. Squadrito and W. A. Pryor. "Oxidative chemistry of nitric oxide: the roles of superoxide, peroxynitrite, and carbon dioxide". In: *Free Radic. Biol. Med.* 25.4-5 (1998), pp. 392–403.

[195] G. Dijkstra et al. "Opposite effect of oxidative stress on inducible nitric oxide synthase and haem oxygenase-1 expression in intestinal inflammation: anti-inflammatory effect of carbon monoxide". In: *J. Pathol.* 204.3 (2004), pp. 296–303.

[196] T. J. Guzik et al. "Nitric oxide modulates superoxide release and peroxynitrite formation in human blood vessels". In: *Hypertension* 39.6 (2002), pp. 1088–1094.

[197] F. C. Tanner et al. "Nitric oxide modulates expression of cell cycle regulatory proteins: a cytostatic strategy for inhibition of human vascular smooth muscle cell proliferation". In: *Circulation* 101.16 (2000), pp. 1982–1989.

[198] J. Scicinski et al. "NO to cancer: The complex and multifaceted role of nitric oxide and the epigenetic nitric oxide donor, RRx-001". In: *Redox Biol* 6 (2015), pp. 1–8.

[199] A. Jahani-Asl and A. Bonni. "iNOS: a potential therapeutic target for malignant glioma". In: *Curr. Mol. Med.* 13.8 (2013), pp. 1241–1249.

[200] V. Somasundaram et al. "Nitric oxide and reactive oxygen species: Clues to target oxidative damage repair defective breast cancers". In: *Crit. Rev. Oncol. Hematol.* 101 (2016), pp. 184–192.

[201] D. C. Chan. "Fusion and fission: interlinked processes critical for mitochondrial health". In: *Annu. Rev. Genet.* 46 (2012), pp. 265–287.

[202] H. Thor et al. "The metabolism of menadione (2-methyl-1,4-naphthoquinone) by isolated hepatocytes. A study of the implications of oxidative stress in intact cells". In: *J Biol Chem* 257.20 (1982), pp. 12419–25.

[203] J. Mauzeroll, A. J. Bard, O. Owhadian, and T. J. Monks. "Menadione metabolism to thiodione in hepatoblastoma by scanning electrochemical microscopy". In: *Proc. Natl. Acad. Sci. U.S.A.* 101.51 (2004), pp. 17582–17587.

[204] D. Donoho, H. Kakavand, and J. Mammen. "The Simplest Solution to an Underdetermined System of Linear Equations". In: *2006 IEEE International Symposium on Information Theory*. 2006, pp. 1924–1928.

[205] R. Alves, F. Antunes, and A. Salvador. "Tools for kinetic modeling of biochemical networks". In: *Nat. Biotechnol.* 24.6 (2006), pp. 667–672.